Targeted EDV^{TM} Nanocells carrying small interfering RNA (siRNA) molecules to overcome drug resistance in Non-small cell lung cancer

by Eva St. Clair

Thesis submitted in fulfilment of the requirements for
the degree of

Master of Science (Research)

under the supervision of

Drs Jennifer MacDiarmid & Himanshu Brahmbhatt (EnGeneIC)

Prof Gyorgy Hutvagner & Dr. Eileen McGowan (UTS)

University of Technology Sydney
Faculty of Life Science

June, 2021

CERTIFICATE OF ORIGINAL AUTHORSHIP

I, Eva St. Clair declare that this thesis, is submitted in fulfilment of the requirements for the award of Master of Science (Research), in the Faculty of Life Science at the University of Technology Sydney.

This thesis is wholly my own work unless otherwise referenced or acknowledged. In addition, I certify that all information sources and literature used are indicated in the thesis.

This document has not been submitted for qualifications at any other academic institution.

This research is supported by the Australian Government Research Training Program.

Signature:

Production Note:
Signature removed prior to publication.

Date: 3/06/2021

Acknowledgments

First and foremost, I would like to thank Dr. Jennifer MacDiarmid and Dr. Himanshu Brahmbhatt for their guidance, encouragement and support to allow me to achieve this master's degree. I feel incredibly grateful to have worked in the innovative company you have built for the past 6 years and cannot thank you enough for your willingness to share your experience and endless knowledge with me. You both inspire me to strive to be the best scientist I can be.

I would like to thank all of the EnGenes for your support over the years. I am incredibly blessed to be working with such lovely people and talented scientists. In particular, thank you to Jocelyn & Natasha for sharing your animal ethics and *in vivo* skills and knowledge. Stacey, for always sharing her extensive tissue culture knowledge and Sharon for being so willing to share her flow cytometry expertise. To Nancy and Steven for their guidance in helping me chose suitable siRNAs, probes and primers and in RT-qPCR analysis. To Lu, Kasia, Estefania and Julia for sharing their knowledge in various *in vitro* experiments, and Ilya, Reema, Vatty and Arash for their guidance in antibody targeting and EDV^{TM} loading and lyophilisation.

To my UTS supervisors, Professor Gyorgy Hutvagner and Dr. Eileen McGowan thank you for your amazing support, encouragement and sharing your extensive knowledge on thesis writing and presentations.

Thank you also to Carmel and David Goggins and the EnGeneIC Cancer Research Foundation that awarded me the Jenna Goggins Scholarship which allowed me to carry out this master's degree. I have heard about what an amazing and courageous woman your daughter Jenna was, and her memory has inspired me throughout my work.

A very big thank you to my own family for their constant support and love and for always being there for me.

Finally, to my husband Sean, thank you for supporting me in everything I wish to achieve, for always making me laugh even during the difficult times and for encouraging me to be the best I can be.

I dedicate this thesis to our beautiful daughter Annabelle, who arrived at the very end of this work and gave me strength and inspiration to complete this master's degree.

Abstract

Background. Over two million people worldwide suffer from lung cancer, the main sub-type (85%) being NSCLC and despite many chemotherapeutics approved for NSCLC, only 2% of patients with NSCLC metastatic disease survive 5 years post diagnosis with *multidrug resistance being the major cause of mortality in NSCLC patients.*

Aim. The overall aim of this project was to evaluate targeted EnGeneIC Dream Vector™ (EDV™) nanocells for loading and delivering small interfering RNA (siRNA) molecules, Polo like kinase-1 (PLK1), Ribonucleoside reductase subunit M1 (RRM1) & Kinesin Spindle Protein (KSP), in order to silence proteins essential to tumour cell survival and proliferation, and to evaluate their therapeutic potential in overcoming the hitherto intractable multiple drug resistance in non- small cell lung cancer (NSCLC).

Methods. The expression of cell cycle genes *PLK*1, *RRM*1 & *KSP* in NSCLC cell lines was measured using RT-qPCR and Western Blot. Efficacy of siRNAs targeting PLK1 (siPLK1), RRM1 (siRRM1) & KSP (siKSP) transfected into NSCLC cell lines was measured by the MTS proliferation assay and Western Blot. Flow cytometric analysis was used to measure apoptosis and cell cycle arrest in NSCLC cell lines transfected with the siRNAs targeting PLK1, RRM1 and KSP. EDV™ nanocells were targeted to the epithelial growth factor receptor (EGFR) and the copy number of siRNAs loaded into the nanocells was measured by staining with an RNA specific dye and measured on a fluorometer compared to known standards. EDV™-siRNAs were used to treat NSCLC cells lines grown as 3D spheroids using the hanging drop plates (Perfecta3D®:HDP1096) and cell proliferation inhibition was assessed using trypan blue cell viability assay. The EDV™s-siRNAs were then tested *in vivo* using the A549-Dox-R a xenograft mouse model, tumours were excised and assessed for gene knockdown by RT-qPCR.

Results and Conclusion. In this study we show that *in vitro* and *in vivo*, EDV™s can effectively deliver targeted-cell cycle-siRNAs to hanging drop 3D spheroids and into a mouse xenograft model to inhibit cell and tumour growth, and that EDV™s can encapsulate and deliver a significant siRNA payload directly inside the tumour cells without affecting non-target tissue. Overall, this study highlights the exciting possibility that siRNAs against mitotic regulators loaded into EDV™s will be safe alone or in combination with drug-loaded EDV™s, and may overcome drug resistance in NSCLC patients. This project has true translational potential for

both delivering hitherto “undeliverable” functional nucleic acids, and for potentially addressing drug-resistance mechanisms in lung cancer.

Table of Contents

Abbreviations

A549-Dox-R	A549-Doxorubicin-Resistant cell line
Ab	Antibody
ACC	Adrenocortical cancer
AF488	Alexa Fluor® 488
AGCA	Australian Government Cancer Australia
AIHW	Australian Institute of Health and Welfare
ALK	Anaplastic lymphoma kinase
ATCC	American Type Culture Collection
BCL2	B-cell lymphoma 2 encoding gene
BRAF	B-Raf Proto-Oncogene
BSA	Bovine Serum Albumin
BsAb	Bispecific Antibody
c-myc	Myc Proto-Oncogene Protein
CA-19-9	Carbohydrate Antigen 19-9
CAR	Chimeric Antigen Receptor
CTLA-4	Cytotoxic T-Lymphocyte-associated Antigen-4
DDT	Dithiothreitol
DNA	Deoxyribonucleic Acid
DOPC	1,2-Dioleoyl-sn-glycero-3-phosphocholine
dsDNA	Double Stranded DNA
dsRNA	Double Stranded RNA
EBSS	Earles Balanced Salt Solution
EMEM	Eagles Minimum Essential Medium
ECACC	European Collection of Animal Cell Cultures
EDTA	Ethylenediaminetetraacetic acid
EDV™	EnGeneIC Dream Vector™
EGFR	Epidermal Growth factor receptor
EML4-ALK	Endocrine Microtubules associated protein-like protein
EMT	Epithelial to Mesenchymal Transition
EphA2	Ephrin type-A Receptor 2
EPR	Enhance Permeation and Retention

ERK	Extracellular Signal-Regulated Kinase
FAK	Focal Adhesion Kinase
FBS	Foetal Bovine Serum
FTI	Farnesyltransferase inhibitors
HDM2	Human Double Minute-2 protein
HER2	Human Epidermal growth factor Receptor 2
Hh	Hedgehog
IC50	Half maximal inhibitory concentration
IFN	Interferon
IL	Interleukin
iNOP	Interfering Nanoparticle
KRAS	Kirsten Rat Sarcoma viral proto-oncogene
KSP	Kinesin Spindle Protein
LCP	Lipid Calcium Phosphate
LODER™	Local Drug Eluter
mAb	Monoclonal Antibody
MAGE-3	Melanoma-associated antigen 3
MAPK1	Mitogen-Activated Protein Kinase 1
MAP	Mitogen-Activated Protein
MEK-1	MAP Kinase/ERK Kinase 1
MET	MET proto-oncogene, receptor tyrosine kinase
MDR	Multi Drug Resistance
MDR 1	Multi Drug Resistant Protein
miRNA	Micro RNA
MESF	Molecules of Soluble Fluorochrome
MNP	Micellar Nanoparticles
mRNA	Messenger RNA
MRP3	Multi Drug Resistance-associated Protein 3
MST	Median Survival time
NEAA	Non-Essential Amino Acid
nm	Nanometer
nM	Nanomolar
NSCLC	Non-Small Cell Lung Cancer

NS-NSCLC	Non-Squamous Non-Small Cell Lung Cancer
NY-ESO-1	Human tumour antigen of the cancer/testis family
ORR	Objective Response Rate
PBS	Phosphate Buffered Saline
PCR	Polymerase Chain Reaction
PD-1	Programmed cell death protein
PDK4	Pyruvate dehydrogenase lipoamide kinase isozyme 4
PFS	Progression-free survival
PLGA	Poly (DL-lactide-co-glycolide acid)
PLK1	Polo-like kinase 1
PTGS	Post-Transcriptional Gene Silencing
PDR	Progressive Disease Rate
QC	Quality Control
RET	Rearranged during Transfection Proto-oncogene
RNA	Ribonucleic Acid
ROS1	ROS proto-oncogene 1, receptor tyrosine kinase
RISC	RNA Induced Silencing Complex
RNAi	RNA interference
RPMI	Roswell Park Memorial Institute medium
RRM1	Ribonucleotide Reductase Subunit M1
RT	Room Temperature
RT-PCR	Reverse Transcriptase Polymerase Chain Reaction
S. Typhimurium	*Salmonella typhimurium*
SCLC	Small-cell lung cancer
siLuc	Luciferase siRNA
shRNA	Short hairpin RNA
siRNA	Small interfering RNA
siPLK1	Polo-Like Kinase 1 targeted siRNA
sLDH	Small layered Double Hydroxide
TKI	Tyrosine Kinase Inhibitor
Tp53	Tumour Protein 53 gene
TRAE	Treatment Related Adverse Effects
VEGF	Vascular endothelial growth factor

WHO	World Health Organisation

List of Figures

List of Tables

Chapter 1 - Introduction

1. Overview

Non-small cell lung cancer (NSCLC) is the leading cause of cancer death around the world [2]. The treatment options for NSCLC are dependent on the stage at diagnosis but generally comprises a combination of chemotherapies, radiation and/or surgery. Targeted therapies, which target a specific mutation or biomarker in patient subsets with NSCLC, have also been developed with limited success [3]. Recently, immunotherapy has emerged as an exciting treatment option for long term disease control, especially if combined with chemotherapy [4]. However, since most patients are diagnosed with advanced disease resistance to current treatment options, even with recently developed immunotherapies, translate into poor clinical outcomes. Therefore, there is a need to develop novel approaches to treat this type of cancer.

The therapeutic potential of using siRNAs in cancer is being actively studied for the purpose of switching off cancer driver genes, or genes that are involved in tumour growth, angiogenesis, metastasis and multi-drug resistance. siRNAi therapies involve delivering a synthetic siRNA into target tumour cells to elicit RNA interference (RNAi), thereby inhibiting the stability of a specific messenger RNA (mRNA) [5]. Many siRNAs are under investigation as potential therapies for NSCLC including those targeting cell cycle regulatory proteins, and 'undruggable' oncogenes, or 'difficult to drug' targets, such as KRAS and MYC [6]. The term "undruggable" oncogenes was originally used to describe proteins that were pharmaceutically unable to be targeted. In this review the term 'undruggable' will be used in the context of not being susceptible to a targeted drug or chemotherapy.

While siRNA is a promising therapeutic approach [5, 7-10], delivering the double stranded RNA into a cancer cell remains challenging. Strategies utilising synthetic nanoparticles, as well as modifications of the nucleic acid to prevent degradation, have been developed, however, while some of these technologies are being deployed in the clinic, most results have had limited success [11, 12]. However, there has been some success with RNAi drug-based therapies for other diseases. The drug company Alnylam, has recently submitted FDA approval for the RNAi, ONPATTRO™ (patisiran) for the treatment of hereditary transthyretin-mediate (ATTR) amyloidosis [13].

The second pressing problem with siRNA therapy is the safe delivery of the siRNA to the cancer cell (target) without prior siRNA degradation, as mentioned. Recently, targeted bacterial nanocells, EnGeneIC Dream Vector™ (EDV™), were used in a phase I clinical trial to successfully and safely deliver a microRNA to patients with recurrent mesothelioma [14]. Additionally, EnGeneIC has dosed siRNA to 'compassionate use patients' (patients who have exhausted all alternative therapies) with siRNAs targeting the multi-drug resistance protein

(MDR1) (unpublished results). These patients had end-stage adrenocortical cancer, no adverse events were associated with the siRNA delivery (Dr Jennifer MacDiarmid, EnGeneIC, and Dr Stephen Clarke, Royal North Shore Hospital (RNSH), personal communication).

Failure to respond to treatment and drug resistance to conventional therapies are problematic. The promising results from the EnGeneIC clinical trials in mesothelioma, and a case study in adrenocortical cancer, prelude this study. The overall aim of this project is to use targeted EDV^{TM} nanocells carrying small interfering RNA (siRNA) molecules to limit replication potential targeting, Polo like kinase -1 (PLK1), Ribonucleoside reductase subunit M1 (RRM1) & Kinesin Spindle Protein (KSP), to overcome drug resistance in NSCLC.

This critical review provides an overview of how far we have come with targeted and non-targeted therapies to date and the current problems with drug resistance focusing on NSCLCs. Specifically, a focus on siRNA use in targeted therapy and siRNA delivery systems are discussed as an introduction to this project. The siRNAs used in this project have been chosen based on this extensive literature review and, practically, from successful preliminary testing in the EnGeneIC laboratory. This project has true translational potential. The ultimate project objective is to test if EDV^{TM} delivered siRNAs can treat/delay remission and could be used in clinical trials.

1.1 Non-small cell lung cancer (NSCLC)

Every year 1.8 million people are diagnosed with lung cancer worldwide, with an estimated 1.6 million deaths [15]. In Australia, in 2018, an estimated 12,740 people will be diagnosed with lung cancer [15] and over 9000 Australians will die from lung cancer. Lung cancers account for an estimated 18.9% of overall cancer deaths [16]. Alarmingly, once lung cancer has been diagnosed, the chance of surviving for more than 5 years is only 16% [17] and there is a high likelihood that the cancer will return.

Lung cancer comprises two main subtypes, namely small cell lung cancer (SCLC) and non-small cell lung cancer (NSCLC), the latter accounting for 85%-90% of all lung cancers [18]. Within the NSCLC subtype, 3 further main sub-types have been described, which are a) squamous cell carcinoma (SCC), b) adenocarcinoma and c) large cell carcinoma. Squamous cell carcinoma begins within the squamous cells, lung cells that line the inside of the airways. These tumours usually form inside the airways near the bronchus. Due to its location, this cancer often produces the most overt symptoms. Adenocarcinoma is a cancer that begins in the glandular cells and is most frequently located in the smaller airways, i.e. bronchioles, previously known as bronchioloalveolar carcinoma. Large cell carcinoma is the most aggressive type of

NSCLC. It can be found in any part of the lung and its growth rate is very fast. This aggressiveness is the major cause of poor prognosis, with shorter survival and recurrence [19]. The recommended treatment options for lung cancers are dependent on the patient Karnofsky performance status, the histology of the cells, the level of disease progression and, importantly, the stage of the cancer. In Australia, the Tumour, Node, Metastasis (TNM) staging system is used to determine diagnosis, prognosis and treatment options. The TNM staging relates to the depth of tumour invasion (T), the extent of any lymph node involvement (N) and the amount of spreading, or tumour metastasis (M) throughout the body [20].

The TNM staging system (I-IV) describes the extent of the tumour growth and whether it has metastasised. Stages I and II generally refer to cancers that have not spread into the surrounding tissue or the lymph nodes, Stage III tumours are larger than Stages I and II and have started to spread into surrounding tissues and Stage IV refers to cancers that have metastasised.

Most patients diagnosed with stage I and II NSCLC have the affected lobe or section of the lung removed by surgery. Surgery is most commonly followed by adjuvant chemotherapy. The first line platinum-based therapies consist of carboplatin or cisplatin. In most cases, due to platinum-based therapy resistance, combinations of 'third generation' regimens such as docetaxel, gemcitabine, irinotecan, paclitaxel and vinorelbine, are used for more efficacious outcomes [21]. Drug choice is determined by whether histology reveals squamous or non-squamous cancer cells. Bevacizumab, a monoclonal antibody (mAb), and pemetrexed, a folate antimetabolite, are the only effective treatments for non-squamous tumours [22]. For those patients with Stage III and IV cancers, surgery is no longer an option. As NSCLC can often show no symptoms in the early stages, this often results in most patients being diagnosed at later stages. The conventional treatment for such patients is chemotherapy in combination with high doses of radiation, but this is associated with debilitating side effects such as nausea, vomiting, diarrhea and painful mouth ulcers, which has led to the emergence of alternative therapies in an attempt to overcome these downfalls.

1.2 Current Drug treatments for NSCLC and multi-drug resistance

Drug treatment in NSCLC is multi-faceted and is dependent on the type/stage of cancer and treatment for the cancer. Currently, treatment for NSCLC patients depends on the stage of disease, the somatic mutations found and the initial response to conventional first-line platinum-based chemotherapy. However, many patients develop resistance to platinum drugs with a resulting, re-emergence of disease [23].

Mortality caused in NSCLC is predominantly caused by two factors, metastasis and drug resistance, both of which are credited to genetic heterogeneity. Tumour heterogeneity results in cancer cells coping with a changing environment and immune responses [24].

There are several well-known mechanisms that result in drug resistance in cancer including drug export pumps (efflux), changes in the gene expression, drug target alteration/modification of drug targets, and the deregulation of DNA repair and apoptotic proteins [25].

Individual tumours often comprise cells with phenotypic and functional heterogeneity resulting from environmental factors, a change in genetics, cellular properties or transformation of the cells themselves [26]. Cancer cells can transform through differentiation, dedifferentiation and transdifferentiation, which is known as cellular plasticity and examples include epithelial-mesenchymal transition (EMT) and subtype transdifferentiation of cells changing from adenocarcinoma to squamous cell carcinoma [24].

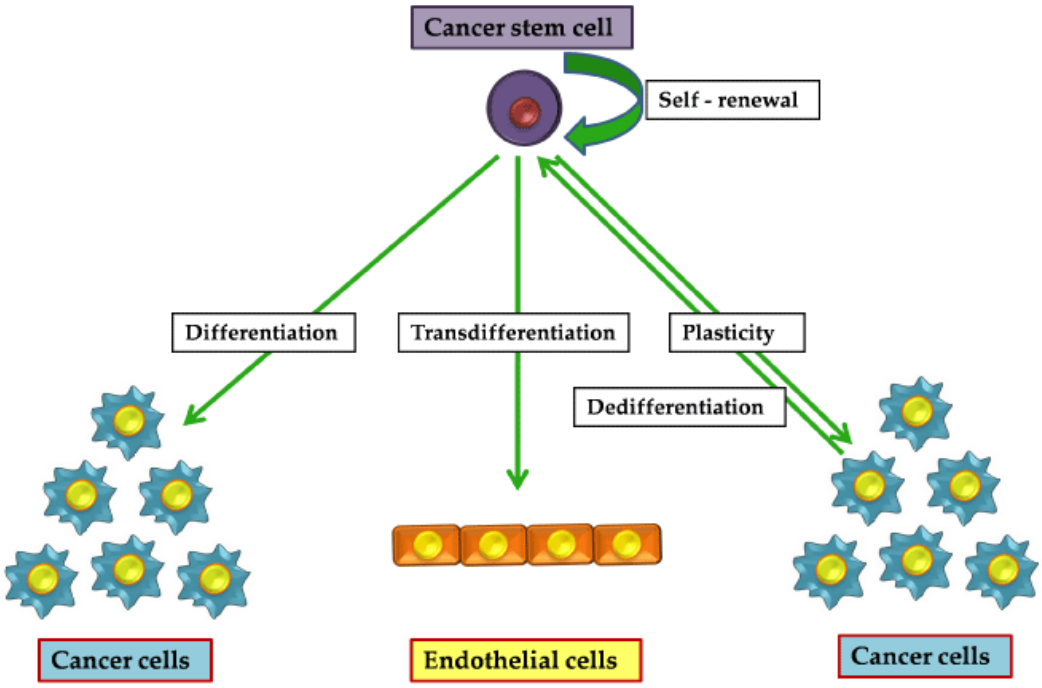

Figure 1.1 Schematic illustrating the different types of cancer cell regeneration. Differentiation is the self-renewal of cancer stem cells, Transdifferentiation is cell changing from one cell type to another and Dedifferentiation is cells that revert to a precursor cell that can divide to produce more differentiated cells [27].

EMT is a crucial mechanism in multicellular organisms as it enables tissue remodelling during morphogenesis and in NSCLC it allows cells to become more invasive with greater metastatic potential [28]. The role of EMT in multi-drug resistance has been intensively studied and it is found to be associated with EGFR-TKI resistance [29]. New mechanisms of resistance are also being uncovered such as pyruvate dehydrogenase kinase 4 (PDK4) which Sun *et al* 2014 reported as a critical metabolic regulator of EMT with associated drug resistance [30]. Phenotypic transition of adenocarcinoma to squamous cell carcinoma occurs within NSCLC and this transdifferentiation and is one of the main causes of TKI resistance in patients and cell heterogeneity and genetic heterogeneity is why treating NSCLC is so difficult [31, 32].

1.2.1 Multidrug Resistance to Chemotherapy in NSCLC

It is estimated that the mutations found in 60% of NSCLC tumours are not "druggable" [33] and thus standard first-line platinum-based chemotherapy remains the initial option, with the aim of inhibiting DNA replication and transcription [34]. Resistance can develop due to insufficient drug reaching the cell nucleus, resulting from low expression of the apoptosis regulator Bcl-2 [35] or high expression of the plasma-membrane transporter 1 [36].

Third generation chemotherapy for NSCLC involves combinations of Carboplatin, Cisplatin Docetaxel, Gemcitabine, Nab-paclitaxel, Paclitaxel, Pemetrexed and Vinorelbine [37]. Melguizo *et al*. 2012 measured levels of multi-drug resistant 1 (MDR1) and multi drug resistance-associated protein 3 (MRP3) in NSCLC treated with carboplatin and paclitaxel to investigate the occurrence of resistance in this regimen [38]. Cell lines treated with paclitaxel showed increased MDR1 expression but not MRP3, in contrast, cells treated with carboplatin showed over-expression of MRP3. Combining paclitaxel and carboplatin, then, resulted in resistance and a poorer outcome for patients. These findings indicated a need for further investigation *in vivo* and in clinical trials, in order to confirm whether the Car-Pac combination should still be the main option for adjuvant therapy in NSCLC patients. Rossi and Maio 2016 reported that third generation cisplatin regimens proved to be more effective than carboplatin and suggested they should be the first choice of platinum-based treatment [39]. Otherwise, a combination of carboplatin, with gemcitabine [40], or the mAb bevacizumab [41], were suggested as alternative therapies in an attempt to lower resistance in NSCLC. Most recently Chang *et al.* 2019 have compared cisplatin with bevacizumab compared to paclitaxel with carboplatin and bevacizumab (PacCBev) and found that the former combination significantly improved progression free survival (PFS) in patients with advanced non-squamous NSCLC

(NS-NSCLC) which may indicate a possible therapy for the third of people who are unable to undergo other targeted therapies [42].

Multidrug resistance is the major cause of mortality in NSCLC with only 2% of patients with metastatic disease surviving 5 years post diagnosis. Thus the need to continue developing new treatments to overcome this resistance is crucial in the fight to defeat this cancer.

1.3 Targeted Therapy for NSCLC

Targeted therapy has come a very long way within the last decade thanks to advances in molecular pathology and the identification of numerous signalling pathways and specific oncogenic driver mutations that lead to harmful cancerous transformation [33]. There have been successful clinical results and benefits of these targeted therapies; however, overcoming the frequent treatment resistance is now the challenge for the delivery of personalised therapies for patients with NSCLC. This section will provide an overview of current targeted therapies that are currently in the clinic or in clinical trials for NSCLC patients. Although many of these targeted therapies have some success in the clinic, drug resistance still remains problematic and is a major cause of recurrence and mortality in NSCLC.

Routinely lung cancer patients are tested for the presence of activating somatic mutations in the epidermal growth factor receptor (EGFR) gene and/or rearrangements of the anaplastic lymphoma kinase (ALK) gene (members of the tyrosine kinase family), which promote cell cycle proliferation. Presence of these mutations are associated with poor prognosis in NSCLC patients [43] .

In the past decade several driver mutations have been discovered, including, EGFR in 10-35% of cases, Kirsten rat sarcoma 2 viral oncogene homolog (KRAS) in 15-25% and less common mutations including serine/threonine-protein kinase B-raf (BRAF), AKT serine/threonine kinase 2 (AKT2), Herceptin 2 (HER2), mitogen-activated protein kinase 1 (MAPK), MAPK/ERK (MEK1), mesenchymal-epithelial transition factor (MET), and Phosphoinositide-3-kinase (PI3K) that phosphorylates Phosphatidylinositol (PIK3CA). Genetic rearrangements of tyrosine kinases, ALK and ROS, and mesenchymal-epithelial transition factor (MET), have also been discovered. With these new discoveries, recently, patients are now also tested for mutations/rearrangements of proto-oncogenes MET, BRAF and RET, all members of the receptor tyrosine kinase family; and KRAS, which belongs to the small GTPase RAS family [44, 45]. Current therapies and therapies in clinical trials targeting NSCLC and problems encountered with these types of therapies are discussed.

1.3.1 Therapies targeting tumours with EGFR mutations and problems with resistance

New targeted therapies have been developed to specifically target EGFR mutations within its tyrosine kinase domain for specific cancers, such as melanoma and lung cancers. EGFR tyrosine kinase inhibitors (TKI), including the EGFR TKI's gefitinib and erlotinib, [46], have been shown to be effective in treating locally metastatic or advanced NSCLC patients who have specific EGFR mutations [47, 48]. Zhou *et al*. 2011 conducted a phase III clinical trial testing erlotinib alone, chemotherapy alone and erlotinib combined with chemotherapy, in patients with EGFR positive mutations in late stage NSCLC [49]. The findings were that overall survival was 20.7 months, 11.2 months and 29.7 months, respectively. While the overall survival has been improved by this treatment, once a patient has received erlotinib or gefitinib, they eventually developed resistance to the respective drug [50].

Problems with EGFR therapy resistance. Several mechanisms of resistance have been found in EGFR tyrosine kinase inhibitors, with 60% of all tumours acquiring resistance caused by a secondary mutation in exon 20 of EGFR (T790M) [51]. As a result of this, second generation, and third generation EGFR TKIs have been identified and developed [52]. Dacomitinib is a second-generation EGFR TKI which has shown strong signalling inhibition in cell lines that have demonstrated resistant to the first generation of EGFR TKIs. This new drug inhibits both the wild-type EGFR as well as the mutated receptor, EGFRT790. Whereas the first generation of TKIs was reversible, hence the development of resistant NSCLCs, this second generation of TKIs is an irreversible inhibitor of EGFR [53]. Mok *et al*. 2017 carried out a clinical trial that compared the effect of dacomitinib and gefitinib where they demonstrated that dacomitinib was more effective showing no signs of adverse effects [54]. The finding of this study supported the use/application of dacomitinib for NSCLC patients that carry the EGFR exon 19 deletion or exon 21 L858R substitution mutations and in 2018 the FDA approved the use of this drug as first-line treatment for such disease [55].

Osimertinib (AZD92991) and naquotinib (ASP8273) are third generation EGFR TKIs and exhibit preferential activity against the tumours harbouring the EGFR T790M mutation. These third generation EGFR TKIs irreversibly bind to their target to prevent the potential drug resistance induced by previous generation inhibitors. Osimertinib was specifically created to overcome the EGFR T790M mutation, which is a common mechanism of drug resistance. Results from a clinical trial conducted by Jänne *et al*. 2015 showed high activity in EGFR T790M-poitive patients treated with Osimerinib, with an objective tumour response rate of 51% [56]. Yang *et al*. 2017 conducted a further Phase I/II trial where a high objective response rate of 62% to osimertinib treatment was observed in patients with EGFRm T790M

advanced NSCLC [57]. In 2017 a phase III trial tested osimertinib versus platinum drugs with pemetrexed as a second line therapy, and the former showed a greater progression free survival of 8.5 months vs 4.2 months respectively [58]. While these results aren't overly impressive later that year Suresh *et al.* 2017 tested osimertinib as a first line therapy with promising results as PFS increased to 22.1 months after treatment. Results from a clinical trial testing the safety and efficacy of naquotinib were also released in 2017 and although overall it was well tolerated by NSCLC patients with the EGFRT790 mutation, the progression free survival was only 6.8 months [59].

The biotechnology company AstraZeneca conducted a phase 1b clinical trial (TATTON) combining osimertinib with either; ascending doses of an anti-PD-L1 mAb Durvalumab (IMFINZI) (refer to section 1.4.3), the MEK 1-2 inhibitor selumetinib or the MET inhibitor savolitinib (AZD6094) [60]. The first two combinations showed increased toxicity in patients with the osimertinib and durvalumab arm being closed early due to these negative results [61]. Conversely osimertinib and savolitinib showed acceptable toxicity and this combination is being further examined in an ongoing clinical trial (SAVANNAH) with MET amplified, EGFR-mutated NSCLC patients with progression after previous EGFR-TKI treatment with results expected in 2022 [62].

AstraZeneca has also conducted a phase III clinical trial in patients with untreated EGFR-mutated advanced NSCLC, testing osimertinib vs other EGFR TKIs. These results showed an acceptable safety profile and a longer overall survival of 38.6 vs 31.8 months respectively in patients [63].

The combination of osimertinib with bevacizumab treatment is being in investigated in a current ongoing clinical trial of NSCLC patients with EGFR-mutated disease which has shown to be a tolerable treatment with efficacy results to come [64]. The same group of researchers have also examined osimertinib and bevacizumab in combination to treat EGFR-mutant lung cancer that has metastasised to the bone *in vivo* [65]. The H1975 bone-metastasis NSCLC mouse model showed tumour regression after combination treatment as well as increased bone remodelling.

Furthermore, pharmaceutical company Eli Lilly Australia have ongoing trials testing osimertinib with ramucirumab (NCT02789345) and necitumumab (NCT02496663) reported by Mazza & Cappuzzo 2017 with results due in 2024 [66]. Disturbingly, resistance to osimertinib and other third-generation irreversible EGFR inhibitors has already been observed. One resistance mechanism has been found to be a mutation in exon 20 of EGFR (C797S) which results in osimertinib being unable to bind to EGFR [66]. Xing *et al.* 2019 investigated the clinical outcomes of the resistance mechanisms of osimertinib and examined the mutations that

are the cause of such resistance [67]. Reflecting the vast amount of literature on NSCLC mutations, EGFR mutations were the highest at 25% followed by MET, Tp53, KRAS, RET, ERB2 and RB1 mutations at 16%, 8%, 4%, 4% and 6.25%. An interesting finding was that transformation to SCLC was associated with the acquired RB1 mutation. Other noteworthy results were that the ERBB2 mutations were only seen in patients that harboured the EGFR-L858R mutation and that 60 patients lost the EGFR-T790M at disease progression while 36 did not. Overall the PFS was significantly longer in patients with acquired EGFR-C797S mutation in comparison to patients with MET amplifications [67]. Interestingly 30% of patients at disease progression had no resistance mechanisms that have been discovered, which reveals the need for further research in this area.

The previously mentioned company Eli Lilly gained an immunotherapy Pegilodecakin (pegulated IL-10, LY3500518) which aims to stimulate the immune system and thus increase tumour attacking T cells. In a phase II clinical trial the company tested this treatment alone and in combination with chemotherapy and the PD-1 check point inhibitor pembrolizumab in NSCLC and renal cancer with results expected November this year [68]. However, in 2019 Eli Lilly conducted a phase III clinical trial in patients with Metastatic Pancreatic cancer using pegilodecakin combined with FOLFOX (folinic acid, 5FU, oxaliplatin) compared to FOLFOX only but this clinical trial did not meet the primary endpoint of overall survival [69].

Currently, other new third-generation EGFR-TKIs are being now being developed in the clinic Olmutinib (HM61713), Nazartinib (EGF816) and Mavelertinib (PF-06747775), with their safety and efficacy being tested [70-73].

1.3.2 Therapies targeting tumours with ALK gene rearrangements and problems with resistance.

The ALK gene was first discovered in 1994 [74]. In 2007, after the screening of many NSCLC tumours, ALK was found to be fused to echinoderm microtubule-associated protein-like protein 4 (EML4) [74]. This rearranged EML4-ALK fused oncogene was shown to stimulate cell proliferation and cancerous growth [74]. In a recent phase III clinical trial, patients who have this rearranged ALK positive lung cancer responded better to the ALK tyrosine kinases inhibitor drug crizotinib, compared to conventional chemotherapy [75]. Crizotinib, which also inhibits MET and ROS tyrosine kinases, has proven to be superior to the earlier second line chemotherapeutics, docetaxel and/or pemetrexed, in patients who have previously been treated

with first line inhibitors/drugs. Shaw *et al*. 2013 showed progression free survival of 7.7 months compared to 3 months for crizotinib and chemotherapy, respectively. Targeting cells and NSCLC patients that carry EGFR rearrangement, or ALK rearranged loci/mutations usually develop resistance to crizotinib, as discussed below [3].

Problems with ALK therapy resistance. Resistance to the TKI inhibitor crizotinib the first ALK TKI (tyrosine kinase inhibitor) has been widely investigated, the mechanisms include mutations in the ALK domain, alterations of ALK copy number [77] and the ability of tumour cells to activate alternate signalling molecules to bypass inhibition [78].

Recently, multiple second generation ALK inhibitors functioning as first line therapies and crizotinib resistance therapies are currently applied in the clinic [75]. Ceritinib is an ALK inhibitor, and was the first of its kind to gain approval for treatment of ALK rearranged and crizotinib-resistant NSCLC. Soria *et al*. 2017 conducted a phase III trial using first-line ceritinib versus platinum-based chemotherapy in NSCLC patients carrying the ALK rearrangement. These showed promising results with progression free survival of 16.6 months versus 8.1 months respectively [79]. More recently, Camidge *et al.* 2018 investigated Brigatinib a next generation ALK inhibitor in NSCLC patients with the ALK-mutation compared to crizitonib and observed a significantly increased PFS of 67% vs 43% respectively [80].

While the results from clinical trials for the ALK gene targeting are encouraging, the numbers of NSCLC patients who harbour ALK or EGFR mutations or are only 13% and 14.5% respectively [3, 75]. The majority of patients are still treated with first line chemotherapy regimen [81].

1.3.3 KRAS mutations as targets for NSCLC and problems with targeted KRAS therapy

KRAS has a complex signalling network with pathways that regulate cell growth, ability to survive, movement, differentiation, angiogenesis and apoptosis [82]. There have been attempts to inhibit the trafficking [83] and localisation [84] of KRAS, and to target the downstream effects of oncogenic KRAS by inhibiting the PI3K/AKT/mTOR pathway which is stimulated in cancer and supports tumour growth [85]. A mutation in the KRAS gene, which occurs in 25.5% of adenocarcinoma NSCLC patients, results in the constant stimulation of the RAS/MAPK (mitogen-activated protein kinase) pathway [86]. The KRAS mutation is often correlated with a tumour being resistant to most available systemic therapies [87]. It is an appealing target for new NSCLC therapies [88] but, despite efforts to develop drugs to

specifically target KRAS, none have been proven effective [89]. Mutations in the KRAS protein confers resistance to erlotinib and gefitinib and have resulted in poor prognosis (as discussed below). Many of the drugs designed to block KRAS, in the main, have not been as promising in the clinic as expected [90].

Treatments and problems with resistance. Treatments include farnesyltransferase inhibitors (FTIs), RAS farnesyl cysteine mimetic drugs (e.g. salirasib) and PI3K inhibitors, respectively [85]. Riley *et al*. 2007 were the first to conduct a trial examining a treatment targeted specifically for positive KRAS-mutant NSCLC patients, using salirasib [91]. This drug targets the removal of KRAS from its membrane-anchoring sites and avoid triggering activation of the signalling cascades [84]. However, this phase II trial showed moderate toxicity and no clinical benefit for the patients involved [91]. KRAS and its association with TKI resistance has been investigated, in 2016 Chabon *et al*. recruited patients who had been treated with a third-generation EGFR inhibitor, rociletinib, 46% of whom showed resistance mechanisms and a few of these have also acquired active mutations in KRAS [92]. Gatalica *et al.* 2015 reported more than half of the NSCLC patients presented with KRAS mutations at the time of resistance to crizotinib or ceritinib, ALK-TKIs [93]. More recently, as previously mentioned, Brigatinib has been successful in overcoming crizotinib resistance, although that needs to be tested in NSCLC patient harbouring the KRAS mutation [80]. From these findings it is evident that targeting KRAS is a complex task. One possible strategy is a combinatorial approach to target several different driver mutations at once, with the use of newly developed SHP2 inhibitors that is currently being investigated [89, 94, 95].

1.3.4 Anti-angiogenic drugs and resistance

Vascularisation is a key requirement for a tumour to grow and stay nourished once it has been established. Angiogenesis, the formation of new blood vessels, is regulated by signalling pathways involving cytokines and several growth factors [96]. Monoclonal antibodies, which act as angiogenesis inhibitors, have been developed to block the growth of new blood vessels. Previously mentioned mAb, bevacizumab (commercially known as Avastin) was the first anti-angiogenic drug on the market and targets the vascular endothelial growth factor (VEGF), a protein that is important in the development of new blood vessels. The blockade of VEGF results in the loss of, or decrease in, blood vessel development that leads to nutrient starvation, followed by cell death within the tumour [97]. Avastin was first approved in 2006 as a first-line treatment in combination with carboplatin/paclitaxel for people with advanced non-squamous NSCLC [98]. However, recently, Avastin based treatment has become less efficient due to

increasing prevalence of drug resistance. This initiated the development of new, alternative drugs to specifically target resistant cells [99-101]. After a successful phase III study which showed its ability to inhibit VEGF when in combination with chemotherapy compared with chemotherapy alone [101]. In 2017 Masuda *et al*. demonstrated that bevacizumab could counteract VEGF-dependent resistance to a NSCLC xenograft model with the EGFR mutation [100]. The findings showed that after tumour shrinkage with erlotinib alone regrowth occurred after long term administration. However, with the bevacizumab and erlotinib combination, regrowth of tumours was successfully inhibited [100]. More recently, Saito *et al*. 2019 tested the erlotinib/bevacizumab combination in patients with advanced NSCLC resulting in improved PFS when compared to erlotinib alone [102].

1.3.5 Therapies targeting tumours with other mutations

Currently, there are a number of alternative signalling pathways that are being targeted for cancer therapeutic treatments including, Herceptin 2 (HER2), BRAF and Hedgehog (Hh) [103]. A clinical trial MyPathway (NCT02091141), run by Hainsworth *et al*. (2017), focuses on these alternative targets [104]. This study has recruited NSCLC patients with tumours types that harbour one of these mutations or alterations [104]. Patients carrying HER2 mutations are being treated with standard doses of the combination of pertuzumab and trastuzumab. Patients with BRAF mutated genotypes are treated with vemurafenib while patients that harbour mutation in Hh are given vismodegib. Trial completion is due for late September 2020 with results to be published 2021.

Early attempts to treat NSCLC patients with RET mutations including carbozantinib and vandetanib have been unsuccessful in clinical trials [105, 106]. Recently, Drilon *et al.* 2020 conducted a Phase I/II clinical trial (LIBRETTO) testing the RET inhibitor, Selpercatinib, in RET-fusion positive NSCLC patients [107]. The researchers reported an objective response rate (ORR) of 85% vs 65% in previously untreated patients vs those previously treated with platinum-based chemotherapy respectively. Notably, in patients with brain metastasis ORR was 91%, proving it a promising therapy for patients with such disease [108].

Overall, targeted therapies are now crucial in the treatment of NSCLC patients. As tumours and the mutations they possess are ever evolving, so will this line of treatment.

1.4 Immunotherapy and targeting NSCLC patients

1.4.1 Overview of immunotherapy:

In the past decade, immunotherapy has made significant advances in the treatment of cancers through an increase in general knowledge of the immune system and the better understanding of anti-tumour immune responses [109]. The use of mAbs and non-specific immunotherapies have shown varied results [110]. However, there are still several problems which need to be overcome and require further investigation.

The molecular properties of the cancer cell are important when it comes to disease progression. However, equally important is the focus on how the cancer cells interact with their tumour environment, and especially with the immune system [111]. Ligands and receptors are key determinants of these interactions [112].

The immune system acts as a protective barrier for potential pathogens. The other major role it plays is to detect and remove abnormal cells, including cancer cells [113]. The immune response is highly regulated to prevent harm to healthy tissue, checkpoint pathways. However, cancer cells have adapted to bypass the immune checkpoint pathways [114]. There are two critical immune checkpoint pathways, the cytotoxic T-lymphocyte-associated antigen-4 (CTLA-4) and programmed cell death protein (PD-1) which both control immune responses driven by T-cells. Cancer cells have evolved to evade these checkpoints.

CTLA-4 is thought to operate in the first stages of the immune response, primarily to be a negative regulator of T cells, reducing their responses to self-antigens to avoid autoimmunity. The difference between CTLA-4 and PD-1 is that the latter operates in the final stages of the immune response to facilitate immune resistance within the microenvironment of the tumour and stop ongoing immune activity occurring in the tissues, which includes signalling to coordinate the maintenance of lymphocytes and self-tolerance [113, 115].

Historically, NSCLC was not considered to be an immunogenic disease, based on failure of NSCLC patients to respond to agents such as interleukin 2 (IL-2). This belief is not the case as more advanced novel immunotherapies have been shown to be significant tools in the advancement NSCLC management. Recently, several novel immune-based therapies have been approved as second- and third line treatments for the previously non-treatable advanced NSCLCs [116-121]. However, current use of immune-based therapies, although proving to be extremely effective in some instances, is only used in advanced NSCLC cases as an adjuvant therapy. Overall, the use of immunotherapy for the treatment of NSCLC offers great hope for people afflicted with this disease [4, 122].

Immunotherapies can be both non-specific and specific which is explained in detail in the following sections.

1.4.2 Non-specific Immunotherapies

Just as antibodies work to aid the immune system in killing cancer cells, there are non-specific immunotherapies which act in a similar manner. Some of these are given as standalone treatments and others have been given in combination with chemotherapies or radiation therapy. Interferons (IFN) are a class of cytokines that can act on both tumour and immune cells, defend the body against disease and have been shown to aid in slowing cancer cell proliferation [123]. In high doses, IFN-alpha stimulates the host's immune system with a strong response seen from a small subset of melanoma patients who had an increase in disease-free survival. However, high levels of toxicity were also observed [124].

Interleukins (IL), including IL2, stimulate the host's anti-tumour immune response. However, systemic IL2 treatment has resulted in severe toxicity [125] and systemic inflammation [126]. IL12 is an important cytokine that controls particular immune responses against cancer cells [127]. Several clinical trials using plasmids loaded with IL-12 have been conducted. In 2008 Daud *et al*. conducted a phase I trial looking at patients with metastatic melanoma and showed 10% presented with full regression after treatment and 42% showed disease stabilisation or partial response [128]. A current clinical trial is testing the checkpoint drug, nivolumab with a newly developed immune stimulation drug, ALY-803, a complex of IL-15 [122]. The trials initial results confirmed safety of this combination as patients were treated via escalating dose concentrations for 6 months, with side effects in most cases being injection site reactions and flu like symptoms, at 90% and 71% respectively.

Recently, Athie *et al*. 2020 reported the discovery of a new long non-coding RNA molecule, (lncRNA) ALAL-1, which acts as a regulator in lung cancer to help cancer cells evade the immune system [129]. . The molecule reduces proinflammatory signalling molecules deterring the congregation of immune cells that could otherwise kill the cancer cells, and thus could be used in future to improve other immunotherapies, although further research is needed [130].

1.4.3 Monoclonal Antibodies targeting the immune system

A growing number of mAbs have been developed to target the immune checkpoints (the regulators of immune activation), for example PD-1, in order to block their inhibitory receptors and stop the growth of cancer [131]. These checkpoint inhibitors include the previously mentioned Nivolumab which has had promising results in both squamous and non-squamous

NSCLC when compared to the chemotherapeutic docetaxel. Brahmer *et al.* 2015 reported that patients with squamous NSCLC had a response rate of 20% to Nivolumab which was greater than the response rate of 9% for docetaxel, and progression free survival 3.5 months and 2.8 months respectively. However, this outcome revealed that 80% of patients had no response to Nivolumab [132]. This was also reflected in a more recent clinical in 2018 where Conolly et al. treated 33 NSCLC patients with Nivolumab, of which 79% of these had progressive disease after treatment and 16% also encountered toxicity [133].

Ipilimumab is a mAb that targets the protein receptor CTLA-4, which is known to downregulate the immune system [134]. CTLs recognize and destroys cancer cells, however this can be stopped by the cancer cells inhibitory mechanisms. Ipilimumab turns off the cancer cell's self-defence 'inhibitory' mechanism, and this drug (mAb) has been tested in a clinical trial for the treatment of NSCLC [135]. Tomasini *et al*. 2011 reported progression-free survival (PFS) of 5.68 months versus 4.63 months using ipilimumab compared to chemotherapy alone, respectively [136].

More recently, Hellman *et al.* 2019 investigated nivolumab and ipilimumab in advanced NSCLC patients with PD-L1 expression and found the combined therapy was more effective than nivolumab alone with overall survival of 17.1 months vs 14.9 months respectively [137]. Over two years this measured to be 40 vs 32.8 months respectively, revealing the combination therapy as a promising treatment over monotherapy going forward.

In a phase II/III study anti-PD1 Pembrolizumab in combination with chemotherapy, resulted in an extra 4 months overall survival, compared to chemotherapy alone [138]. Monoclonal antibodies that are directed against the PD-1 ligand, including atezolizumab, avelumab and the previously mentioned durvalumab have all entered the clinic. Herbst *et al*. 2013 engineered the MPDL3280A mAb (Atezolizumab) and conducted a study to investigate the function, biomarkers and how safe it was to inhibit PD-L1 [139]. It was found that patients with PD-L1 positive tumours had an ORR of 39% and progressive disease rate (PDR) of 12%, while in patients with PD-L1 negative tumours the ORR and PDR were 13% and 59% respectively proving it a relatively effective treatment. In 2017, Rittmeyer *et al*. conducted a phase III clinical trial testing atezolizumab compared to docetaxel, reported findings of how the median survival time (MST) improved by 13.8 months and 9.6 months respectively [140]. More recently, Yang *et al.* 2019 reported findings of the phase Ib clinical trial testing an anti-PD1 antibody sintilimab in combination with pemetrexed and platinum chemotherapy in non-

squamous NSCLC which showed promising efficacy [141]. This treatment was further investigated in a phase III trial (ORIET11) where there was a significant increase in PFS in the sintilimab-combination group than the placebo-combination group at 8.9 verses 5 months respectively with acceptable safety [142].

1.4.4 Therapeutic Vaccines – immunotherapeutic targeting NSCLC

Cancer vaccines can be either preventative or therapeutic vaccines. Prominent preventative vaccines include the Human Papilloma virus, which is known to cause cervical cancer, and the Hepatitis B vaccine, which prevents liver cancer. Conversely, cancer treatment vaccines are a type of immunotherapy that are prescribed to patients who already have cancer and work to improve the body's biological resistance and capability to fight cancer cells.

The vaccines for NSCLC that are currently in clinical trials focus on targeting antigens, such as MAGE-3 which target proteins found in 42% of lung cancers [143]. MAGE-A3 is a tumour-associated cancer-testis antigen that is differentially expressed in NSCLCs and has been used in several clinical trials as an immunotherapy and safety has been favourable. However, results showed no difference in patient overall survival in treatment versus placebo groups, as reported by Vansteenkiste *et al*. in 2016 [144]. In 2018 a phase II clinical trial run by the H. Lee Moffitt Cancer Center and Research Institute, investigated the safety and immunogenicity of a vaccine made with recombinant MAGE-A3 protein combined with an immunological adjuvant AS15 (recMAGE-A3+AS15) with or without the immunostimulant, poly-ICLC in melanoma patients. However, this treatment was deemed to be ineffective and the study has been terminated [145].

Other clinical trials involves the use of Epidermal Growth Factor (EGF) vaccine which induces Abs against the EGF receptor [146]. EGFR is overexpressed in many NSCLC patients and the human recombinant CIMAvax-EGF vaccine can target and block the receptor which will prevent proliferation of the tumour cells.

Earlier this year, Popa *et al.* 2020 reported findings of a phase III trial testing the CIMAvax-EGF vaccine in NSCLC patients with stage IIIB/IV disease. The vaccine was found to induce an EGF-specific immunological response in treated patients which was associated with clinical benefit [147].

1.4.5 Immune cell modulation

Another form of immunotherapy involves removing a person's T-cells, altering them in the laboratory to have specific proteins or receptors that are then re-introduced into the patient in the aim that they will then have the ability to target and destroy cancer cells. This type of therapy is called chimeric antigen receptor (CAR) T-cell therapy.

Li *et al*. 2018 engineered human T-cells so that they expressed EGFR-CAR to be targeted to NSCLC tumour cells and the treatment has seen positive results both *in vitro* and *in vivo* with anticancer efficacy and tumour regression demonstrated respectively [148].

Another clinical trial in the United States, has recruited patients whose tumours have tested positive for the protein NY-ESO-1[149]. A subset of T-cells is taken from the patient and the T-cells are exposed to Ny-ESO-1 in cell culture. The treated T-cells are re-introduced into the patient and these T-cells recognise tumour cells expressing NY-ESO-1. The results from this clinical trial will be released in 2021 [149]. Clinical trials in the early stages have also focused on targeting CD19 as it is an antigen that is expressed on many B-cells, however not on other cells which minimises the risk of "on target-off tumour" toxicity [115].

Immunotherapy treatments are a promising option for treating NSCLC patients and will likely end up being used as first line or a concurrent treatment in order to have the greatest effect.

1.5 Overview of siRNA targeting and its current use in NSCLC treatments

RNA Interference (RNAi) or Post-Transcriptional Gene Silencing (PTGS) is a biological process discovered by the Nobel Prize winning Fire and Mello [150]. Double stranded RNA is processed into siRNA by Drosha and Dicer where they are then loaded into the RNA-induced silencing complex (RISC), thus becoming unwound into short RNA molecules which inhibit the expression and translation of genes by silencing specifically targeted mRNA molecules. While there are naturally occurring siRNAs within the body, synthetic siRNA can be manufactured and are currently been used in scientific research with several siRNA-based therapeutic clinical trials focusing on cancer treatment [151-153]. Short hairpin RNA (shRNA) is an artificial RNA molecule with a tight hairpin turn that can induce long-term silencing of target gene expression via RNAi [154].

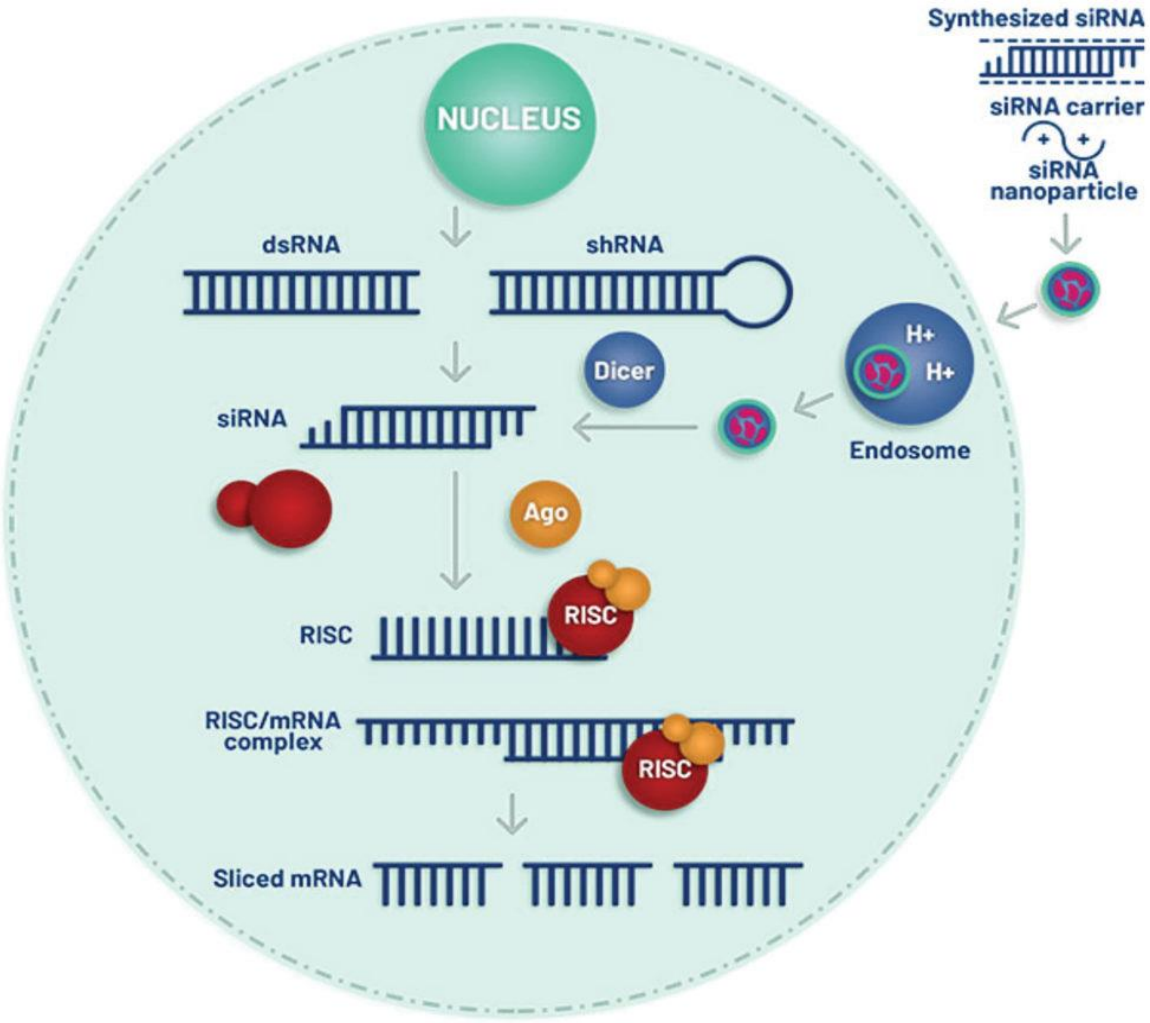

Figure 1.2 Schematic representation of RNA interference by siRNA

RNA Interference is a biological process where siRNA via a nanoparticle enter the cytoplasm of a cell and are loaded into the RNA-induced silencing complex (RISC).The siRNA becomes unwound into small RNA molecules via Argonaute 2 in the RISC complex which inhibit the expression and translation of genes by silencing specifically targeted messenger RNA molecules [155].

1.5.1 NSCLC siRNA targets.

Molecular profiling has revealed mutations in 50% of NSCLC patients which shows the immense heterogeneity of the disease. Molecular targets for siRNA specifically include genes that control and regulate tumour activity, including EGFR, ALK, ROS1, HER2, BRAF, RET and Kirsten rat sarcoma viral (KRAS) [156], as well as TP53 [157], VEGF [158], survivin [159] and the matrix metalloproteinases [160]. Attempts to achieve knockdown of one or several of these genes simultaneously in order to inhibit cell proliferation, migration and invasion, and stop angiogenesis in cancer is under investigation [161].

1.5.1.1 KRAS

The mutation of the KRAS oncogene is one of the most prevalent in NSCLC, and as previously discussed is often the hardest to treat as it correlates with the highest rate of resistance [88]. A new approach to address this is to inhibit ALK/ROS1 and MET concurrently, which was investigated by Jänne *et al*. 2016 using the irreversible EGFR inhibitor dacomitinib in combination with the MET/ALK/ROS1 receptor tyrosine kinase inhibitor crizotinib. However, they were unable to show any significant anti-tumour activity and there was a high degree of toxicity [56].

At protein and mRNA levels siRNA can downregulate mutant KRAS [162] Golan *et al*. 2015 conducted a clinical trial using an RNAi-based anti-mutated KRAS treatment in pancreatic cancer [163]. The Local Drug EluteR (LODER^{TM}) is a drug delivery platform developed by Silenseed Ltd. to insert RNAi therapies contained within a "specialised bio-polymeric scaffold" to the core of solid tumours [164]. Using the LODER^{TM} technology, Golan *et al*. 2015 treated patients with an siRNA drug developed against KRAS (siG12D-LODER^{TM}) followed by Gemcitabine [163]. This combination was found to be well tolerated by the patients. In 70% of the treated patients, this combined treatment demonstrated potential efficacy resulting in a decrease in the tumour marker CA19-9 [163].

Perepelyuk *et al*. 2017, developed a novel delivery system for anti-mutant KRAS treatment for NSCLC (AKSLHN) [162]. They used a nanoparticle carrier aimed to effectively deliver siRNA to the tumour in a mouse model. In this model, mice were treated with monotherapy as well as in combination with Erlotinib. Toxicity levels were low and tumour burden in the AKSLHN alone group showed regression over 4 weeks of treatment, whilst the combination group showed no sensitivity *in vivo* [162]. These results reveal that AKSLHN may be a possible treatment for mutant KRAS expressing NSCLC in the future. Xue *et al.* 2014 showed effective nanoparticle delivery of siRNA targeting KRAS (siKRAS) resulting in reduced expression of the gene as

well as MAPK signalling *in vitro*, with increased apoptosis and a reduction in the growth of tumours *in vivo* [165]. More recently, Mehta *et al.* 2019 used bovine serum albumin (BSA) nanoparticles on A549 cells *in vitro* to successfully deliver siRNA-KRAS specifically targeting the G12S mutation [166]. However, these BSA nanoparticles are yet to be tested for safety or efficacy in an animal model.

Cyclin-dependent kinase-4 (CDK4) downregulation and its interaction with KRAS Mutant NSCLC was investigated by Mao *et al*. 2014. Using micellar nanoparticles, they delivered siRNA targeting CDK4 (MNP_{siCDK4}) in the A549 NSCLC xenograft model and showed inhibition of growth [165, 167, 168].

1.5.1.2 Polo like kinase-1 (PLK1)

PLK1 is crucial for cell division, promotes mitotic entry and regulates mitotic progression, thus it is highly significant in tumour progression and has been proven as a valid target in cancer [169]. PLK1 inhibitors have been developed such as rigosertib [170] and volasertib [171]. A phase III clinical trial conducted by O'Neil *et al*. 2015 tested rigosertib in combination with gemcitabine for patients with metastatic pancreatic cancer. However, there was no improvement found in patients receiving this treatment versus gemcitabine as a monotherapy [172]. Ellis *et al*. 2015 conducted a phase II trial with advanced NSCLC patients testing volasertib as a monotherapy and in combination with pemetrexed. While toxicity was not increased there was no significant increase in efficacy compared to chemotherapy alone [173]. De Martino *et al.* 2018 explored the use of a PI3K inhibitor in combination with volasertib where a synergistic effect between the two was found *in vivo* while treating an immunocompetent allograft T4888M ATC model and tumour growth was successfully inhibited [174]. Most recently, Affatato *et al.* 2020 investigated another PLK1 inhibitor, onvansertib in combination with paclitaxel in a mucinous ovarian xenograft model MCAS, which caused greater tumour regression than treatments delivered alone [175]. While these results are somewhat promising they are yet to be tested in a NSCLC mouse model.

Inhibitors to PLK1 in NSCLC, including rigosertib and volasertib, have overall been disappointing in the clinic, and thus more recent studies have investigated the use of siRNA as treatment to target this gene in lung cancer [176]. *PLK*1 has been proven to be overexpressed in NSCLC [177]. McCarrol *et al*. 2015 targeted PLK1 and delivered siRNA-PLK1 to a NSCLC orthotopic mouse model (H1299) and decreased tumour growth [176]. Greco *et al*. 2016 used

PLK1-1 siRNA loaded in exosomes delivered to bladder cancer cell lines and were able to knockdown the gene *in vitro* [178].

The p53 tumour suppressor gene is often mutated in NSCLC, usually in the DNA binding region of the gene [179]. Siebring-van Olst *et al*. 2017 conducted a genome wide siRNA screen of human NSCLC cells to assess regulators for p53 and found 10 genes that were validated as p53 inhibitors which could be new potential targets for siRNA treatment [157]. The gene is usually inactivated in 50% of cancer which causes its tumour suppressor function to be lost [180]. It has been found that p53 is negatively regulated by PLK1 which as discussed is often overexpressed in NSCLC, making it an appealing target for treatment [181].

As mentioned, expression of PLK1 has been found in many cancer cells [182, 183], and currently siRNA therapeutics are being developed to target this gene in a range of cancers. Demeure *et al*. 2016 describe TKM-080301, a lipid nanoparticle formulated with siRNA targeting against PLK1 in Adrenocortical cancer (ACC) [184]. Their phase I/II study run by Tekmira Pharmaceuticals focused on 16 ACC patients with refractory disease. Results were encouraging with anti-tumour efficacy being observed, 1 patient with a 13% reduction of tumour diameter [184].

There have also been attempts to use a combination of siRNAs to target 3 oncogenes involved in cell proliferation and angiogenesis simultaneously, human double minute-2 protein (HDM2), c-myc and VEGF using a lipid/calcium/phosphate nanoparticle in an NSCLC mouse xenograft model (A549) and were able to achieve reduction of tumour growth [161].

1.5.1.3 Kinesin Spindle Protein (KSP)

KSP plays an important role in mitosis, during spindle formation and chromosome division. Hu, Wang & Zhang *et al.* 2016 conducted *in vitro* studies using siRNA to target VEGF and KSP in A549 (NSCLC) cells. In this study, MTT assays were used to measure cell proliferation and quantitative polymerase chain reaction (qPCR) to measure gene expression. After transfecting cells with siRNAs there was a decrease in cell proliferation. Inhibition of cell proliferation was greater when cells were transfected with a combination of siRNAs, in comparison to transfections with single siRNAs [185]. There have been attempts to silence these genes in other types of cancers by Alnylam Pharmaceuticals. The pharmaceutical company developed an RNAi therapeutic ALN-VSP02 to treat liver cancer: a lipid nanoparticle-formulated with siRNAs targeted to VEGF-A and KSP. The phase I trial (2012) showed preliminary activity against several types of cancer, however, the safety levels and efficacy of the treatments were not acceptable [186]. More recently, Alnylam Pharmaceuticals

attempted a clinical trial with siPLK1 for solid tumours where the siRNA was delivered by liposomes. However, the particles accumulated in the liver and patients experienced abnormal liver function tests [151].

1.5.1.4 Ribonucleoside reductase subunit M1 (RRM1)

RRM1 and Ribonucleoside reductase subunit M2 (RRM2) are regulatory components of ribonucleotide-diphosphate reductase that regulate cell proliferation, suppression of cell migration, tumour metastasis, and synthesise the deoxyribonucleotides for DNA synthesis [187, 188]. RRM1 & RRM2 have been proven to be overexpressed in many cancers and increased expression is often is related to resistance to chemotherapy [188, 189]. Gemcitabine is used as a treatment for NSCLC and RRM1 & RRM2 are involved in the metabolism of this drug [190]. In a study conducted by Souglakos *et al.* 2008 the expression of RRM1 and RRM2 was measured by real time qPCR (RT-qPCR) of primary tumours of untreated patients who were then treated with docetaxel/gemcitabine. 79% of patient tumours overexpressed RRM1 & RRM2. Those with low levels of RRM1 and RRM2 had a significant response from treatment ($p<0.001$) and greater overall survival ($p=0.02$) respectively [190]. These results suggest that using siRNA to target RRM1 and/or RRM2 is a potential therapeutic to overcome drug resistance.

The receptor tyrosine kinase EphA2 has been seen as a desirable target as it is often overexpressed in many cancers [12]. siRNA-EphA2-DOPC is a drug that has been developed by the MD Anderson Cancer Clinic which once internalised can bind to EphA2 DNA and mRNA, causing disruption to transcription and translation and thus causing cell inhibition (Clinical Trial #NCT01591356). In the current phase I trial siRNA-EphA2-DOPC is being tested for safety in patients with advanced disease with results expected July 2021 [12].

In summary, the cell cycle proteins discussed are important in tumour growth and turning them off means that the cells get “stuck” and can’t progress to division, ultimately causing tumour growth inhibition. To advance the use of targeted siRNA in NSCLC, siRNA-PLK1 & siRNA-KSP were chosen as candidates for further stu dy in this project. The decision to use these specific siRNA targets was based on their importance in the literature findings, however equally important the decision was based on their efficacy in preliminary studies in the EnGeneIC laboratory. While siRNA therapies have developed significantly the main obstacle for each treatment is how to effectively deliver it to the tumour cells.

1.6 Problems with siRNA delivery

1.6.1 Naked siRNA delivery

One of the major downfalls of administering siRNA directly to patients is the potential for off-target effects which are often related to partial complementarily of the sense or antisense strands to an unintended target [191]. Challenges faced in the successful application of Naked siRNA for therapeutic purposes included poor cellular penetration, immunogenicity, degradation of RNAses in the blood stream, rapid renal clearance and aggregation in the blood [5, 192].

1.6.2 Nanoparticles for drug delivery

Over the last few decades, nanomedicine has become popular. Nanoparticle-based delivery systems are now a major part of cancer research. This type of therapy delivery is currently under investigation for NSCLC patients. Liposomes, micelles, lipid nanoparticles, protein-based particles and polymeric nanoparticles are all currently being developed [193]. The leaky vasculature of the tumour microenvironment allows molecules to enter via the Enhanced Permeation and Retention effect (EPR) so that they accumulate in the tumour [194]. Doxil® a liposome formulation of Doxorubicin, developed by Petros & DeSimone 2010, was one of the first generation nanoparticles to utilise the EPR effect [195]. However, the limitation of this kind of treatment was the lack of specificity for the cancer which resulted in severe side effects.

Xue *et al.* 2014, developed the 7C1 compound, made from polyethyleneimine which undergoes a chemical reaction with $C_{14}PEG_{2000}$ resulting in nanoparticle formation. The 7C1 nanoparticle has been well tolerated in mice [165]. They investigated the effect of the delivery of siLuciferase (siLuc) and miR-34 and found positive injection levels of miR-34 increased by 27-fold compared to the mice treated with siLuc [165]. Dong *et al***.** 2014 reported that delivery of a small layered Double Hydroxide (sLDH) – Liposome Composite System, which are approximately 200 nanometre (nm) in size, showed low toxicity effects when they were used to deliver DNA to a colon cancer cell line (HCT-116). This type of delivery was 3-times more efficient than the delivery of sLDH alone [196].

In 2016, Krivitsky, *et al*. developed a nanocarrier centred on animate poly alpha glutamate which interacts electrostatically with siRNA and thus forms a polyplex (siRNA + Polymer), which can protect the siRNA from RNAase degradation [197]. Polyak *et al*. 2017 reported that they delivered this polyplex to mice bearing ovarian or lung tumours and caused 38% and 33%

knockdown, respectively, of the targeted Rac1 gene, as well as formed a PLK1 targeted siPLK1-polyplex which caused 73% tumour regression *in vivo* [192].

Su *et al*. 2011 developed a lysine containing interfering nanoparticle (iNOP), for the systemic delivery of RNAi and loaded it with both miRNA and siRNA [198]. As previously mentioned McCarroll *et al*. 2015 utilised the iNOPs, loading them with siRNA targeted to the PLK1 gene [176]. The iNOP-7-PLK1 siRNA treatment showed a 50% decrease of whole lung bioluminescence with the *in vivo* orthotopic model of NSCLC. However, full tumour regression did not occur [176].

A hybrid nanoparticle (AKSLHN) was developed by Perepelyuk *et al*. 2017 and as previously discussed delivered anti-mutant KRAS to a mouse model of NSCLC in combination with erlotinib. However, no tumour regression was reported with this combination therapy [162]. As previously mentioned Mehta *et al.* 2019 used BSA-nanoparticles on A549 cells *in vitro* to successfully deliver siRNA-KRAS specifically targeting the G12S mutation, although this needs to be tested *in vivo* [166].

Recently, Elbatanony *et al.* 2020 have investigated the use of PLGA nanoparticles loaded with the TKI Afatinib in lung cancer [199]. Using A549 spheroids they were able to penetrate the tumour cells effectively and cause growth inhibition *in vitro* and thus this treatment will now be further investigated in a pre-clinical mouse model.

1.6.3 siRNA delivery via the EDV™ nanocell (EnGeneIC Dream Vector) ™

A nanoparticle delivery system that has demonstrated successful delivery of numerous cancer therapeutics including chemotherapies, siRNA and microRNA, while targeting tumours with a significant degree of specificity is the EnGeneIC Dream Vector™ (EDV™), developed by MacDiarmid *et al*. 2007 *(Fig. 1.3)* [168, 200-207]. The EDV™ is derived from a *min*CDE-chromosomal deletion mutant of *Salmonella enterica* serovar Typhimurium (S. Typhimurium). This mutation depresses polar sites of cell division, which enables the bacteria to divide at it pole in addition to normal cell division. This cellular fission at polar sites forms the EDV™ [168].

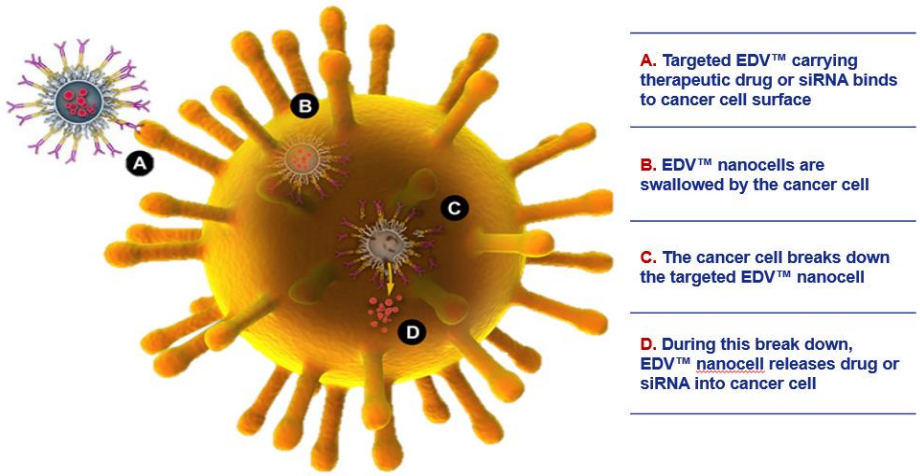

Figure 1.3 Schematic showing the efficacy of the EDV™ by targeting cancer cells via bispecific antibody interaction with cancer cell surface receptors. EDV™ is a lipid vehicle derived from bacteria used to carry drug therapy to tumour cells. Bispecific antibodies on the surface of the EDV™ binds to receptors on the cancer cell. The EDV™ is then incorporated into the cell via endocytosis, the EDV™ vesicle is rapidly broken down in the cancer cell releasing its drug (i.e. siRNA) contents into the cancer cell, resulting in specific cancer cell death (Schematic kindly provided by EnGeneIC Pty Ltd).

The EDV™ is a globally unique and versatile technology that combines targeted drug delivery and immune-oncology [202]. The unique and beneficial properties include the presence of a surface antibody that can target EDV™ nanocells by binding to specific molecules on cancer cells [168]. The EDV™ can also transport significantly larger therapeutic doses than other nanoparticles, which are released once it has been endocytosed by the cancer cell. EDV™ nanocells have been shown to deliver functional nucleic acids as well as drugs and therefore have the potential to combat drug resistance. MacDiarmid *et al*. 2009 successfully inhibited MDR1 expression *in vitro* and successfully reversed drug resistance in Doxorubicin resistant tumours in a mouse xenograft model when siRNA against MDR1 was delivered by targeted EDV™ nanocells, the result being significant tumour regression. EDV™ nanocells were also loaded with scrambled siRNA which did not elicit a response or cause any tumour regression. This emphasizes that non-specific siRNA effects were not significant and that targeting the tumour with the bispecific antibodies (bsAbs) was of the greatest importance [168].

Another distinctive feature of the EDV™ is the unprecedented quantity of toxic drug or functional nucleic acid (siRNA or microRNA) that can firstly be loaded into the nanocell and subsequently be delivered to the tumour site [206, 208]. Compared to other drug delivery

approaches the EDV^{TM} offers a significant improvement in the efficacy of drug delivery to patients [168, 209].

Glover *et al*. 2015 used EDV^{TM} nanocells loaded with microRNA-7 (miR-7) to target adrenocortical cancer *in vivo.* After10 doses of treatment significant tumour reduction was seen between mir-7 loaded EDV^{TM}s compared to the siRNA nonsense loaded EDV^{TM} treatment group. In vivo off target effected were also investigated, and while there was no increase of miR-7 expression in other organs, there was an increased expression of miR-7 in the xenografts. This alludes to minimal off target effects occurring from this delivery system, which can often be of concern with miRNA replacement therapy [210]. Reid *et al*. 2013 reported administration of EGFR targeted EDV^{TM} nanocells loaded with synthetic mimic microRNA 16 (mir-16) to a mesothelioma xenograft in nude mice. Previously they had found that the downregulation of miR-16 was 2-10 fold greater than in normal mesothelioma cells and with this treatment they were able to restore miR-16 levels, resulting in inhibition of tumour growth [208].

Furthermore, a phase I study showed successful delivery of therapeutic miR-16a via EDV^{TM} nanocells to end stage mesothelioma patients which showed promising results and was well tolerated in patients [204]. One patient in particular had a "complete metabolic response" to treatment, improved respiratory function as well as a partial response and decreased tumour volume were evident from a positron emission tomography (PET) scan *(Fig. 1.4).*

The high degree of safety the EDV^{TM} displays has been demonstrated in several clinical trials [203]. In a phase I safety trial with end-stage recurrent glioblastoma patients were treated with EGFR targeted EDV^{TM} nanocells loaded with doxorubicin and the treatment was well tolerated [201]. Clinically and commercially EDV^{TM} nanocells are beneficial as they have a long shelf life measured by up to 3 years (EnGeneIC Pty Ltd in-house data). Currently a phase I/IIa trial now enrolling patients at a major US research hospital to address a significant unmet medical need in recurrent glioma, with one patient treated with whose tumours have already shrunk [211]. In 2020, the immune modulatory effects of EDV^{TM} were also reported in mouse models and human cancer patients and were found to induce both the innate and adaptive immune responses resulting in antitumour effects [260].

In summary, unlike most nanoparticles currently being developed the EDV^{TM} is not just a delivery particle. It has biological activity in its own right hence immune stimulation, while all other particles are inert. EDV^{TM} can carry any payload, can be targeted and only extravasates into target tumour environment when other nanoparticles are too small and so disperse throughout the body causing side effects, especially liver toxicity [166, 198-205, 260].

All of the advantages described above make the EDV^{TM} a considerably appropriate and advantageous option for the delivery of siRNA and potentially overcoming drug resistance in NSCLC.

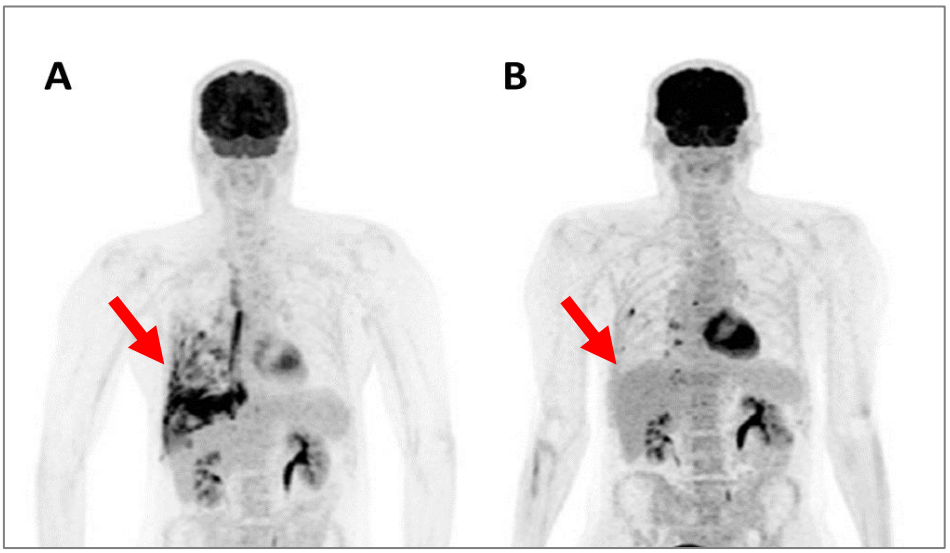

Figure 1.4. PET scans revealing tumour regression in a mesothelioma patient treated with EDV^{TM}s. CT scans of a mesothelioma patient **A)** before beginning EDV$^{TM}_{miRNA16a}$ treatment and **B)** after 8 weeks of treatment. Tumour regression was accompanied by improved functioning of the respiratory system (Kao *et al.* 2015)

1.7 Summary

In summary, first-line treatment for NSCLC is generally a combination of chemotherapy, radiation and/or surgery. Emerging therapies include targeting unique mutated gene products (proteins) and immunotherapy which involves utilising a patient's immune system to fight cancer. An important issue is that most patients are diagnosed with late stage disease with poor outcomes. Drug resistance emerges in most patients effecting more toxic treatments.

The therapeutic potential of using siRNAs in cancer is being actively studied for the purpose of switching off cancer driver genes, or genes that are involved in tumour growth, angiogenesis, metastasis and multi-drug resistance. While siRNA is a promising therapeutic approach [7-10] delivery of siRNAs to the cancer cell is challenging. Strategies utilising synthetic nanoparticles, as well as modifications of the nucleic acid to prevent degradation, have been developed, however with ambiguous results.

Recently, EDV^{TM} technology was used in a phase I clinical trial to successfully and safely deliver microRNA16a to patients with recurrent mesothelioma following at least 2 lines of

standard treatment [207]. These promising results set the baseline for siRNA treatment of other cancers that respond poorly to conventional treatments.

Recurrence, mainly due to multidrug resistance is the major cause of mortality in NSCLC patients. This project is designed to specifically address the urgent unmet needs of NSCLC patients who have little or no hope of effective treatment.

1.9 Significance of project

Over two million people worldwide suffer from lung cancer, the main sub-type (85%) being NSCLC. Despite many types of chemotherapy approved and readily available for NSCLC, only 2% of patients with NSCLC metastatic disease survive 5 years post diagnosis.

Previously, EnGeneIC discovered that small interfering RNA (siRNA) duplexes freely enter whole bacterially derived nanocells (EDV^{TM}s) and effect tumour stabilisation and regression in mouse xenograft models [168]. The targeted EDV^{TM} nanocell delivery of siRNA targeted to the multi-drug resistance gene, MDR1 reversed drug resistance in a uterine cancer model [168]. This study provides strong evidence that using siRNA as a therapy has potential in cancer therapy. In order to dramatically increase overall survival in patients with intractable lung cancers and to address the major problem of drug resistance, it may be useful to study if there is a synergistic effect when siRNA therapies are combined. Furthermore, targeted EDV™ have the potential to safely deliver functional nucleic acids to compromised patients and at the same time, eliciting an innate and adaptive immune response.

In this project, I will use targeted EDV^{TM}s in a model of drug resistance which is an intractable issue in NSCLC. This project has true translational potential. An important project objective is to also recognise if any of the EDV^{TM} siRNAs identified in this study have therapeutic potential for lung cancer and could be committed to phase I NSCLC clinical trials.

1.8 Hypothesis & Aims

Hypothesis: Specific siRNAs delivered directed to NSCLC using targeted EDV^{TM} nanocells have potential to overcome multiple drug resistance in NSCLC.

Overall Aim: The overall aim of this project is to use targeted EnGeneIC Dream Vector^{TM} (EDV^{TM}) nanocells carrying small interfering RNA (siRNA) molecules directed against the genes that regulate proteins essential to tumour cell survival and proliferation and to evaluate their ability to overcome the intractable multiple drug resistance in non- small cell lung cancer (NSCLC).

Specific aims:

1) Test the expression of and efficacy of siRNA targeting the genes *PLK*1, *RRM*1 & *KSP* in NSCLC cell lines.
    a) This aim will be achieved through cytotoxicity assays, PCR analysis, Western Blot and cell cycle analysis by flow cytometry
2) Test the efficacy of siRNA loaded into EDV^{TM} nanocells targeting the genes *PLK*1, *RRM*1 & *KSP* in NSCLC.
    a) To achieve this aim EDV^{TM}s will be loaded with siRNA and the siRNA copy numbers will be measured
    b) 3D spheroids of NSCLC cells will be treated with the EDV^{TM}s and tested for growth inhibition by cell viability assays and gene knockdown by PCR analysis.
3) Test the efficacy of siRNA loaded into EDV^{TM} nanoparticles *in vivo* using an established mouse xenograft model.

Chapter 2. Methodology

2.1 Design Rationale:

The first hypothesis of this study is that targeted EDV ^{TM} delivery of siRNAs targeting genes which are essential to division and cycling in cancer cells may provide a solution to drug resistance in NSCLC. EnGeneIC had previously developed an NSCLC cell line which is resistant to Doxorubicin (A549-Dox-R). The cell line was established in 2016; therefore, the drug resistant status of the experimental cell line was tested using a well-established cytotoxicity assay, the MTS (3-(4,5-Dimethylthiazol-2-yl)-2,5-diphenyltetrazolium bromide) based proliferation assay. The parental A549 NSCLC cell line and the other NSCLC cell lines were chosen for this study due to their successful transfection efficiency and ability to grown into spheroids. The MRC-5 non-cancerous lung fibroblast cell line was chosen as a negative control. The expression of cell cycle genes *PLK*1, *RRM*1 & *KSP* in NSCLC cell lines was measured using RT-qPCR and Western Blot. Efficacy of siRNAs targeting PLK1 (siPLK1), RRM1 (siRRM1) & KSP (siKSP) transfected into NSCLC cell lines was measured by the MTS proliferation assay and Western Blot. Flow cytometric analysis was used to measure apoptosis and cell cycle arrest in NSCLC cell lines transfected with the siRNAs targeting *PLK*1, *RRM*1 and *KSP*. EDV^{TM} nanocells were targeted to the epithelial growth factor receptor (EGFR) and the copy number of siRNAs loaded into the nanocells was measured by staining with an RNA specific dye and measured on a fluorometer compared to known standards. EDV^{TM}-siRNAs were used to treat NSCLC cells lines grown as 3D spheroids using the hanging drop plates (Perfecta3D®: HDP1096) and cell proliferation inhibition was assessed using trypan blue cell viability assay. The EDV^{TM}s-siRNAs were then tested *in vivo* using the A549-Dox-R a xenograft mouse model, tumours were excised and assessed for gene knockdown by RT-qPCR.

2.2 Methodology overview.

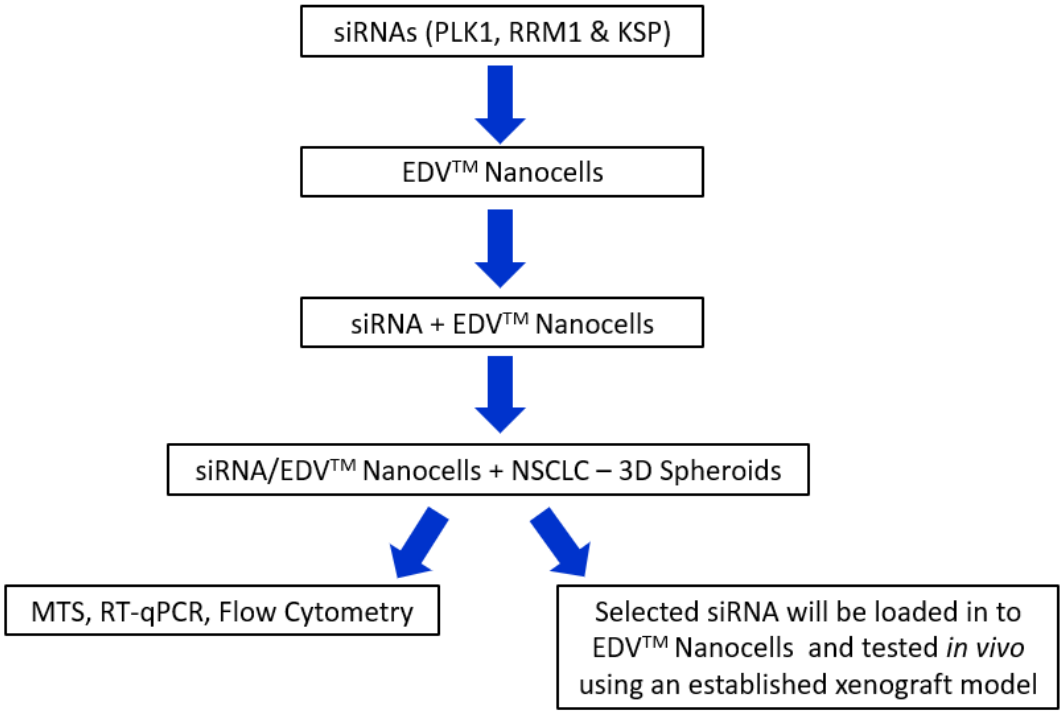

Figure 2.1 Overview of methodology. In brief, efficiency of selected siRNAs (PLK1, RRM1 and KSP) on gene and protein knockdown were verified by Flow Cytometry, Western Blot and MTS assay. EDV™s were loaded with siRNA and the effectiveness of siRNA-EDV™ treatment was tested in NSCLC 3D spheroid cultures and measured by cell viability assay, PCR and flow cytometry. SiRNA-EDV™ was tested using a xenograft mouse model.

2.2.1 Cell Culture

The following cell lines, used in several experiments, were cultured at 37^0C with 5% CO_2. The cell lines, and their growth medium were as follows:

A549 lung carcinoma (ATCC® CCL-185™) was purchased from American Type Culture Collection (ATCC) was grown in Dulbecco's Minimum Essential Medium (DMEM) (Sigma, Cat#D8437) + 10% fetal bovine serum (FBS) (Bovogen, Cat#14106SFBS).

A549-Dox-R Drug (Doxorubicin) Resistant lung carcinoma cell line developed by EnGeneIC from parental A549 lung carcinoma (ATCC® CCL-185™)) cell line was grown in DMEM + 10% FBS + 800ng/ml Doxorubicin (Sigma, Cat#25316-40-9)

H358 (ATCC® CRL-5807™), H2122 (ATCC® CRL-5985™), & HCC827 (ATCC® CRL-2868™) NSCLC cell lines were purchased from ATCC and were grown and maintained in ATCC formulated RPMI (Gibco, Cat#A10491) + 10% FBS.

H441 & H23 NSCLC cell lines were gifts from the Peter MacCallum Cancer Centre, and were grown and maintained in ATCC formulated RPMI (Sigma, Cat#R8758) + 10% FBS.

The MRC-5 (Cat #05090501) lung cell line was purchased from the European Collection of Authenticated Cell Cultures (ECACC) cell line was maintained in Eagles Minimum Essential Medium (with Earles Balanced salt solution and 1% non-essential amino acids) (EMEM (EBSS + NEAA)) (Sigma, Cat#M5650) + 2mM L-glutamine (Sigma, Cat#59202C) + 10% FBS.

2.2.2 Induction of Clinically Relevant Drug Resistance in A549 Cell Line

Drug dose was based on the IC50 previously determined in the EnGeneIC laboratories: Doxorubicin (IC50 – 250 nanomolar (nM)). A549 cells were grown to ~60-70% confluence in T25 flask and were initially grown in the presence of Dox. Media was replaced with fresh drug after 2-3 days. After 5 days, media was replaced with fresh media +10% serum and cells were left to recover normal growth pattern. Once growth pattern was resumed the Doxorubicin (Dox) IC50 was re-added to culture and cells were grown in the presence of drug for 5 days (fresh drug added every 2-3 days) and then left to recover in drug free media. When cells stopped dying in response to Dox, the Dox concentration was doubled, and the cycle treatments were continued until Dox concentration reached 800ng/ml and cells no longer died in response to this concentration. Cells were then cultured under constant Dox pressure (800ng/ml).

2.2.3 Cytotoxicity Assays

Cells were cultured to 80% confluence in T75 flasks with complete medium. Spent media was removed and cell monolayer washed with PBS (Sigma Cat#D8537) and 3mL of Trypsin-EDTA (Sigma Cat#T4174) was added to detach cells. Cells were then counted, using trypan blue (Sigma Cat#T8154), on an automated cell counter or haemocytometer. Cells (5000 cells per well) were then seeded in flat bottomed, clear, 96-well tissue culture treated plates, at the above indicated cell concentrations, in 100µL of complete medium. For each drug, 30 wells were seeded, which was enough for three replicate wells for the 'cells only controls', three replicate wells for each of the eight different drug concentrations and also three spare wells. Wells on the edge were filled with media alone and not used. Plates were incubated overnight at 37^0C with 5% CO_2.

Dilution series of each drug were made at twice the final drug concentrations in the range of 0.5-5000nM in each corresponding well. 100µL of each drug concentration was added to the existing 100µL of medium (containing cells) to make a 1:1 dilution of drug to media (carried out for each of the three replicate wells for all drugs and concentrations). 100µL of media alone was added to each of the "cells only control" wells. Plates were then incubated for a further 72 hours. Cytotoxicity assays were carried out in 3 biological replicates.

2.2.4 MTS viability assays and data analysis

Media containing cytotoxic drug was collected from all wells into a spent media bottle and discarded into the cytotoxic waste container. CellTiter 96® AQueous MTS Reagent Powder (Promega, Cat# G1112) was diluted 1:6 in complete media, was added to each well. MTS diluted 1:6 in complete media was also added to six wells that contained no cells. These formed the "blank control" wells. Cells were incubated at 37°C in the dark until the "cells only control" wells turned dark brown. The absorbance of all plates was read at 490nm using a plate reader and the MTS protocol on KC junior. Cell viability for each treatment was then calculated against the cells only control. These percentages were then plotted against the nM drug concentrations using GraphPad Prism 8 software and half-maximal inhibitory concentrations (IC50) were calculated off the curve on the graph.

2.2.5 Measuring expression of PLK1, KSP and RRM1 in NSCLC cell lines

2.2.5.1 RNA Extraction – to purify total RNA from cultured cells.

Cells were seeded in T75 flasks, cell lines included were A549, A549-Dox-R, H358, H2122, H441 and H23. The cell monolayer was washed with PBS and cells were trypsinised for 4 minutes. When cells had lifted, the reaction was neutralised with 7mL media. Cells were centrifuged for 5 minutes and then counted using an EVE automated cell counter. The cell pellet was resuspended in 1mL of medium and a volume corresponding to $5x10^5$ cells was removed for each sample. Cells were washed once in PBS and collected by centrifugation at 300g for 5 minutes. RNA was extracted from cell lines using ISOLATE II RNA Mini Kit (Bioline, Cat#BIO52073) using the manufacturer's instructions.

2.2.5.2 cDNA reaction: synthesise first-strand cDNA.

cDNA was synthesised using the SuperScript® VILO™ cDNA Synthesis Kit (Thermo Fisher Scientific, Cat#11754050). Each reaction combined 4uL of 5X VILO™ Reaction Mix, 2uL 10X SuperScript™ Enzyme Mix, 20uL of DEPC-treated water with the required uL amount of RNA for 20ng. Tube contents were gently mixed, and a quick centrifugation was performed to collect all mixture at the bottom of the tubes. Samples were incubated in the PCR machine using the following thermal profile; 25°C for 10 minutes, 42°C for 60 minutes, 85°C for 5 minutes and then the reaction was terminated, and samples held at 4oC. cDNA was then diluted prior to qPCR.

2.2.5.3 RT-qPCR.

A master mix was prepared with 6pmol/µl forward and reverse primers, 5uL SYBR green mix 2x Concentration (Sigma, Cat# FSUSGMMRO) and 3uL DEPC dH2O (ThermoFisher, Cat#750023). 9uL of master mix was aliquoted into each well. 1uL (10ng) of the cDNA prepared solution was added to its required well of a PCR plate. The cycling conditions were 50ºC for 2mins, 95ºC for 10min, followed by 40 cycles of denaturation (95ºC, for 15sec) and annealing and extension (58ºC for 30sec). RT-qPCR was carried out using 7500 Software v2.3 and analysed using DataAssistTM v3.01 [212].

Table 2.1 Sequence of Primers

Primers	**Sequence 5'->3'**	**Reference**
PLK1-F	GGCAACCTTTTCCTGAATGA	[213]
PLK1-R	AATGGACCACACATCCACCT	[213]
RRMI-F	CGCTAGAGCGGTCTTATTTGTT	[214]
RRMI-R	TTGCTGCATCAATGTCTTCTTT	[214]
KSP-F	CATCCAGGTGGTGGTGAGAT	[215]
KSP-R	TATTGAATGGGCGCTAGCTT	[215]
HGAPDH-F	AGATCCCTCCAAAATCAAGTGG	[216]
HGAPDH-R	GGCAGAGATGATGACCCTTTT	[216]

2.2.6 siRNA Transfections of NSCLC cell lines with siPLK, siRRM1, siRRM2 & siKSP

Table 2.2 Validated siRNA sequences

Target	Sequence	Ref.
Nonsense	5'-TTC TCC GAA CGT GTC ACG T dtdt-3'	[217]
Nonsense2	Confidential	Confidential
PLK1	5′-GCA CAT ACC GCC TGA GTC T-3′	Dharmacon
KSP	5′-AAC TGA AGA CCT GAA GAC AAT-3′	Qiagen
RRM1	5′-GCA AAC TCA CTA GTA TGC ACT TCT A-3′	[218]
RRM2	5′-GCG ATT TAG CCA AGA AGT TCA-3′	[219]

Cells were seeded at $2.5x10^4$ cells/well in 24 well plates and incubated overnight at 37^0C with 5% CO_2. To seed, the cell monolayer was washed twice with Dulbecco's PBS. The cells were then trypsinised for 3 minutes until detached and neutralised with their respective medium. Cells were then centrifuged at 300g for 5 minutes and counted on the EVE automated cell counter. Once cells were resuspended, cell numbers were calculated and cells were seeded in 500uL at $2.5x10^4$ cells/well.

For each transfection sample (in 24 well plates), the oligomer-Lipofectamine RNAiMAX® (Life Technologies, Cat#13778150) complexes were prepared as follows. 20pmol of siRNA was diluted in 50ul Opti-MEM (Life Technologies, Cat#31985070)

The serum medium was reduced and the sample was mixed gently. 1ul of Lipofectamine RNAiMAX® was diluted in 50ul Opti-MEM reduced serum medium and mixed gently, followed by incubation for 5 minutes at room temperature. After incubation, the diluted oligomer was combined with the diluted Lipofectamine RNAiMAX® prepared as described above. The sample was mixed gently and incubated for 20 minutes at room temperature. The oligomer- Lipofectamine RNAiMAX® complexes were added to each well containing cells and medium (final concentration of 30nM) and cells were incubated at 37^0C with 5% CO_2. Media was changed 24hr post transfection. The effect of the transfected siRNA on the cells was determined by cell viability assay (MTS). All treatment wells in the experiments were conducted in duplicates. Controls used: Lipofectamine® only, and cells transfected with siRNA against a non-targeted siRNA; E-Nonsense (siNon) (EnGeneIC Ltd proprietary).

2.2.7 Detecting protein expression and knockdown of NSCLC cell lines after siRNA transfection by Western Blot

2.2.7.1 Cell Culture

Cell lines were seeded in T25 flasks at $3x10^5$ cells/mL in 5mL/flask and cultured at 37^0C with 5% CO_2. Cells were collected after 48hours (as described below) and 3 biological replicates were performed.

2.2.7.2 Protein extraction

Cells were washed 2x with DPBS. 500uL of RIPA buffer (Sigma, Cat#R0278) was added with 1uL of protease inhibitor to up to up to $1x10^6$ cells in each well. Using a cell scraper scrape the cells off the T25 flasks. Transferred the cell/buffer mixture from each flask into an Eppendorf tube. Vortexed vigorously for 15s and placed the samples on ice for 1h and vortexed every 15mins. Centrifuged the samples at 12,000g for 5min, then carefully transferred the supernatants to fresh tubes, trying not to disturb the pellets (if any) collected at the bottom of the tubes. Samples were stored at -20 degrees until time of use.

2.2.7.3 Quantification of protein concentration

The Biorad RD-DC kit (BIO-RAD, Cat #5000122) was used for protein quantification, as per manufacturer's instructions.

2.2.7.4 Protein Gel electrophoresis and Transfer

For each sample, required amount of protein (uL) was mixed with 5uL of Novex™ Tris-Glycine SDS Sample Buffer (ThermoFisher, Cat#LC2576) and 2uL of dithiothreitol (DTT) (Sigma, Cat#3483-12-3) (20-25uL in total). Note: equal amount of protein were used for all samples, and the total volume was made up to 20-25uL with water. A master mix of running buffer and DDT with 5uL and 2uL, respectively, was made for each sample. Equivalent amounts of protein containing 7uL master mix and water to make equal volumes of sample were placed on the Eppendorf tube heater for 5min at 80^oC then centrifuged the samples at 5000g for 10secs so that all the contents in each tube were collected at the bottom. Using a NuPAGE® Novex® 4-12% Bis-Tris Gels, 1.5 mm, 10 well (Thermofisher, Cat#NP0335Box) gels, the sticker at the bottom of the gel cast was carefully removed and the comb gently pulled out to expose the wells. The gel was placed into a gel tank filled using 1x MOPs buffer (NuPAGETM MOPs SDS running buffer (Thermofisher, Cat#NP0001) is 20x, for 1x add 50mL to 1L of deionised

water). Each well in the gel was gently flushed out using a 1mL pipette and then the entire content of each sample was carefully transferred into each well. 5uL of Novex Sharp Pre-stained Protein Standards (Thermofisher, Cat#LC5800) was loaded into one of the wells of each gel. The gel was run at 150 volts until dye had past the wells and then ran at 200 volts for about 45mins, until the dye displayed on the gel moved to the bottom of the gel cast.
Immediately following SDS-PAGE, the gels were transferred to nitrocellulose membranes (iBlot stacks; Life Technologies, Cat# IB23002) using iBlot2 (Life Technologies).

2.2.7.5 Probing the membrane with antigen-specific antibodies

The membranes were submerged in SuperBlock™ Blocking Buffer (Thermofisher, Cat# 37535), and placed on a shaker (low-setting) for 30mins/RT Membranes were incubated in 1:4000 anti-PLK1 (mouse), 1:1000 anti-RRM1 (rabbit) 1:4000 RRM2 (mouse) and 1:500 KSP (eg5) primary antibody overnight at 4°C with rotation in 10mL of 1:10 SuperBlock™ Blocking Buffer in PBST (1X PBS + 0.1% Tween 20 detergent (Sigma, Cat#P2287). The membranes were washed in PBST 3 times/15mins. The membranes were incubated in 1:5000 HRP-conjugated anti-mouse or 1:5000 HRP-conjugate anti-rabbit antibody in 1:10 SuperBlock™ Blocking Buffer with DPBST for 1h/RT in the dark on the shaker. Membranes were further washed in PBST 3x/15mins. To develop the membranes, 1ml of ECL® substrate (Bio-Rad, Cat#1705060) was added for 3min/RT. Membranes were visualised using ChemiDoc MP (Biorad). The following day the membrane was blocked in SuperBlock™ Blocking Buffer (40mins/RT) on the shaker (low-setting), incubated with 1:7000 anti-ACTIN (mouse) primary antibody (1h/RT) in 1:10 SuperBlock™ Blocking Buffer with DPBST in a 50mL tube on rotation. Further washing in PBST 3x/15mins, followed by 1:5000 HRP-conjugated anti-mouse incubation in 1:10 SuperBlock™ Blocking Buffer with DPBST for 1hr/RT in the dark in a rotating 50mL tube. Membranes were washed in PBST 3x/15mins and developed and visualised as mentioned above.

Table 2.3 Primary Antibodies

Primary Antibodies	***Source***	***Dilution***
Anti-human PLK1	Abcam, Cambridge, UK	1:4000
Anti-human RRM1	Abcam, Cambridge UK	1:1000
Anti-human RRM2	Abcam, Cambridge UK	1:4000
Anti-human KSP	Biolegend, USA	1:500
Anti-human Actin mAb	MerckMillipore USA	1:7000

Table 2.4 Secondary Antibodies

Antibody	*Source*	*Dilution*
goat anti-mouse polyclonal horseradish peroxidase (HRP)-conjugated	Abcam, Cambridge, UK	1:5000
anti-rabbit monoclonal HRP-conjugated	Abcam, Cambridge UK	1:5000

2.2.8 Apoptosis staining of non-small cell lung cancer cells transfected with siPLK, siRRM1, siRRM2 & siKSP measured by flow cytometry

The levels of apoptosis of NSCLC cell lines and a normal lung cell line after transfection with siPLK, siRRM1, siRRM2 & siKSP were measured by flow cytometry. After cell culture and cell transfection as described in **section 2.2.7** cell pellets were resuspended in 500uL Annexin V Binding Buffer (Thermofisher, Cat#V13246) (at a concentration of ~$1x10^6$ cells/ml).

2.2.8.1 Cell Staining

5uL of Annexin V FITC Conjugate and 2uL of DAPI solution were added to each cell suspension (except unstained tubes). Samples were incubated for 10 mins/RT in the dark.

2.2.8.2 Flow cytometry

Cell fluorescence was determined immediately on Gallios Flow cytometer with 488nm excitation laser with detection in green (FL1; Annexin-V FITC reagent) and red (FL4; PI stain) detectors. Compensation was applied after running single stained and unstained controls. Gating as follows; Live Cells (Annexin V-, PI-), Early Apoptotic cells (Annexin V+, PI-), Late Apoptotic cells (Annexin V+, PI+) and Necrotic cells (Annexin V-, PI+).
Data was analysed using GraphPad Prism 8.

2.2.9 Cell cycle staining of non-small cell lung cancer cells transfected with siPLK, siRRM1, siRRM2 & siKSP measured by flow cytometry

Cells were plated at $4x10^5$ cells/well, after 24hrs NSCLC cells were transfected with siNonsense, siPLK1, siRRM1, siRRM2 & siKSP in 6 well plates as described in **section 2.2.7.** 24 hours post transfection spent media was collected from the wells and transferred to 15mL

falcon tubes. The cell pellet was then resuspended in cold DPBS, fixed with 100% ice cold ethanol dropwise gently vortexing then incubated at 4ºC/1h. Cells were then centrifuged at 400g/8mins/4ºC and resuspended in cold DPBS and this was repeated twice. RnaseA and propidium iodide were added to each sample for final concentration of 0.2-0.5ug/mL and 10ug/mL respectively. Cells were incubated for 30mins/37ºC and then kept in the dark at 4ºC until analysis. Samples were analysed on FACS cytometer at 488nm. Data was analysed using GraphPad Prism 8.

2.2.10 Loading of siPLK1, siRRM1 and siKSP into EDV™s and Targeting EDV™s for the EGF Receptor

Loading and targeting of EDV™s as previously described [168]. In brief, targeting of minicells was achieved using bispecific antibodies, in which one arm recognises the O-antigen component of the minicell surface LPS and the other, a cell-surface receptor specific for the mammalian cell to be targeted, in this case Vectibix. Loading EDV™s involved significant amounts of washing by centrifugation of the EDV™s in various pH levels of PBS. The EDV™s were incubated with the siRNA overnight at 37^{O}C and the following day went through another series of washes before Vectibix was added and incubated for 30mins at RT. EDV™s were again washed thoroughly. Quality control (QC) was performed, and they were then freeze dried by the EnGeneIC manufacturing team. Further QC, including endotoxin testing, cell binding assay and sterility were then performed before batch release.

2.2.11 Measuring siRNA copy number of EDV™s after loading of siRNA

Known concentrations of siRNA were diluted in 1x10^{9} EDV™s to generate a standard curve using a fluorometer. Empty EDV™s do not contain RNAs and were used as our negative control. The newly loaded EDV™s were stained using with an RNA specific dye (QuantiFluor RNA System®, Promega, Cat#E3310) which detects the siRNAs in the EDV™s and measured using a fluorometer. Raw fluorescent values were used against the standard curve to calculate the siRNA concentrations within the EDV™s. Copy numbers calculated using the following equation.

Where: X=amount of amplicon (ng)

N=length of dsDNA amplicon

660g/mole=average mass of 1 bp dsDNA

Number of copies (molecules) = Xng*6.0221x10^{23} molecules/mole

(N*660g/mole)*1x10^{9}ng/g

2.2.12 Anti – EGFR Antibody Binding Capacity measured by Flow cytometry

The Quantum™ MESF (Molecules of Soluble Fluorochrome) kit (Bangs Laboratories, Cat#815) contains one blank population and a series of four fluorescent microsphere populations labelled with varying amounts of Alexa Fluor® 488. The assignment of fluorescence intensity MESF units was performed through direct comparison of fluorescence measurements from solutions of the pure fluorochrome with those from microspheres surface-labelled with the same fluorochrome.

2.2.12.1 Cell Culture and Staining

Cells were harvested by washing monolayer gently with PBS. The wash was discarded and 4ml of accutase® (Sigma, Cat#A6964) was added back to flasks and incubated until the monolayer had detached. The cells are detached from the flask by washing down the surface of the flask repeatedly. Cells were manipulated until a single cell suspension was achieved and then centrifuged at 300g for 5 mins. Cells were then resuspended in 1ml PBS 1% BSA and a cell count was performed. Aliquots of 1 x 10^6 cells/100ul were placed in Eppendorf tubes. One drop of Quantum Simply Cellular anti-mouse IgG microspheres (Bangs Laboratories, Cat#815) was added to the microcentrifuge tube then 50µL staining buffer and then the contents of the tube were gently mixed by tapping. One tube for each antibody capture population (1 – 4) was prepared. 2ug (10uL) of Anti-EGFR AF488 antibody (Santa Cruz, Cat#SCZSC-120AF488) was added to each bead population and samples (did not add to blank beads) smoothly and rapidly to obtain the tightest distribution, and then gently tapped the tube to mix. 2ug (5uL) of the isotype control antibody was added to the aliquot of cells smoothly and rapidly so to obtain the tightest distribution, the tube was tapped gently to mix. All samples were then incubated in the dark for 30 minutes at 4^0C after which 1mL of MACs Running buffer was added and samples were centrifuged; Beads at 2500g for 5 minutes and sample tubes at 300g for 5 minutes. All samples were further washed 2 times by adding 1ml buffer and centrifuging for 5 minutes at 300g. Samples and beads were then resuspended in 400µL MACs Running buffer and were run on the flow cytometer.

2.2.12.2 Flow cytometry

Stained bead populations and the blank were run individually. Microspheres were analysed on the flow cytometer at the test-specific instrument settings (PMT voltages and compensation). A flow rate of 100-200 events per second was used and 10,000 events are collected per bead population. Channel values were recorded and data was analysed by the QuickCal® v. 2.3 Data Analysis Program which generated the antibody binding capacity values.

2.2.13 Measuring cell number & cell viability of NSCLC hanging drop spheroids treated with siRNA loaded EDV™s

NSCLC 3D spheroids were made using specialised hanging drop plates (Perfecta3D®: HDP1096) and treated with EGFR targeted EDV™s loaded with siNonsense, siPLK1, siRRM1 & siKSP. Cells were seeded at 1000-3000 cells per well in 50uL/well and allowed to grow for 2-5 days until 300um was reached then treated with $5x10^8$ EDV™s/spheroid. Spheroids were treated for 24-72 hours. Treatments included cells only, EGFR-EDV or EDV alone, EGFR-EDV-siNonsense, EGFR-EDV-siPLK1, EGFR-EDV-siRRM1 & EGFR-EDV-siKSP. For treatment, each lyophilised EDV vial was reconstituted with 600ul of trehalose and incubated at RT/30mins. Reconstituted EDV™s were then centrifuged at 12,000g/10mins. EDV™ pellets were then resuspended in DPBS and centrifuged at 12,000g/8mins. The cell pellet was resuspended in culture media at a concentration of $5x10^8$ EDV™s /30µl. 20µl of media was removed and 30µl of media/ EDV™s suspension was added or 30µl of media without EDV™s to cells only treatment. Media in the outside wells were refilled with additional 5µl media every 2 days. Spheroids were treated for 24-72hrs.

2.2.13.1 Cell viability Assay

The entire content of treatment wells (spheroid+media) was collected and spheroids were allowed to settle by gravity. Supernatant removed was removed spheroids washed twice with DPBS using gravity to pellet them. Supernatant was removed and 100uL of 0.25% Trypsin/EDTA was added. Samples were incubated at 37°C/5mins or until the spheroids are dissociated into single cells. Trypsin was inactivated with complete media. Cell counts and cell viability was determined using trypan blue staining and counted using a haemocytometer.

2.2.14 Xenograft mouse models

Cell were grown in T175 flasks and cultured as described in **section 2.2.3**. After counting cells were centrifuged at 300g/5mins, supernatants were discarded, and pellets were resuspended in cold serum free media and pooled into 1 tube. Cells were centrifuged at 300g/5mins,

supernatant was discarded. A549-Dox-R cells 5×10^6 cells were injected in 100µL Serum Free RPMI with 100µL BD Matrigel basement membrane matrix-growth factor reduced (Matrigel), phenol red free (BD Biosciences), e.g. $5x10^6$ cells in 200µL/mouse ($2.5x10^7$/mL).

6mL of Matrigel was added to the cell pellet containing $3x10^8$ cells and made up to the final volume of 12mL with cold serum free media. Cells were kept on ice and $5x10^6$ cells were injected into the left flank 50 mice immediately.

50 mice were used because xenografts grow at different rates and only 80% of mice develop tumours that grow 100-150mm3 (EnGeneIC in house data). These were randomised into groups as per Table 2.5. Excess mice were used for dissection and tail vein injection training purposes. Each group comprised 7 mice which is the number needed for efficacy testing and statistical significance of the treatments. When tumours reached $150mm^3$, $2x10^9$ EDV^{TMs} were injected via the tail vein, 3 times per week for 2 weeks as per Table 2.5.

Tumours were measured at each dosing point. Tumours from these mice have been excised and RNA from the tissue will be extracted for RT-qPCR to assess knockdown of the genes being targeted. *Animal Ethics Approval: 01/2018 (EnGeneIC Pty Ltd Animal Care and Ethics Committee)*

Table 2.5 In vivo experiment treatment schedule

Treatment group	***No. animals***	***Pretreat ****	***Treat #***	***Monitor ‡***	***End ¶***
Saline	*7*	*A549-Dox-R cells at $5x10^6$/200µL (media Matrigel), injected subcutaneously on the right flank of each mouse*	*100µL Saline injected i.v.3x a week for 2 weeks*	*1.Daily* *2.Tumour volume measured 3x a week* *3. Mice weighed 2x a week*	*Tumours >1.5 cm^3 or when there is a significant difference between controls and treatment groups* *Tumours excised for PCR analysis*
$^{EGFR}EDV_{siNonsnense}$	*7*	*A549-Dox-R cells at $5x10^6$/200µL (media Matrigel), injected subcutaneously on the right flank of each mouse*	*$1x10^9$ (100µL) $^{EGFR}EDV_{siNonsense}$ injected i.v.3x a week for 2weeks*	*1.Daily* *2.Tumour volume measured 3x a week* *3. Mice weighed 2x a week*	*Tumours >1.5 cm^3 or when there is a significant difference between controls and treatment groups* *Tumours excised for PCR analysis*

Treatment group	*No. animals*	*Pretreat **	*Treat #*	*Monitor ‡*	*End ¶*
$^{EGFR}EDV_{siPLK-1}$	7	*A549-Dox-R cells at $5x10^6$/200µL (media Matrigel), injected subcutaneously on the right flank of each mouse*	*$1x10^9$ (100µL) $^{EGFR}EDV_{siPLK-1}$ injected i.v.3x a week for 2weeks*	*1.Daily 2.Tumour volume measured 3x a week 3. Mice weighed 2x a week*	*Tumours >1.5 cm^3 or when there is a significant difference between controls and treatment groups Tumours excised for PCR analysis*
$^{EGFR}EDV_{siRRM1}$	7	*A549-Dox-R cells at $5x10^6$/200µL (media Matrigel), injected subcutaneously on the right flank of each mouse*	*$1x10^9$ (100µL) $^{EGFR}EDV_{siRRM1}$ injected i.v.3x a week for 2 weeks*	*1.Daily 2.Tumour volume measured 3x a week 3. Mice weighed 2x a week*	*Tumours >1.5 cm^3 or when there is a significant difference between controls and treatment groups Tumours excised for PCR analysis*
$^{EGFR}EDV_{siKSP}$	7	*A549-Dox-R cells at $5x10^6$/200µL (media Matrigel), injected subcutaneously on the right flank of each mouse*	*$1x10^9$ (100µL) $^{EGFR}EDV_{siKSP}$ injected i.v.3x a week for 2 weeks*	*1.Daily 2.Tumour volume measured 3x a week 3. Mice weighed 2x a week*	*Tumours >1.5 cm^3 or when there is a significant difference between controls and treatment groups Tumours excised for PCR analysis*
$^{EGFR}EDV_{Dox}$	7	*A549-Dox-R cells at $5x10^6$/200µL (media Matrigel), injected subcutaneously on the right flank of each mouse*	*$1x10^9$ (100µL) $^{EGFR}EDV_{Dox}$ injected i.v.3x a week for 2 weeks*	*1.Daily 2.Tumour volume measured 3x a week 3. Mice weighed 2x a week*	*Tumours >1.5 cm^3 or when there is a significant difference between controls and treatment groups Tumours excised for PCR analysis*

Total number of animals: **42**

*Pretreat **
Treat #
Sample †
Monitor ‡
End ¶

2.2.15 RT-qPCR measuring gene knockdown in tumour xenografts

Tumours were extracted and a 3-4mm^3 section was placed in a tube with 350uL Lysis Buffer RLY (Bioline, Cat#BIO52073) where tissue was broken up using an electronic pellet pestle

(Sigma, Cat# Z359971). A further 300uL lysis buffer was added to each tube before spinning. Samples were stored at -80ºC until further experiments could be run.

2.2.15.1 RNA Extraction – to purify total RNA from cultured cells.

RNA was extracted from cell lines using ISOLATE II RNA Mini Kit (Bioline, Cat #BIO52073) using the manufacturer's instructions. Quantitation of RNA was performed using a spectrophotometer with the 260/280 & 260/230 values recorded.

2.2.15.2 cDNA reaction: synthesise first-strand cDNA.

cDNA was synthesised using the SuperScript® VILO™ cDNA Synthesis Kit (Thermo Fisher Scientific, Cat#11754050). Each reaction combined 4uL of 5X VILO™ Reaction Mix, 2uL 10X SuperScript™ Enzyme Mix, 20uL of DEPC-treated water with the required uL amount of RNA for 20ng. Tube contents were gently mixed, and a quick centrifugation was performed to collect all mixture at the bottom of the tubes. Samples were incubated in the PCR machine using the following thermal profile; 25°C for 10 minutes, 42°C for 60 minutes, 85°C for 5 minutes and then the reaction was terminated, and samples held at 4oC. cDNA was then diluted prior to qPCR.

2.2.15.3 RT-qPCR.

For each qPCR reaction 5uL TaqMan advance mix (Applied Biosystems, Cat#4444557), 0.5uL 20x TaqMan Probe mix *(Table 2.5)* and 2.5uL DEPC dH2O was made up as a master mix and 8uL was aliquoted into each well. 2uL of the cDNA prepared solution was added to its required well of a PCR plate. The cycling conditions were 50ºC for 2mins, 95ºC for 10min, followed by 40 cycles of denaturation (95ºC, for 15sec) and annealing and extension (60ºC for 1 minute). RT-qPCR carried out using 7500 Software v2.3 and analysed using DataAssistTM v3.01.

Table 2.6 TaqMan Probes

TaqMan™ Gene Expression Assay (Thermo Fisher Scientific Cat#4331182)	Gene Expression
B2M	Hs99999907
GAPDH	Hs99999990
GUSB	Hs99999908
KIF-11	Hs00189698
PLK1	Hs00153444
RRM1	Hs01040698

Chapter 3. Characterisation of cell cycle regulation through inhibition of PLK1, RRM1 and KSP using siRNA (siPLK1, siRRM1 & siKSP) in NSCLC cell lines

3.1 Background

Cell cycle regulatory genes are major targets for drug resistant cancers. As discussed in *sections 1.5.1.2 – 1.5.1.4,* the cell cycle regulatory genes, PLK1, KSP and RRM1 play integral roles in cell division and regulating mitotic division [185, 220-223] and are often overexpressed in advanced NSCLCs and associated with drug resistance [176, 177, 224-226] . Therefore, this chapter focuses on the expression of cell cycle regulatory genes and whether siRNAs (siPLK1, siRRM1 & siKSP)) targeted against these genes cause knockdown of protein expression and determine their effect on a drug resistant cell line. Depending on the influence of knockdown by the specific siRNA, the siRNAs will be loaded into EDV^{TM}s for delivery to the NSCLCs.

Aim 1. Test the knockdown efficiency of siRNA to decrease gene expression of essential cell cycle regulators PLK1, RRM1 & KSP in NSCLC cell lines.

To achieve this aim:
First, we confirmed the drug sensitivity of the A549-Dox-R lung cancer cell line (constructed by EnGeneIC in 2016).
Secondly, we investigated the expression of cell cycle regulatory genes and silencing using siRNA on cellular apoptosis and cell cycle arrest.

3.2 Results

3.2.1 The A549-Dox-R NSCLC cell line is drug resistant to Doxorubicin

A drug resistant cell line (A549-Dox-R), originally constructed by EnGeneIC in 2016, was reevaluated for drug resistance. The MTS proliferation assay was used to determine drug resistance to doxorubicin (Dox) in the A549-Dox-R cell line compared to the parental A549 cell line. Cells were treated at a concentration range of 0.5-5000nM Dox for 72 hours after which cell toxicity was measured. The IC50 value was calculated using GraphPad Prism in direct comparison to the parent A549 cells. As shown in *Fig. 3.1A,* the average IC50 of 964nM, the A549-Dox-R cell line was three-times more resistant than the original A549 cell line, with an average IC50 of 316nM *(Fig. 3.1B),* confirming a significant increase ($p = 0.0004$) in drug resistance using a standard t-test (*Fig. 3.1C).*

A.

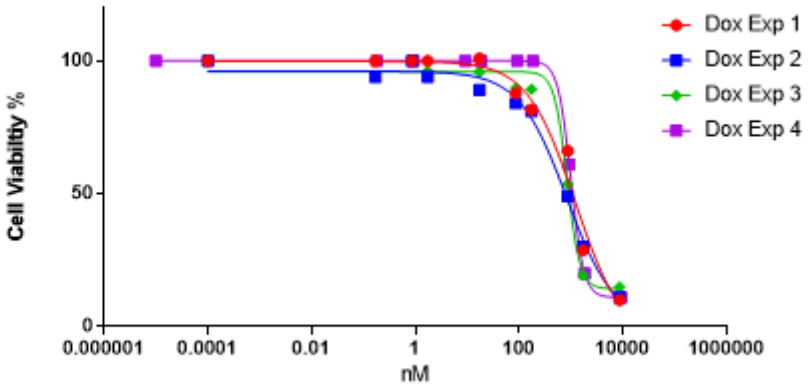

B.

	Dox Exp 1	Dox Exp 2	Dox Exp 3	Dox Exp 4
IC50	1204	825.5	840.6	987.4

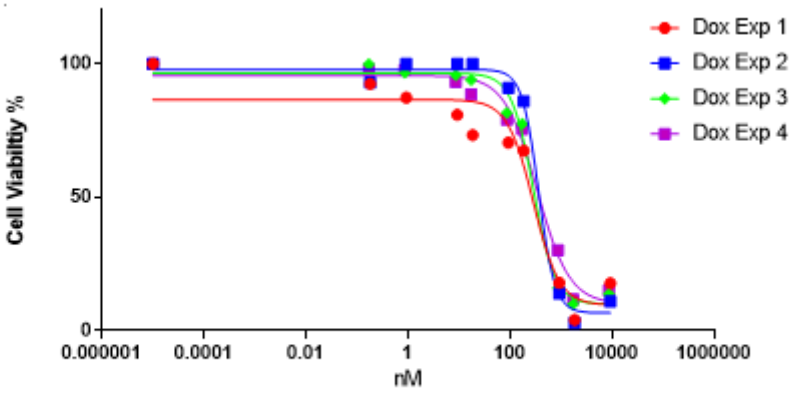

	Dox Exp 1	Dox Exp 2	Dox Exp 3	Dox Exp 4
IC50	285.1	359.1	283.2	335.2

C.

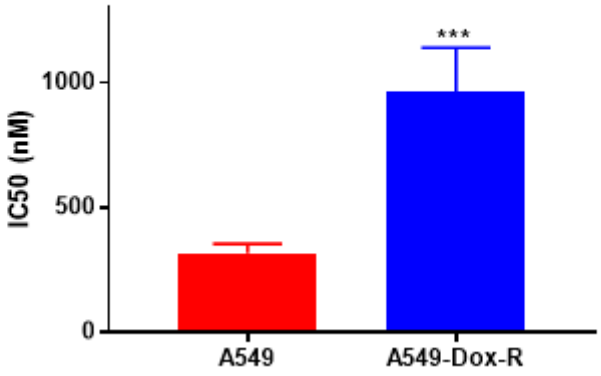

Figure 3.1 A549-Dox-R NSCLC cell line is drug resistant to Doxorubicin. To determine the IC50 concentration of *(A)* A549-Dox-R and *(B)* parent A549 cell lines, cells were seeded at a seeding density of 5000 cells in 96 well plates and treated with doxorubicin or media alone for 72 hours at a concentration range of 0.5-5000nM. At 72h MTS reagent was added and absorbance read at 490nm using an ELISA plate reader. Cell toxicity was measured using the MTS proliferation assay and the IC50 values were calculated using GraphPad Prism. Each graph represents the growth curves of quadruple independent biological experiments: Each point represents the mean of 3 technical replicates, n = 4. IC50 calculated as nanomolar (nM). *C* represents the IC50 of A549 cell line compared to A549-Dox-R cell line.
*** $p = 0.0004$ (t-test)**.**

3.2.2 *PLK*1, *KSP* & *RRM*1 RNA levels are elevated in NSCLC cell lines

As previously mentioned, the 3 genes, *PLK*1, *RRM*1 & *KSP* have been shown to be overexpressed in advanced NSCLC and associated with drug resistance [177].

Using real-time qPCR, this experiment aimed to determine the relative expression of *PLK*1, *RRM*1 & *KSP* compared/normalised to the expression of the control housekeeping gene GAPDH. MRC-5, a normal lung cell line was used as a comparative control (cancer vs normal expression). In repeated experiments, *Figure. 3.2A and 3.2B,* we observed the same pattern of expression in the A549-Dox-R cell line, where *PLK*1 was >7-fold and >10-fold *respectively,* compared to MRC-5. The expression level of *RRM*1 and *KSP* was >2-fold. The NSCLC cell line H358 also expressed *PLK*1 >3-fold *(Fig. 3.2A)* and >10-fold *(Fig. 3.2B),* and the parental A549 *(Fig. 3.2B)* had >5-fold expression of *PLK*1 compared to the MRC-5 normal lung cell line.

These results confirmed that *PLK*1 is overexpressed in several NSCLC cell lines, particularly noteworthy was the significant overexpression in the drug resistant cell line. Hence these cell lines were used in further studies to examine the consequences of the knockdown of *PLK*1 expression levels with siRNA. The expression levels of *RRM*1 and *KSP* was less consistent, not all NSCLC cells overexpressed these genes, importantly though, *RRM*1 and *KSP* are also overexpressed in the drug resistant A549-Dox-R cell line.

A.

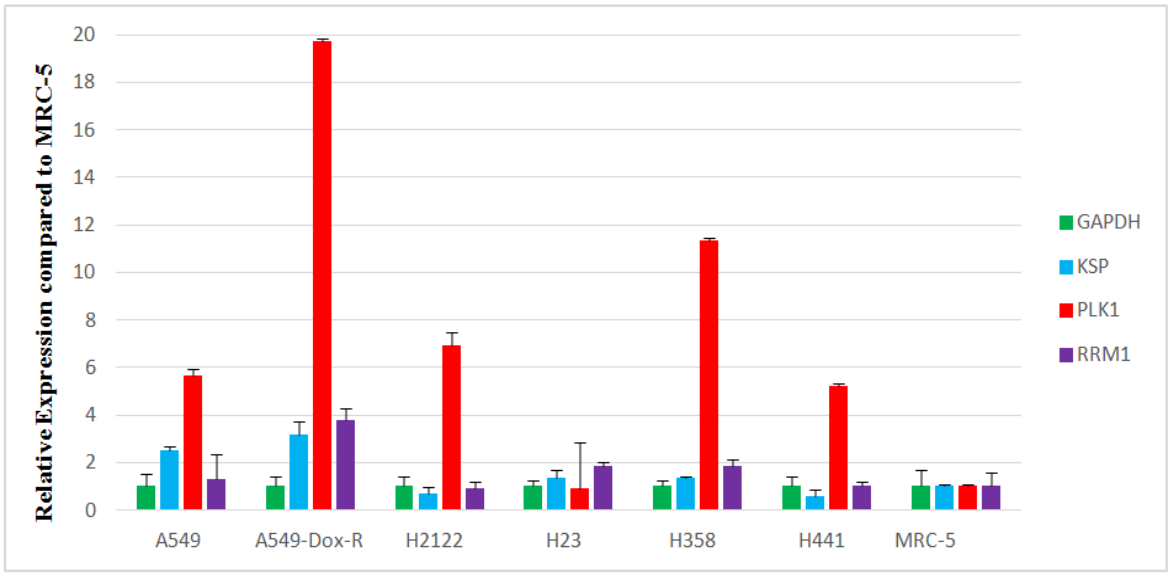

B.

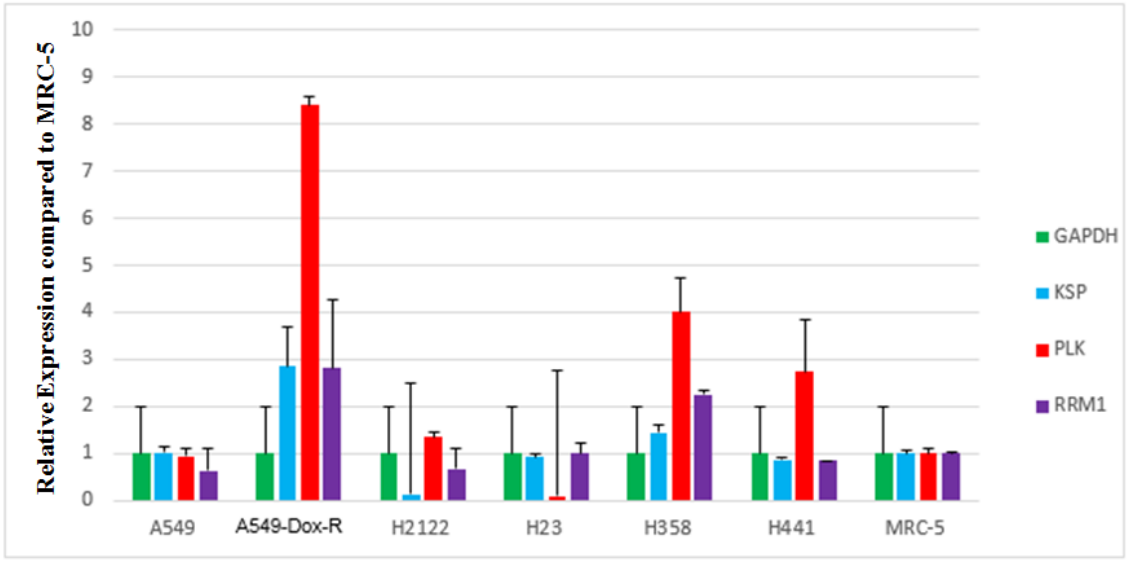

Figure 3.2 *PLK*1, *KSP* & *RRM*1 levels are elevated in NSCLC cell lines. The expression of three genes, *PLK*1 (red), *KSP* (blue) and *RRM*1 (purple), was tested in 6 NSCLC cell lines and one control, MRC-5 lung cell line using RT-qPCR. Top panel and Bottom panel *(A and B)* are graphical a representation of duplicate biological experiments. The housekeeping gene (green) used was *GAPDH*. RT-qPCR carried out using 7500 Software v2.3 and analysed using DataAssist™ v3.01. Error bars +/- Std dev of technical triplicate ($p<0.05$)

3.2.3 PLK1, RRM1 & KSP protein levels are elevated in NSCLC cell lines

The function of PLK1, *RRM*1 and *KSP* genes is driven by their translated proteins. Thus given that qPCR data only shows RNA levels that do not necessarily manifest into equivalent protein expression levels, western blots were performed to further validate expression of PLK1, RRM1 & KSP as well as RRM2 protein expression in NSCLC cell lines compared to the normal lung fibroblast MRC-5 cell line *(Fig. 3.3)*. Although overall the results were statistically non-significant we did observe that PLK1 expression increased 3-fold and 2.5-fold in the A549-Dox-R and A549 cells lines respectively while KSP was expressed >2.5-fold in H441 cell line compared to MRC-5 *(Fig. 3.4)*. RRM1 was expressed at >1.3-fold in A549-Dox-R although all other cell lines had reduced expression in comparison with MRC-5.

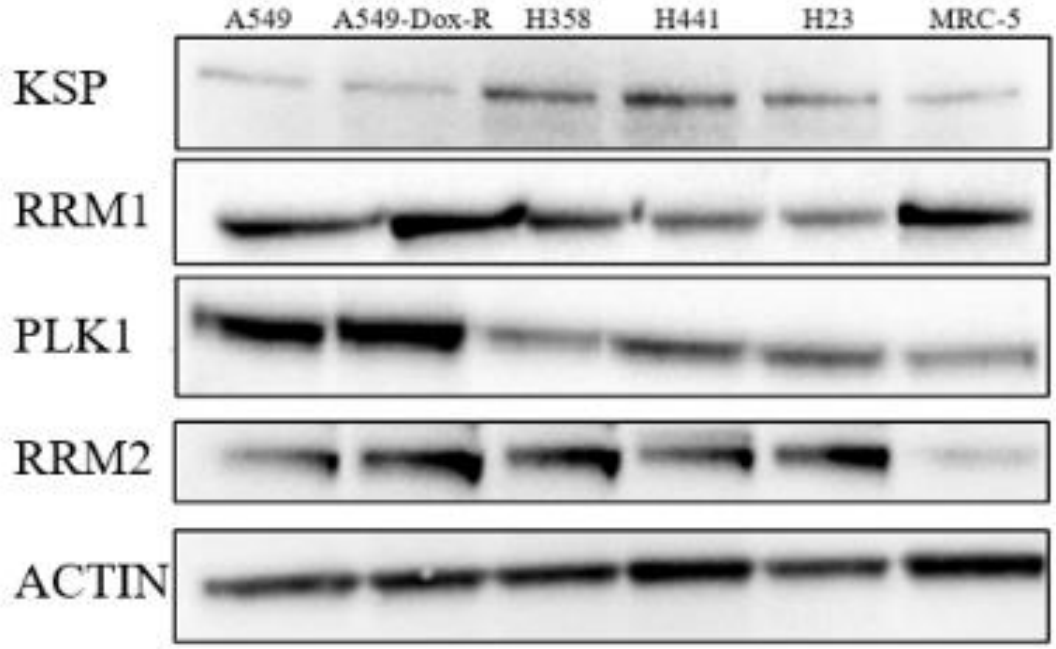

Figure 3.3 Protein expressions are increased in NSCLC cell lines. Analysis demonstrated an increase in PLK1, RRM1, RRM2 & KSP protein expression of NSCLC cell lines compared to the normal lung cell line MRC-5. Bands compared against ACTIN control and MRC-5 cell line. Images taken using Bio-Rad Image Lab™ Software v6.01.

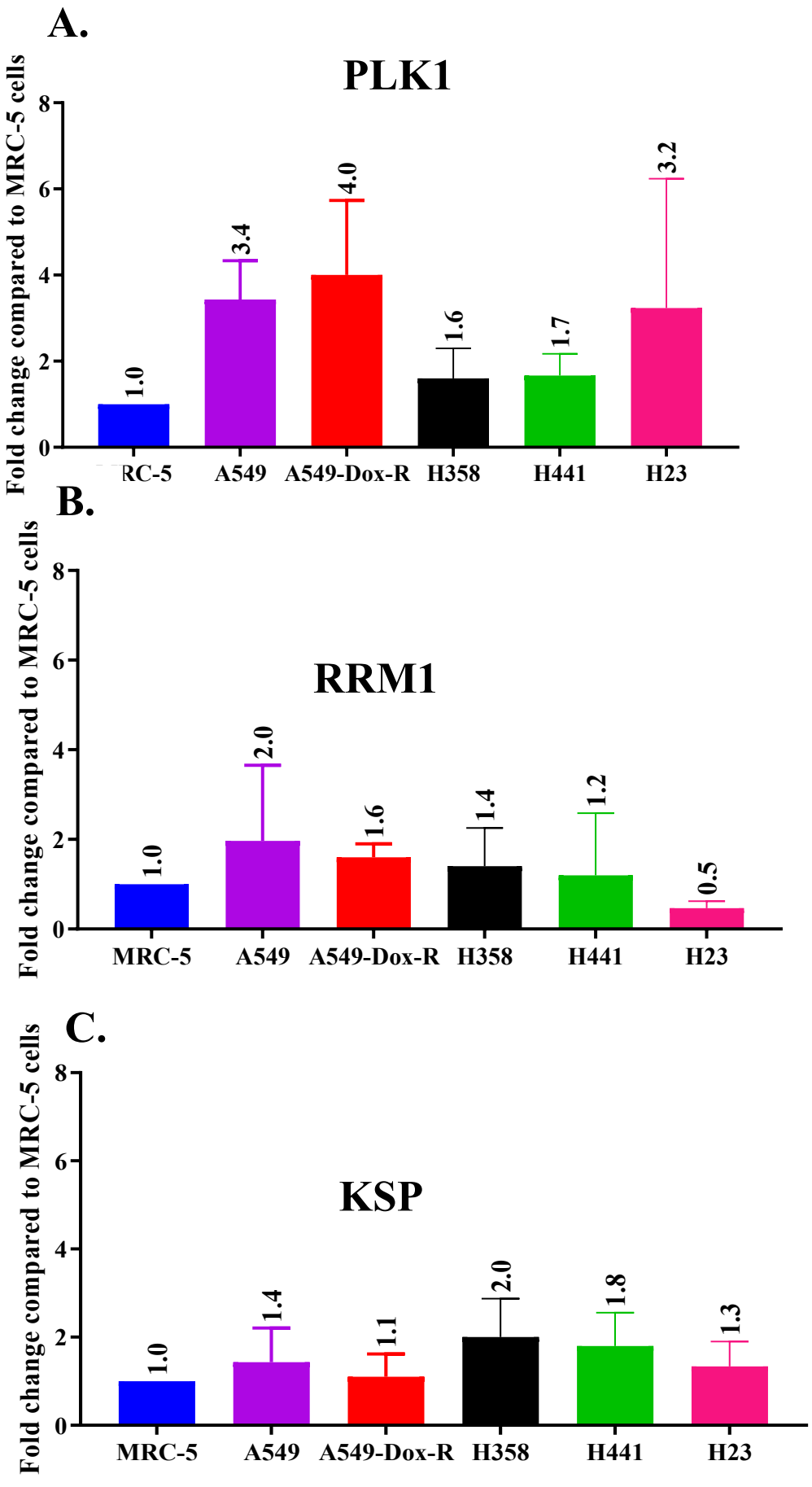
A.
PLK1
Fold change compared to MRC-5 cells
0
2
4
6
8
1.0
3.4
4.0
1.6
1.7
3.2
RC-5
A549
A549-Dox-R
H358
H441
H23
B.
RRM1
Fold change compared to MRC-5 cells
0
2
4
6
8
1.0
2.0
1.6
1.4
1.2
0.5
MRC-5
A549
A549-Dox-R
H358
H441
H23
C.
KSP
Fold change compared to MRC-5 cells
0
2
4
6
8
1.0
1.4
1.1
2.0
1.8
1.3
MRC-5
A549
A549-Dox-R
H358
H441
H23

Figure 3.4 Relative protein expression of PLK1, RRM1, KSP and RRM2 in NSCLC cell lines. Protein was extracted from NSCLC cell lines and expression was measured using Bio-Rad Image Lab™ software v6.01. MRC-5 non-cancerous cell line served as the negative control and data was normalised to ACTIN. Experiments were completed in biological triplicates and averages are displayed. 2-Way ANOVA with a follow-on Tukey test. No statistical significance recorded.

3.2.4 siRNAs inhibiting PLK1, RRM1, RRM2 & KSP cause protein knockdown

In this study one of our main aims was to silence the genes, *PLK*1, *KSP, RRM*1 and *RRM*2 in order to halt tumour cell proliferation. *PLK*1 encodes for a protein that regulate cell cycle, mitosis, cytokinesis and repair damaged DNA [220, 227], similarly *KSP* encodes for a motor protein involved in stages of mitosis specifically involving chromosome assembly and spindle formation [185, 223, 228]. *RRM*1 and *RRM*2 encode the two subunits of ribonucleotide reductase, an enzyme that is responsible in the formation of deoxyribonucleases from ribonucleases which is crucial in DNA replication during S phase of the cell cycle [221, 222, 229, 230]. H358 and A549 cell lines were chosen for this experiment as they exhibited the greatest expression of our proteins of interest overall. Western Blot was used to assess the inhibitory effect of siPLK1, siRRM1, and siKSP on protein expression post 24hrs (*Fig. 3.5 & Fig. 3.6).* Cells only and cells transfected with a siNonsense (scrambled siRNA), which should not affect the RNA or protein expression, were used as negative controls. siKSP caused 37%, 26% and 24% knockdown while siRRM1 caused 93%, 95% and 90% knockdown in A549, A549-Dox-R and H358 respectively. siPLK caused 75%, 79% and 73% % protein expression knockdown in the cell lines respectively.

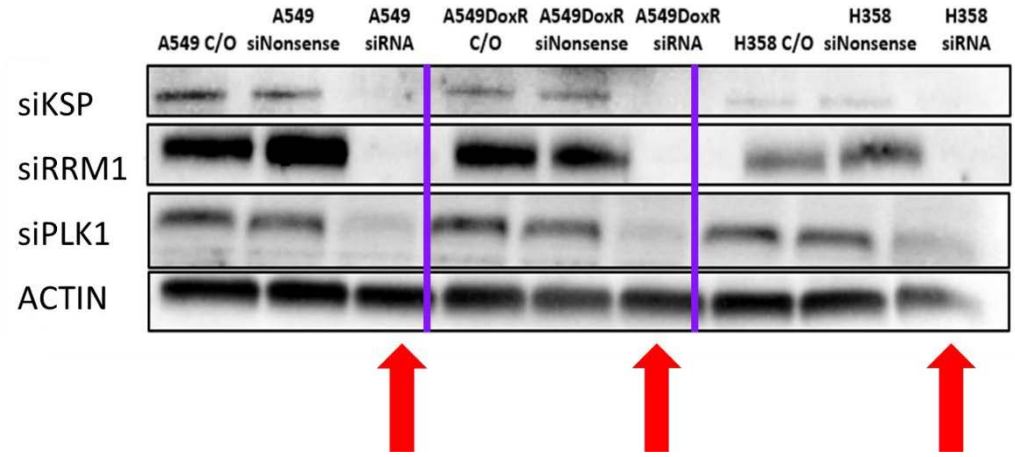

Figure 3.5 siRNA knockdown of PLK1, RRM1 & KSP confirmed by Western Blot. NCSLC cells transfected with PLK1 and KSP and Nonsense siRNAs compared to untransfected cells post 48hs were analysed by western blot. Actin was used as a loading control. The images are representative from one experiment. Experiments were completed in biological triplicates.

A.

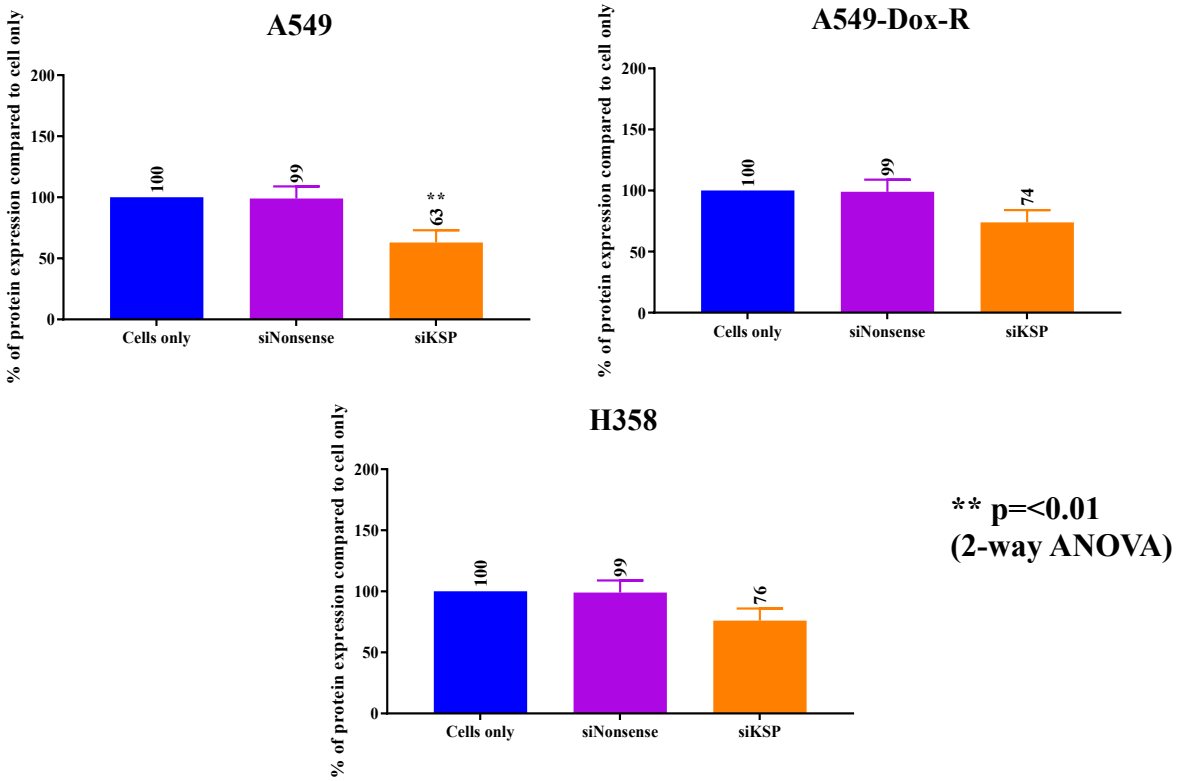

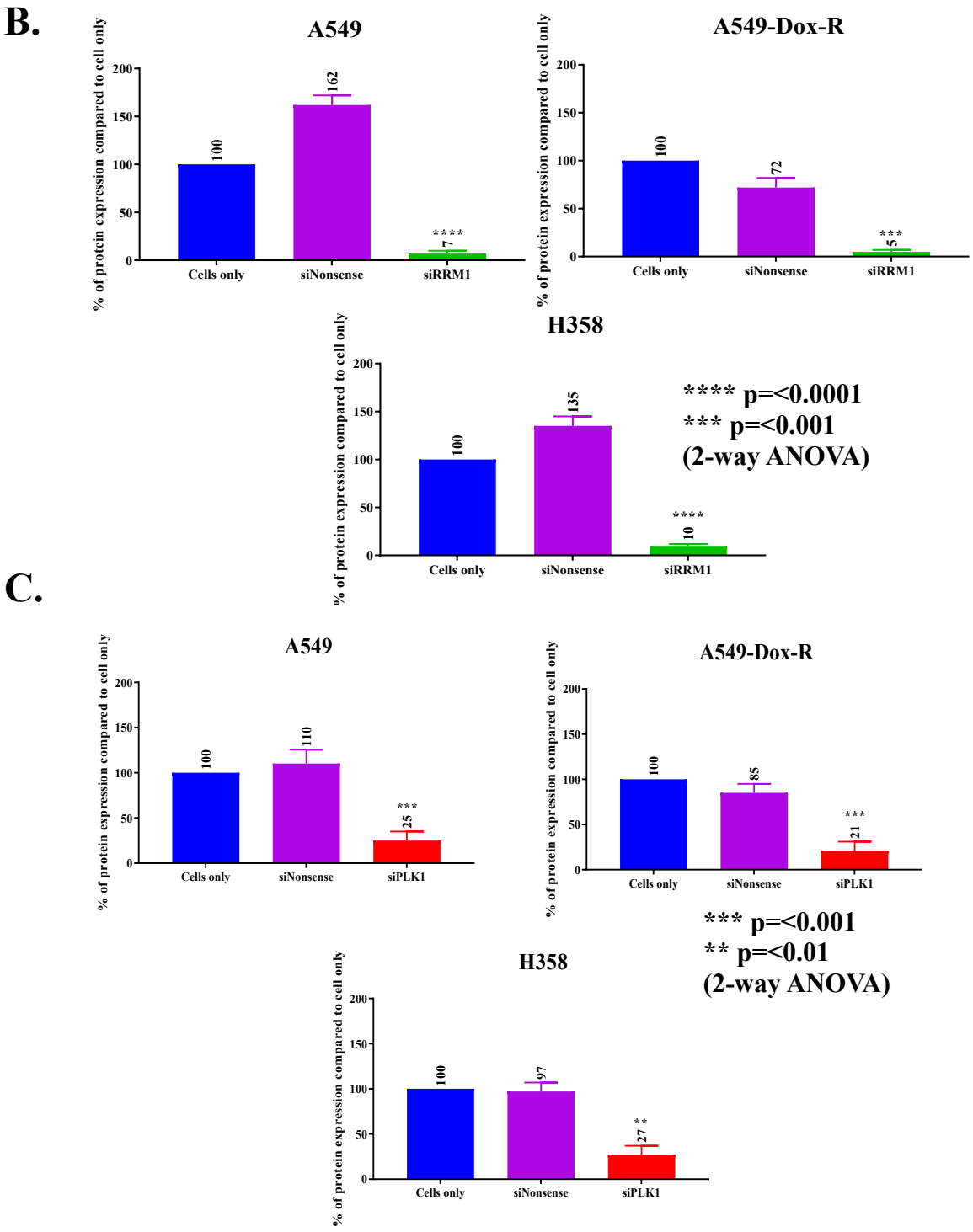

Figure 3.6 Knockdown of KSP, RRM1 and PLK1 protein analyses. Quantitation of protein expression from western blots shown in *Figure 3.5* revealed knockdown of protein expression in NSCLC cell lines post-transfection with KSP (Fig. A), RRM1 (Fig. B) and PLK1 (Fig. C) siRNAs. Data was normalised to ACTIN. 2-Way ANOVA with a follow-on Tukey test. Experiments were completed in biological triplicates with averages of the independent experiments displayed.

3.2.5 siRNAs inhibiting PLK1, RRM1 & KSP decreased cell viability in NSCLC cell lines

Using Lipofectame^{TM} as a transfection agent, siRNA targeted to *PLK*1 (siPLK1), *RRM*1 (siRRM1), *RRM*2 (siRRM2) & *KSP* (siKSP) were transfected into A549, A549-Dox-R & H358 *(Figs. 3.7A, B & C)* and post 72 hours cell death was measured using the MTS assay. The A549 & A549-Dox-R *(Figs. 3.7A & B)* transfection with siPLK1 resulted in significant cell death 83% and 76% respectively, and the cell line H358 *(Fig 3.7C)* showed 74% cell death. Transfection with siRRM1 showed 82% cell death in the A549 cell line *(Fig. 3.7A)* and A549-Dox-R and H358 were 63% and 60% respectively. siRRM2 showed to be the least effective with only 47%, 33% and 55% cell death in A549, A549-Dox-R and H358 cell lines respectively. The most effective siRNA proved to be siKSP with 82%, 88% and 89% cell death in A549, A549-Dox-R and H358 *(Figs. 3.7A, B & C)* cell lines respectively.

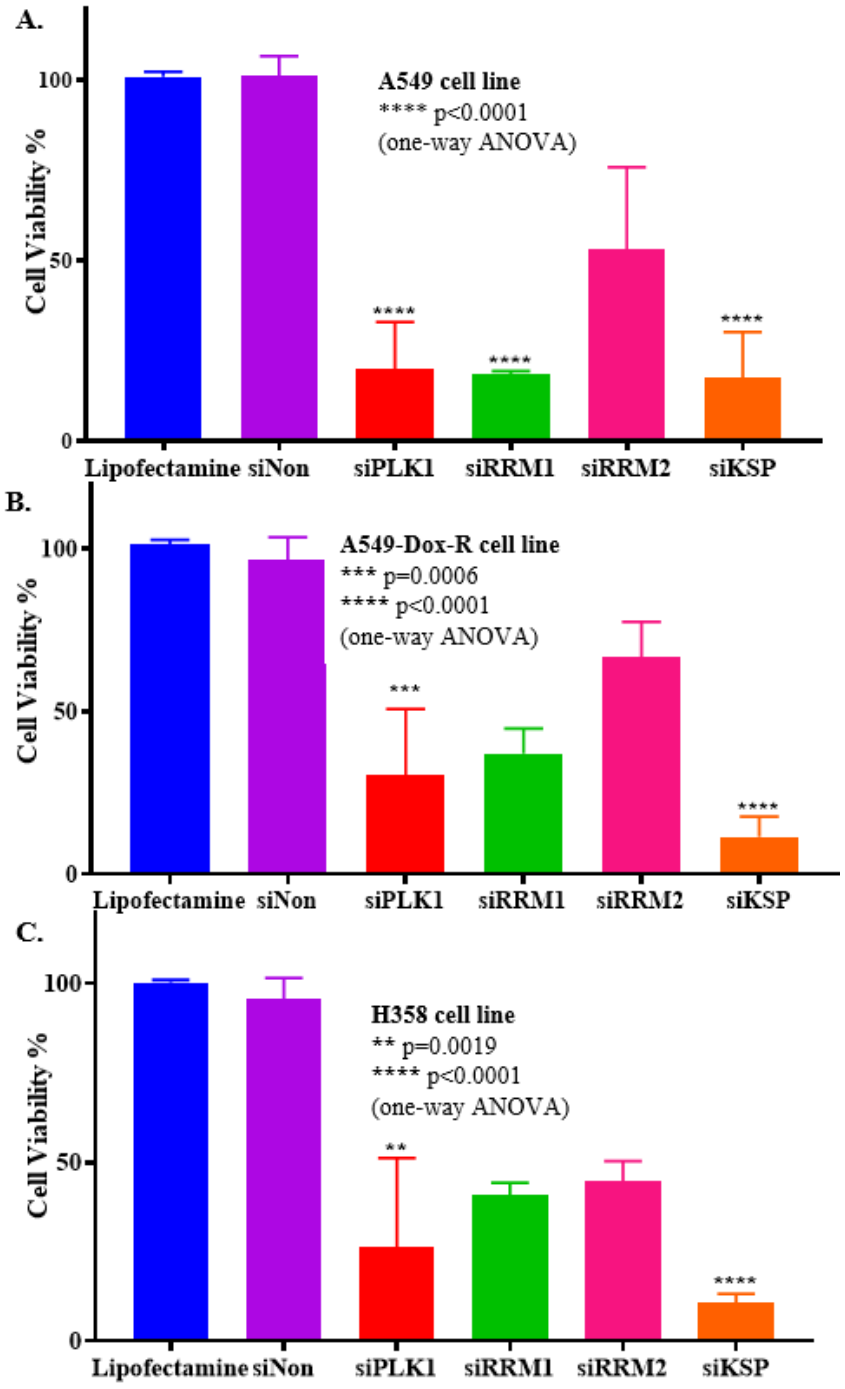
A.
Cell Viability %
100
50
0
A549 cell line
**** p<0.0001
(one-way ANOVA)
****
****
****
Lipofectamine
siNon
siPLK1
siRRM1
siRRM2
siKSP
B.
Cell Viability %
100
50
0
A549-Dox-R cell line
*** p=0.0006
**** p<0.0001
(one-way ANOVA)
***
****
Lipofectamine
siNon
siPLK1
siRRM1
siRRM2
siKSP
C.
Cell Viability %
100
50
0
H358 cell line
** p=0.0019
**** p<0.0001
(one-way ANOVA)
**
****
Lipofectamine
siNon
siPLK1
siRRM1
siRRM2
siKSP

Figure 3.7 Cell viability is significantly decreased in cell lines transfected with siRNA targeted to *PLK*1, *RRM*1 (siRRM1), *RRM*2 (siRRM2) and *KSP* (siKSP). Parental A549 *(A)*, A549-Dox-R *(B)* and H358 *(C)* lung cancer cell lines were transfected with Lipofectamine® only control (blue), siNon (purple), and siPLK1 (red), siRRM1 (green), siRRM2 (pink) and siKSP (orange). Viability of cells was measured and compared against Lipofectamine control 72hrs post transfection as determined by MTS Assay, absorbance was read at 490nm. Data analysed using GraphPad Prism 8. 2-Way ANOVA with a follow-on Tukey test ($p<0.001$). n=3 data presented as mean, error bars +/- Std dev.

3.2.6 Inhibition of PLK1, KSP & RRM1 induces apoptosis in NSCLC cell lines

Flow cytometric analysis measuring programmed cell death (apoptosis) is an effective tool to assess the efficacy of a stimuli or treatment in promoting death in cancer cells [231]. Given that siPLK, siRRM1, siRRM2 & siKSP caused a reduction in cell viability (section 3.5) we next investigated the stages of apoptosis in NSCLC cells and a normal lung cell line. Apoptosis was evident 48hrs after the inhibition of PLK1, RRM1, RRM2 & KSP followed by Annexin V and propidium iodide staining and measured by flow cytometry.

Figure 3.8 shows the clear shift of cells from live cells (control groups (*Fig. 3.8A-B*)) to early and subsequently late apoptosis by siPLK1*(Fig. 3.8E)* and siKSP *(Fig. 3.8F)* treatments. A slight shift was also seen in cells treated with siRRM1*(Fig. 3.8C)* and siRRM2 *(Fig. 3.8D)* indicating a level of early apoptosis.

Overall, there were significant levels of apoptosis in all NSCLC lung cancer cell lines except H441 transfected with siPLK1. A549 *(Fig. 3.9A),* A549-Dox-R *(Fig. 3.9B),* H358 *(Fig. 3.9C),* and H23 *(Fig. 3.9D)* recording 50%, 70%, 55% and 54% total apoptosis respectively compared to the normal lung cell line MRC-5 *(Fig. 3.9F).* siKSP also caused significant total apoptosis in the previously mentioned cell lines, especially A549 and H23 with 65% and 75% respectively.

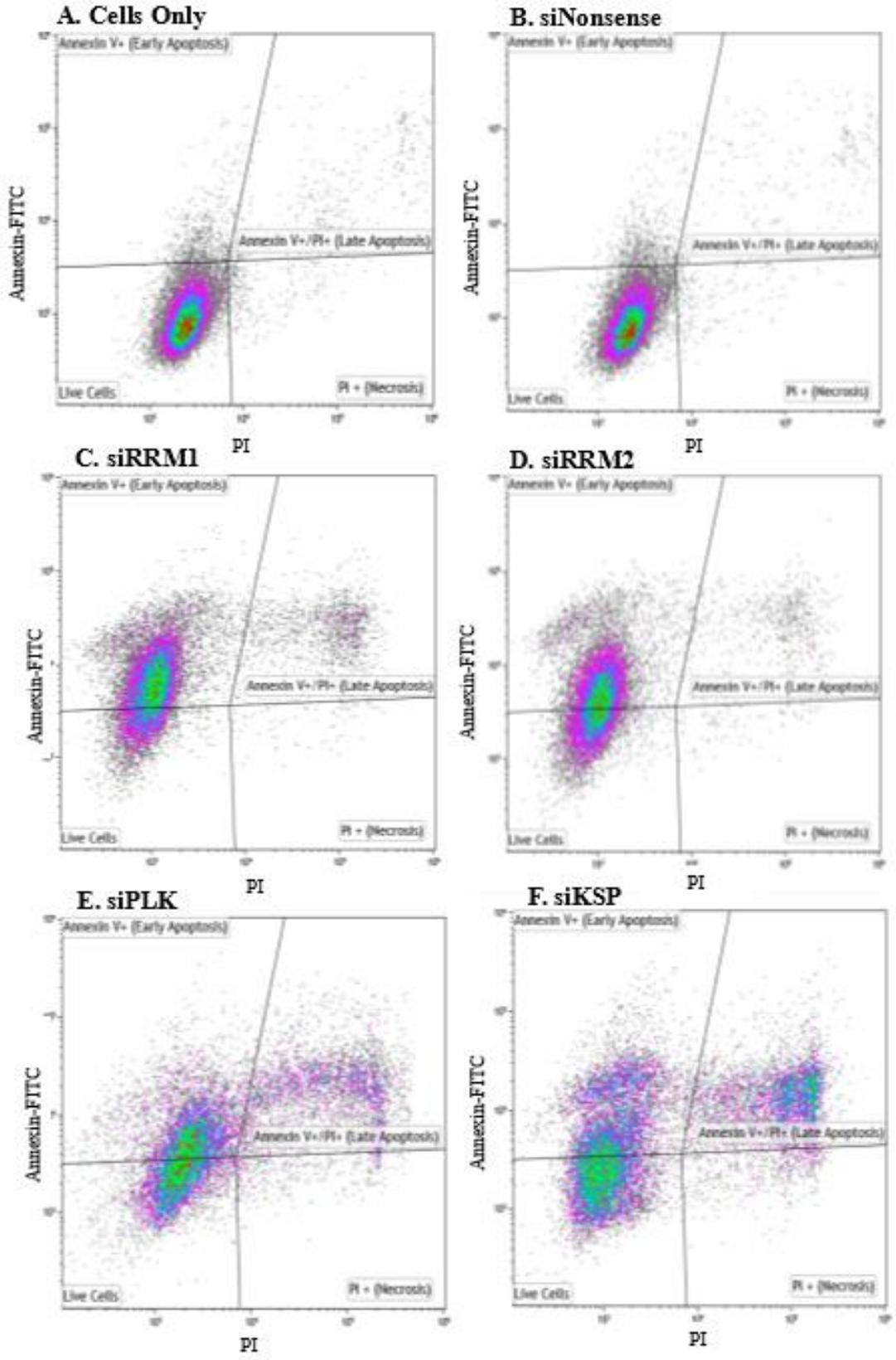

Figure 3.8 A significant shift from early to late apoptosis in A549 cell line. Cells transfected with, siRRM1 *(C),* siRRM2 *(D),* siPLK1 *(E)* & siKSP *(F)* compared to negative controls *(A & B).* Images collected using Gallios 6C Flow Cytometer and Kaluza Analysis v2.1.

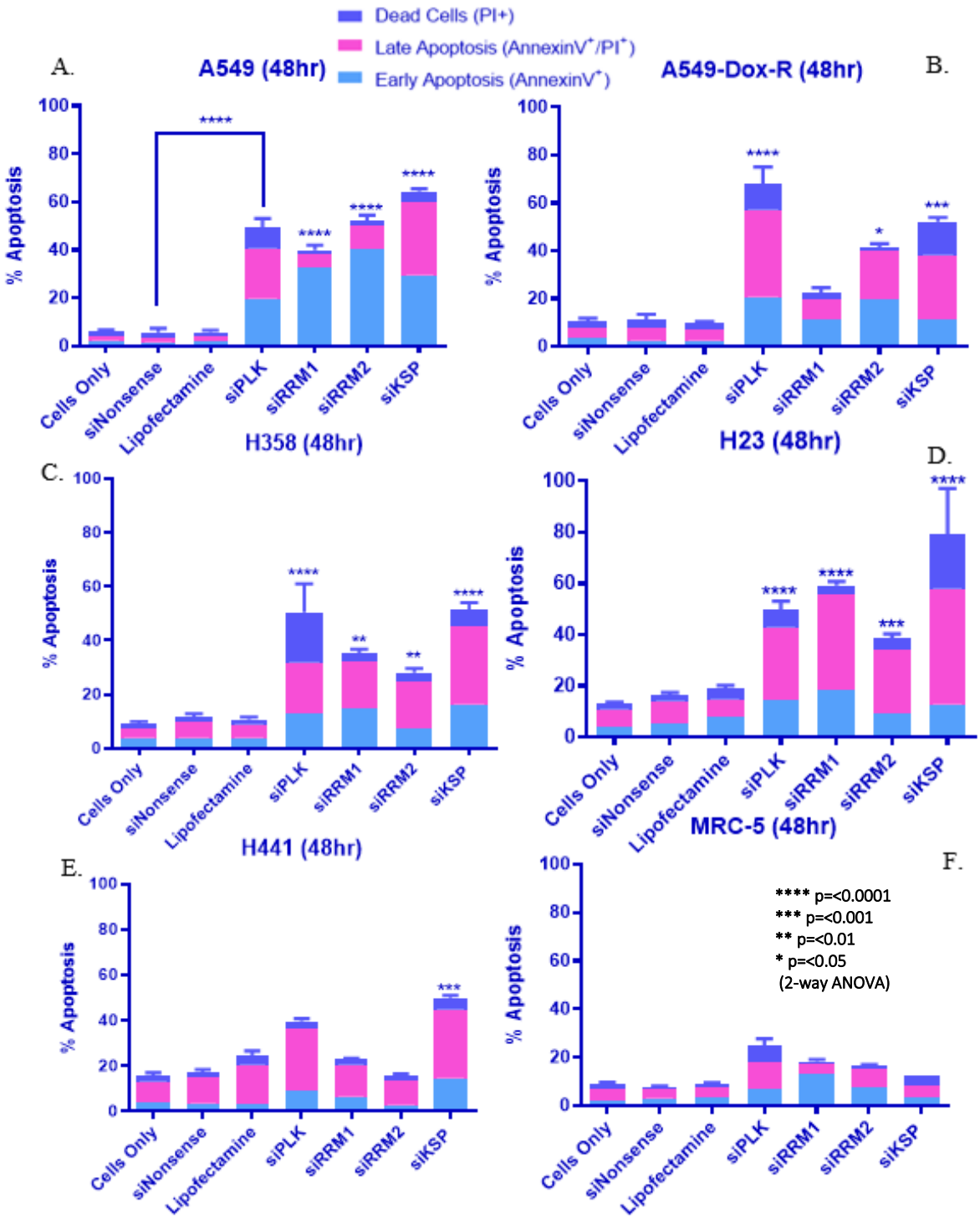

Figure 3.9 Significant levels of apoptosis were measured in NSCLC cell lines transfected with siPLK1, siRRM1, siRRM2 and siKSP compared to the normal cell line MRC-5. NSCLC cell lines *(A-E)* and a normal lung cell line *(F)* transfected with siRNA and after 48hrs stained with Annexin V and propidium iodide. Early (Blue) and Late (Pink) apoptosis levels as well as dead cells (Purple) were measured by flow cytometry and data analysed using GraphPad Prism 8. 2-Way ANOVA with a follow-on Tukey test. n=3 biological triplicates with data presented as mean, error bars +/- Std dev.

3.2.7 Inhibition of PLK1 & KSP causes cell cycle arrest in the NSCLC cell lines

PLK1, KSP and RRM1 are critical in cellular proliferation during the cell cycle and thus they are the proteins of interest. PLK1 plays a vital role in the mitotic spindle formation while KSP enables centrosomes to separate during prophase causing the migration to opposite poles and ultimately a functional bipolar spindle [168]. Using flow cytometry, cell cycle phases of NSCLC cell lines and a normal lung cell line transfected with siPLK, siRRM1, siRRM2 & siKSP, were measured post 24hr after propidium iodine staining, shown in *Figures 3.10 and 3.11.* Cell cycle arrest in the G2 phase of the cell cycle was demonstrated in all NSCLC cell lines post treatment with PLK1 and KSP siRNAs compared to Nonsense siRNA.

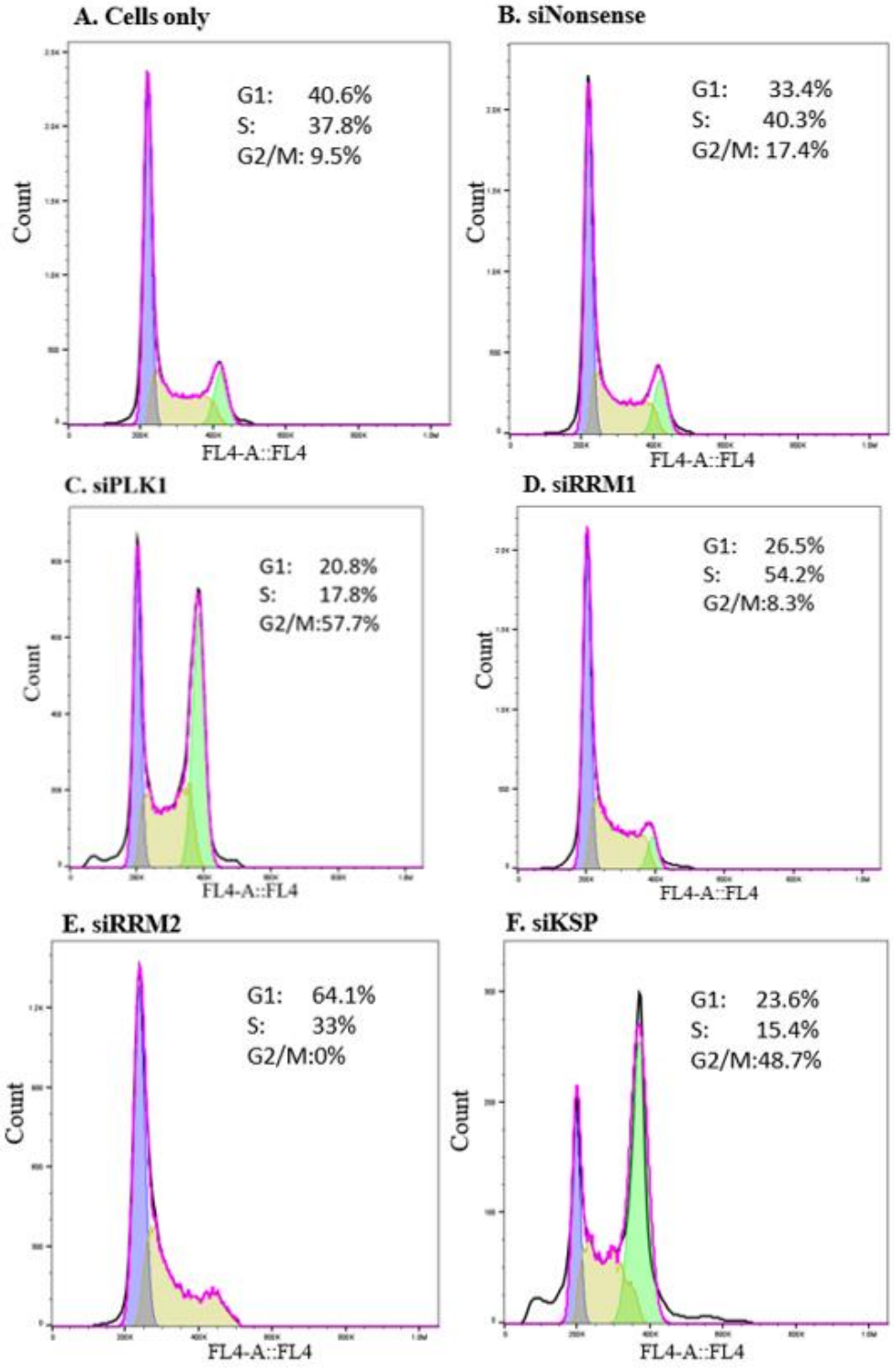

Figure 3.10 A549 cell line undergoes cell cycle G2 arrest. NSCLC cell lines were transfected with siRNA as described in *Figure 3.7*. Post 24hrs after transfection a G2 arrest (green peak) was measured with siPLK1 *(C)* and siKSP *(F)* and a G1 arrest (purple peak) after transfection with siRRM2 *(E)*. Images collected from FlowJo_V10 analysis.

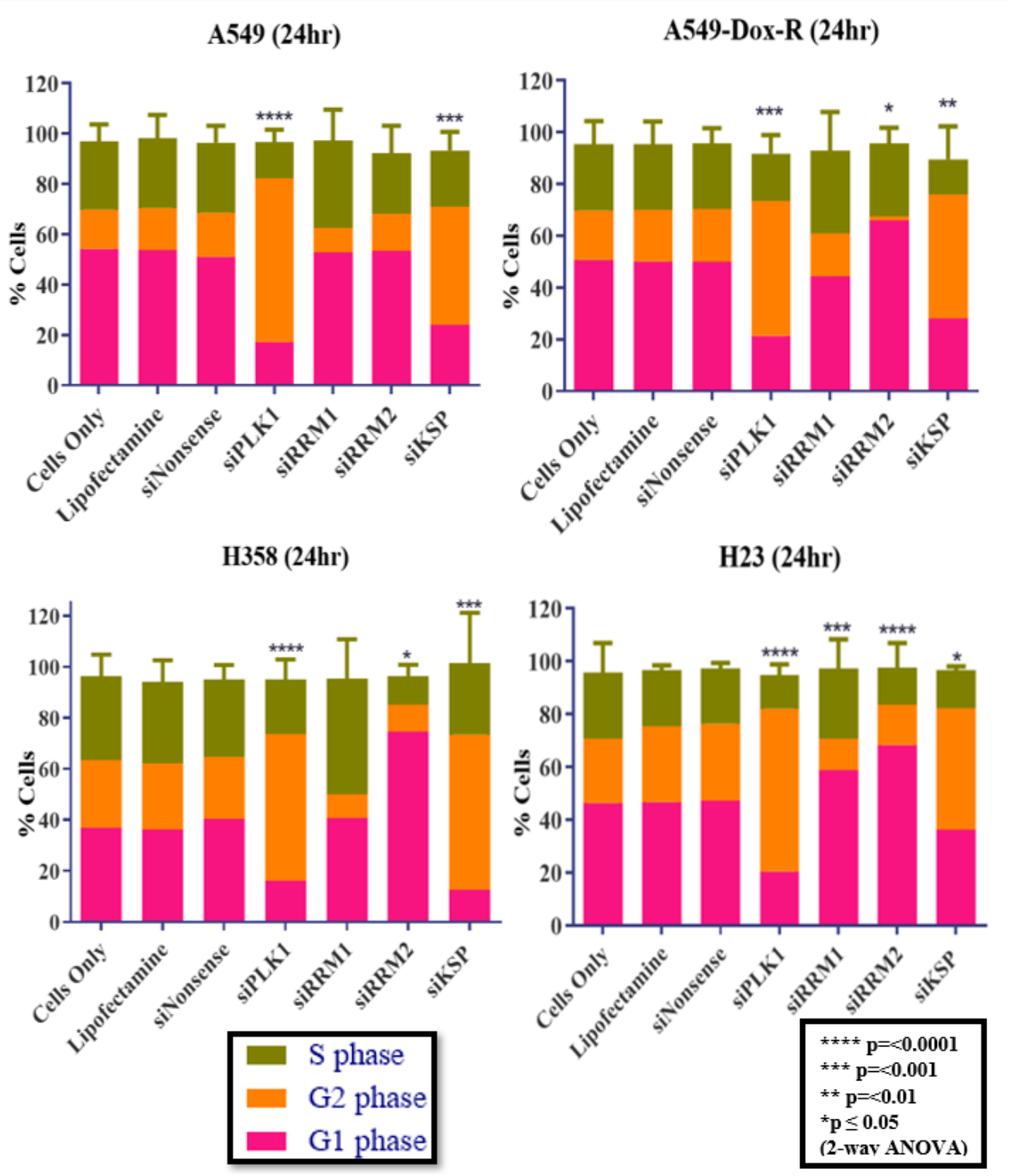

Figure 3.11 Cell cycle G2 arrest occurred in NSCLC cell lines transfected with siPLK1 and siKSP post 24hrs measured by flow cytometry. NSCLC cell lines were transfected with siRNA as described in *Figure 3.7* and post 24hrs stained with propidium iodide. Cell cycle G1 phase (pink), G2 phase (orange) and S phase (Green) were measured by flow cytometry and data analysed using FlowJo (V10, Tree Star, Inc., Ashland, Oregon) and GraphPad Prism software. 2-Way ANOVA with a follow-on Tukey test. n=3 data presented as mean, error bars +/- Std Dev.

3.3 Discussion and Conclusions

A common feature of drug resistant lung cancer cells is the overexpression of *PLK*1, *RRM*1 & *KSP* making them potential targets for treatment of drug resistant NSCLCs [176, 224-226, 232]. One of the major goals of this study was to investigate the potential of siRNAs to these target genes and determine their potential in clinical use in resistant tumours.

To determine the effectiveness of siRNAs in knocking down genes of interest, we used an *in vitro* drug resistant cell-based model (A549-Dox-R) developed previously in our laboratory. In order to establish the optimal conditions for the further experiments, the drug resistant status of this cell line was confirmed. The MTS assay is extensively used to test the drug sensitivity in cancer cell lines [233, 234]. In order to validate the resistance of the A549-Dox-R cell line we conducted MTS assays determining the IC50 compared to the parental A549 cell line, the results revealed a 3-times greater resistance to doxorubicin in the A549-Dox-R cell line. Once the resistance had been established and before proceeding with further experiments, it was imperative to confirm the status of gene expression in our NSCLC cell lines of interest. Previous studies have shown elevation of *PLK*1 [176, 224, 232, 235, 236], *KSP* [226, 237-239] and *RRM*1 [187, 225, 240] in a broad range of cancers. In our own experiments using RT-qPCR we established a profile of gene expression in various NSCLC cell lines compared to a normal lung cell line MRC-5. Similar to *McCarrol et al.* 2015 we found that *PLK*1 was overexpressed in 5/6 of NSCLC cell lines tested, and which included the H441 cell line [176]. The expression of *RRM1* and *KSP* was less consistent. Not all NSCLC cells overexpressed these genes but they were overexpressed in in the drug resistant A549-Dox-R cell line. In subsequent western blot analysis, we found similar results in PLK1 expression being overexpressed in majority of cell lines and KSP and RRM1 expression was again variable. Interestingly the level of expression in our drug resistant cell line did not correlate between experiments as both KSP and RRM1 showed very little increase in protein expression compared to mRNA expression, an anomaly that has previously been witnessed [241, 242]. Post-transcriptional regulations and/or technical reasons could explain these differences. *Marcotte et al.* 2012 explored the major factors regulating protein expression and found a correlation between protein levels and their corresponding mRNAs. However, this could only account for 40% of variation. Further research found that the remaining 60% of variation could be explained by the specific genetic functions; genes that are highly metabolic were found to have high protein:mRNA ratios whereas proteins that are involved in transcriptional regulation had higher degradation and thus

lower ratios [241]. KSP and RRM1 are regulatory proteins and therefore may be degraded rapidly, accounting for the decrease in expression that was measured. Another reason for differing mRNA to protein expressions could be rationalised by the use of different housekeeping controls chosen for RT-PCR and Western Blot respectively. A study looking at rat retinal development adopted the two previously mentioned methods and their housekeeping controls were scrutinised. Housekeeping genes *Rn18s* and *Hprt1* in RT-PCR as well as loading controls β-actin, cyclophilin and α-tubulin showed great variability in Western Blot. *GAPDH* and *Mapk1* proved the most stable in RT-qPCR and MAPK was the greatest stably expressed in Western Blot results [243]. Going forward we could expand and optimise the experiment in this study by testing various housekeeping genes/proteins, especially those found to be most stably expressed for both methods and comparing results.

Overall, these preliminary results confirmed that PLK1 is overexpressed in several NSCLC cell lines, and hence provided confidence in using these cell lines in further studies to examine knockdown of PLK1 expression levels with siRNA.

As previously discussed, potential target genes were chosen for this study from extensive reviewing of the literature and from results produced by the experiments earlier in this chapter [185, 189, 220, 223, 232, 240]. Our subsequent studies aimed to investigate the efficiency of the siRNA of these genes, on our drug resistant cell line alongside other NSCLC cell lines.
Western blot analysis confirmed significant knockdown of PLK1 and RRM1 in A549, A549-Dox-R and H358 from siRNA treatment while KSP knockdown was not significant.
Interestingly there was a high level of protein knockdown post siRRM1 treatment in A549, A549-Dox-R and H358 NSCLC cell lines of just under 80% for all three cell lines which did not completely correlate with our initial Western Blot experiments, where protein expression of RRM1 was only 1.5-2-fold greater than the non-cancerous cell line. From these results it was confirmed that the level of protein expression does not always relate to the level of protein knockdown after treatment of siRNA targeted to the genes encoding such protein. An explanation for this is that the effectiveness of an siRNA is not dependent on level of protein expression and rather depends on its complementarity to the target gene as well as the transfection efficiency of the cell line under study [244]. Further investigation could be carried out in order to explore this anomaly, which may include performing a longer siRNA transfection or using a different type of antibody.

In the following *in vitro* experiments, there was an overall a significant reduction in proliferation as well as increased apoptosis and cell death in the A549, H358, and A549-Dox-R cell lines post *PLK*1 and *KSP* knockdown.

Characterisation of cell cycle regulation using flow cytometry, revealed significant levels of apoptosis in all NSCLC lung cancer cell lines tested, post inhibition of *PLK*1. These results correlated with the results from initial experiments in this study that showed A549 and A549-Dox-R having increased PLK1 expression compared to the normal lung cell line MRC-5 as well as significant PLK1 knockdown of NSCLC cell lines after siPLK1 treatment. These findings were also consistent with other studies, where significant apoptosis after PLK1 downregulation was observed in both ovarian and melanoma cell lines [239].

Initial experiments showed very little KSP expression in all cell lines and the knockdown efficiency was not significant. However, interestingly in subsequent *in vitro* experiments siKSP caused significant cell death as well as cell cycle arrest. Significant cell death with siKSP treatment has also been observed previously in a study using a hepatocellular carcinoma cell line [237]. Overall in the cell cycle analysis, we observed a significant G2 arrest in all NSCLC cell lines transfected with siPLK1 and siKSP, which is also consistent with other studies using colon cancer cells and correlates with their close involvement in mitotic progression stages [168].

In initial experiments RRM1 gene and protein expression was not significant in any cell line although knockdown efficiency with siRRM1 was significant. This correlated with subsequent experiments where siRRM1 caused significant cell death and apoptosis in the A549 cell line.

In conclusion siRNAs encoding for mitotic proteins PLK1 and KSP were shown to be the most effective in causing cell death in NSCLC cell lines *in vitro*.

Chapter 4. Efficacy of EDV^{TM}s loaded with siRNA (*PLK*1, *RRM*1 & *KSP*) determined in 3D cell culture models

4.1 Background

When siRNA is delivered intravenously, it typically disperses through the blood stream and travels to several different organs with little specificity, ie. Systemic delivery [245]. Therefore to deliver siRNAs directly to the tumour site in this study we are using the EDV^{TM} technology developed by EnGeneIC, as described in Chapter 1. A unique characteristic of the EDV^{TM} nanocell is its size of 400nm, which means it will bypass the gaps between blood vessels of normal organs; however, where the blood vessel environment is leaky, a feature of tumour growth, the EDV^{TM} can enter the tumour environment through these leaky blood vessels [168].

A common feature of many cancers, especially NSCLCs, is the presence of the EGF receptor (EGFR) on the surface of the cells [246, 247]. In this study our EDV^{TM}s were designed with a bi-specific antibody to target EGFR. Prior to testing the efficacy of our EDV^{TM}-siRNAs in 3D culture, EGFR expression on the cell lines used was measured to determine whether expression levels were adequate to utilise the unique properties of the EDV^{TM} technology.

When siRNA is loaded into nanoparticles, the number of siRNA copies (copy number) can be measured. Loading siRNA into nanoparticles has previously proved challenging and resulted in a low-entrapment efficiency [248-250]. At EnGeneIC, successful loading of siRNA is determined by measuring the siRNA copy number per EDV^{TM}, which needs to fall within our Quality Control guidelines set for a measurable clinical outcome being >3000copies/ EDV^{TM} (EnGeneIC in house data). Therefore, it was important to investigate if the siRNA copy number in the EDV^{TM}s loaded at > 3000 copies [168].

In the previous Chapter the efficacy of siRNAs on NSCLC cell lines was examined in 2D culture. Although 2D culture provides useful information, a 3D model is more representative of a tumour environment because it mimics cell-cell communications, where cell-matrix exchanges, have both increased spatial depth and cell bonding [251]. Therefore, in this Chapter, we explore and compare the efficacy of siRNAs (PLK1, RRM1 & KSP) encapsulated in EDV^{TM}s using 2 different 3D model cell culture techniques: the conventional method of spheroid culture using low attachment 96 well plates; and the hanging drop method, where the spheroid is suspended as a droplet.

Aim 2. Test the efficacy of siRNA loaded into EDV^{TM} nanocells *in vitro* to decrease gene expression of *PLK*1, *RRM*1 & *KSP* in NSCLC and to result in cell cycle arrest

To achieve this aim:

First, the presence of EGF receptors on the A549 cell lines were investigated and cell lines assessed for antibody-targeted EDV^{TM} binding.

Secondly, EDV^{TM}s were loaded with siRNAs and targeting *PLK*1, *RRM*1 and *KSP* and their copy number measured.

Finally, EDV^{TM}s loaded with the siRNAs were used to treat NSCLC 3D hanging drop spheroids.

4.2 Results

4.2.1 Epidermal Growth Factor receptors are highly expressed in NSCLC cell lines

A unique property of the EDV^{TM} nanoparticle is that it can be decorated with a bi-specific antibody, where one arm binds to the EDV^{TM} and the other arm is free to target and bind to receptors on cancer cells. Our initial experiment was to confirm EGFR status of our NSCLC cell lines through flow cytometry using Quantum simply cellular microspheres to quantitate the number of EGF receptors per cell using the X-Med values of each peak. Firstly, antibody-receptor binding of the anti-EGFR AF488 antibody was optimised *(Fig. 4.1A)* and subsequently the quantity of EGFR receptors was measured on the *A549 (Fig. 4.1B)* and A549-Dox-R *(Fig. 4.1C)* cell lines. Both cell lines showed a high number of EGF receptors per cell, with 349,699 and 387,103 respectively *(Fig. 4.1D),* confirmation that both cell lines could be targeted with EDV^{TM} nanocells targeted with an EGFR antibody.

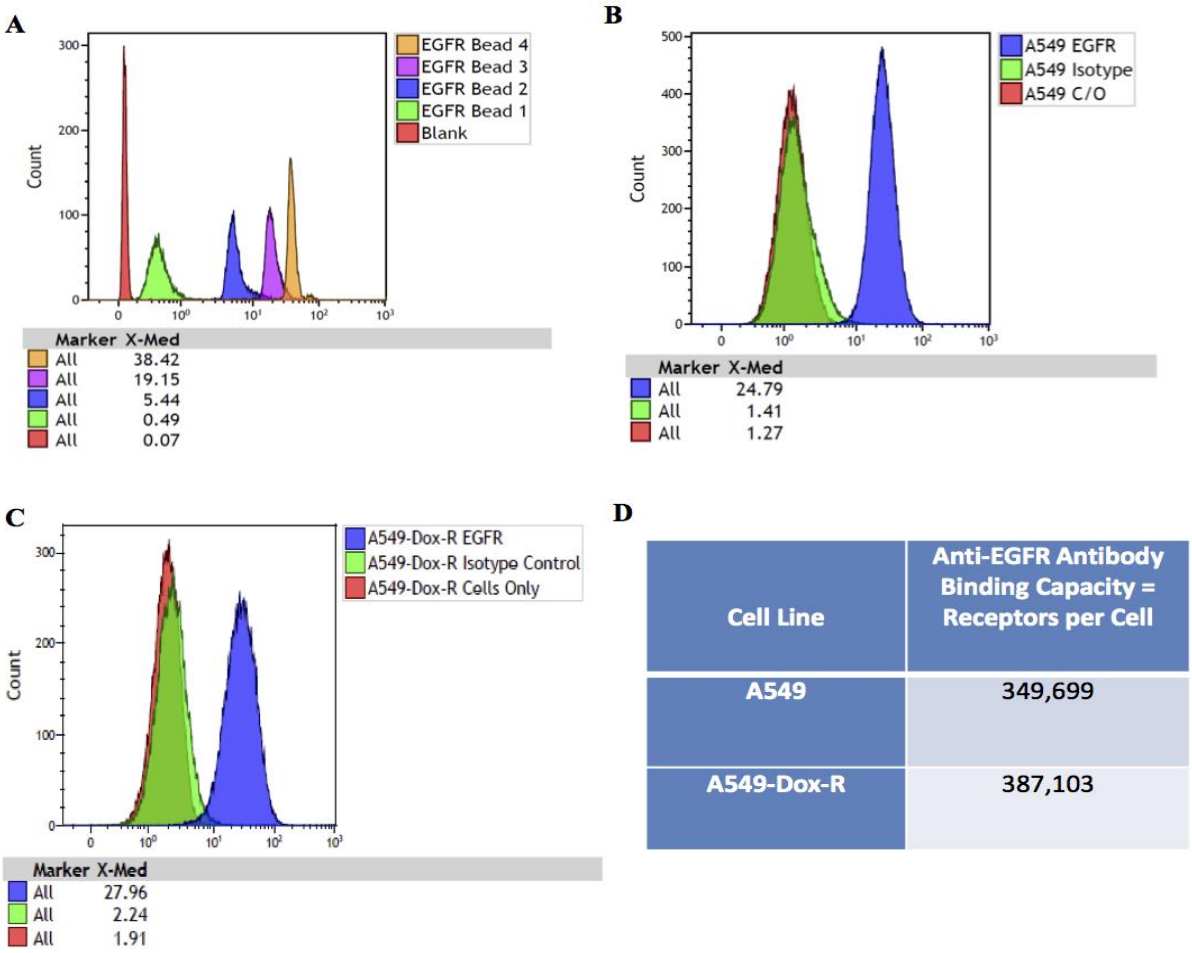

Cell Line	Anti-EGFR Antibody Binding Capacity = Receptors per Cell
A549	349,699
A549-Dox-R	387,103

Figure 4.1 A549 Parental & A549-Dox-R cells express significant numbers of the Epidermal Growth Factor Receptor. Optimisation of the Antibody binding capacity of the anti-EGFR AF488 antibody as determined by flow cytometry (A). Values of X-Med are the median of each peak used to quantify receptor number on control microspheres (beads) 1-4 which are labelled with varying amounts of Alexa Fluor® 488 (AF488). (B) A549 & (C) A549-Dox-R cells were harvested and incubated with Isotype control antibody or Anti-EGFR AF488 antibody, the cells only sample received no treatment. The Isotype control is a primary antibody that lacks specificity to the target but matches the class and type of the EGFR AF488 antibody. The Isotype control was used as a negative control to help differentiate non-specific background signal from specific antibody signal. The samples were analysed via flow cytometry where the surface expression and significant antibody binding capacity of EGFR on A459 cells was exhibited compared to the isotype negative control. (D) Quantification of receptors per cell were generated with the Bangs Laboratories QuickCal program using the median values (X-Med) of peak.

4.2.2 siRNAs are efficiently loaded into EDV^{TM}s

In this experiment the copy numbers for each of the siRNAs targeting *PLK*1, *RRM*1 and *KSP*, samples were measured by staining with an RNA specific dye and measured on a fluorometer. The copy number for siPLK, siRRM1 and siKSP after loading into EDV^{TM}s was 5186, 22880 and 10670 respectively *(Fig. 4.2)*.

EDV spiked siRNA measurement

Samples	RFU	Actual Concentration (ng/uL)
-ve	62	
+ve	610	
	337	10
	221	5
	139	2.5
	103	1.25
	72	0.3125
	68	0.15625
	66	0.078125
EDV	65	0

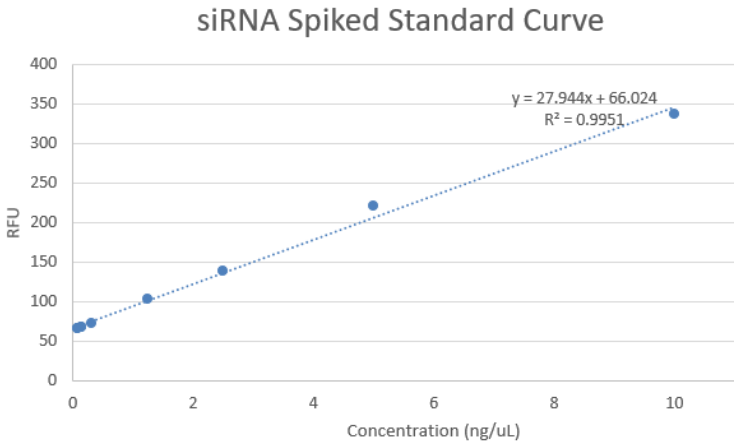

EGFR EDV siPLK1
Amount/1E9 EDV
112.93ng
Copy Number/EDV
5186

EGFR EDV siRRM1
Amount/1E9 EDV
469.39ng
Copy Number/EDV
22880

EGFR EDV siKSP
Amount /1E9 EDVs
218.89ng
Copy Number/EDV
10670

Figure 4.2 Copy numbers of siRNA in EDV^{TM}s. Copy number of siRNAs were measured in EDV^{TM}s against a standard curve and calculated using ENDMEMO RNA copy number calculator [1]. Known concentrations of siRNA were diluted in 1x10^{9} EDV^{TM}s to generate a standard curve using a fluorometer and used to estimate the copy number for *PLK*1, *RRM*1 and *KSP* siRNAs after loading into EDV^{TM}s. Raw fluorescent values were used against the standard curve to calculate the siRNA concentrations.

4.2.3 Hanging Drop method improves uptake of EDV^{TM}s loaded with siRNA in A549-Dox-R spheroids after 72hrs compared to the conventional ultra-low binding plate method.

In this experiment we compared 2 different techniques to culture the spheroids. The hanging drop method (described in section 2.2.13), differs from the conventional method of making spheroids in low attachment 96 well plates in that instead of the spheroid sitting at the bottom of the well and it is suspended in a droplet. The hanging drop technique allows for a greater surface area exposed to treatment; thus, we predicted this technique would result in greater efficacy for EDV^{TM}s to bind to cell surfaces and subsequently release their payload within the cell. A549-Dox-R cells were seeded using both the Hanging Drop spheroid method and the ultra-low binding plate spheroid method. Cells were treated with EDV^{TM}s loaded with siRNA for 72 hours. As predicted, there was a significant increase in the level of cell growth inhibition when using the hanging drop plate *(Fig. 4.3A)* compared to the normal low binding plate *(Fig. 4.3B)*

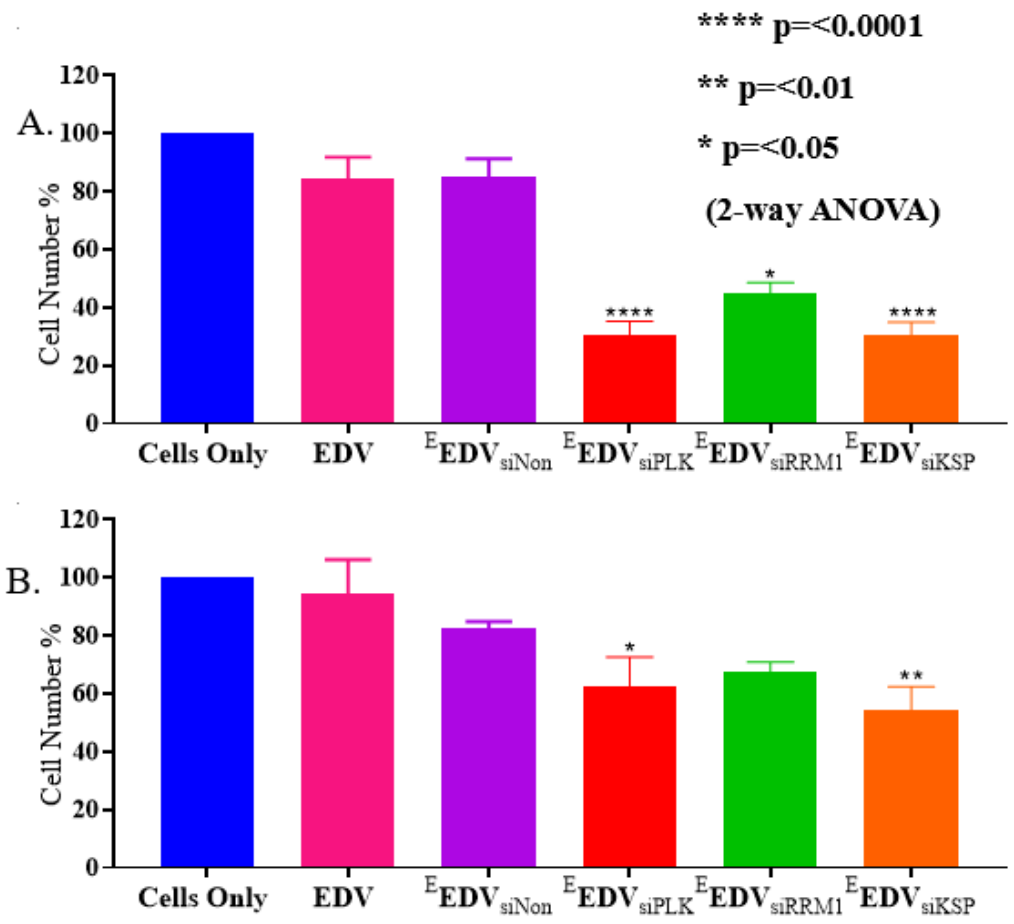

Figure 4.3 Cell growth is inhibited NSCLC hanging drop spheroids after treatment with EDV^{TM}s loaded with siRNAs for 72hrs compared to conventional spheroids. Cells were seeded in hanging drop plates *(A)* or ultra-low attachment plates *(B)* and spheroids were allowed to grow until approximately 300uM when they were treated with 5x10^{8} EDV^{TM}s /spheroid. Post 72 hours spheroids were collected, and cell number was determined via Trypan Blue staining. Data analysed using GraphPad Prism 8. 2-Way ANOVA with a follow-on Tukey test. n=3 data presented as mean, error bars +/- Std Dev.

4.2.4 EDV^{TM}s loaded with siRNA targeting PLK1, RRM1 & KSP inhibit cell proliferation in hanging drop spheroids

For all further experiments, we used the novel 3D 'Hanging Drop' spheroid technique since it had proven to be more efficient than the conventional low attachment 96 well plates, allowing all surfaces of the spheroid to be exposed to targeted EDV^{TM}s. Spheroids were treated with EDV^{TM}s loaded with siPLK, siKSP and siRRM1. Experiment 1 measured cell viability and Experiment 2 examined cell proliferation as these are two distinct properties of cells and it was important to determine that if cell death was not occurring whether cell growth inhibition was being achieved. In Experiment 1 cell viability was reduced in all cell lines, most significantly in the H358 *(Fig. 4.4C)* cell line with 34% viability after EGFR-EDV-PLK1 compared to 91% viability of the negative control EGFR-EDV-siNON. While the viability between the A549 *(Fig. 4.4A)* and A549-Dox-R *(Fig. 4.4B)* wasn't statistically significant, there was a reduction in the size of the spheroids in treated groups, therefore in Experiment 2; NSCLC hanging drop spheroids treated with EDV^{TM}s loaded with siRNA targeting *PLK*1, *KSP* and *RRM*1 *(Figure 4.5)*, cell numbers were measured. In these studies, significant inhibition of cell proliferation, measured by counting cell numbers, was observed in all cell lines A549, A549-Dox-R & H358 *(Figs. 4.5 A, B & C)*. Cells treated with EGFR-EDV-siPLK1 demonstrated inhibition of 54%, 70% and 45%, respectively. EGFR-EDV-siRRM1 caused 54%, 55%, and 29% inhibition in the above cell lines respectively. Finally, in the A549, A549-Dox-R, H358 cell lines, inhibition of cell proliferation was 53%, 70% & 54% respectively after treatment with targeted-EGFR-EDV-siKSP.

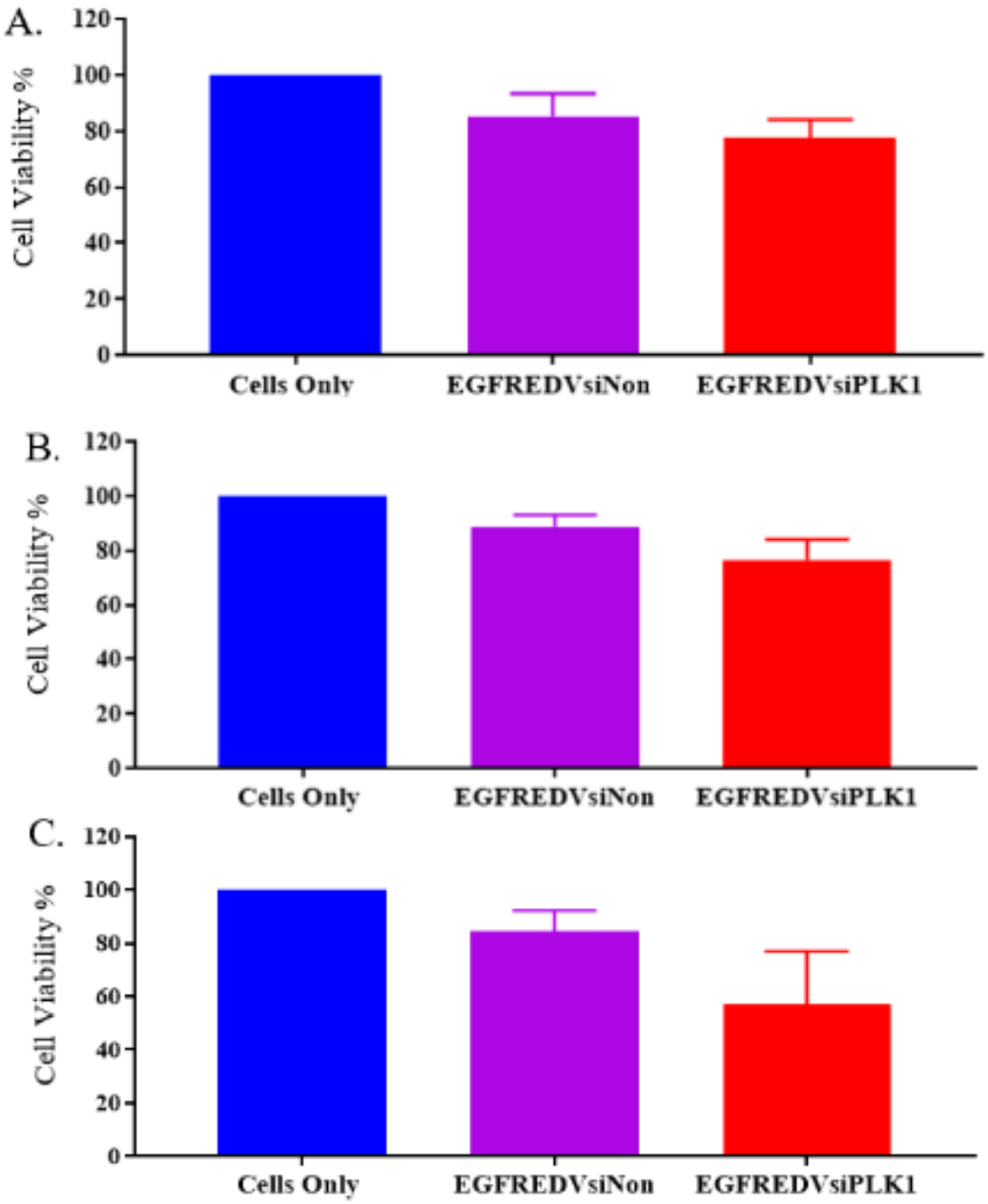

Figure 4.4 Cell viability is decreased in NSCLC hanging drop spheroids after treatment with EDV^{TM}s loaded with PLK1 siRNA. A549 *(A),* A549-Dox-R *(B)* and H358 *(C)* Spheroids were allowed to grow until approximately 300nM when they were treated with 5x10^{8} EDV^{TM}s /spheroid. Post 72 hours spheroids were collected and cell viability was determined via Trypan Blue staining. Data analysed using GraphPad Prism 8. 2-Way ANOVA with a follow-on Tukey test. n=3 data presented as mean, error bars +/- Std dev. No statistical significance ($p>0.05$).

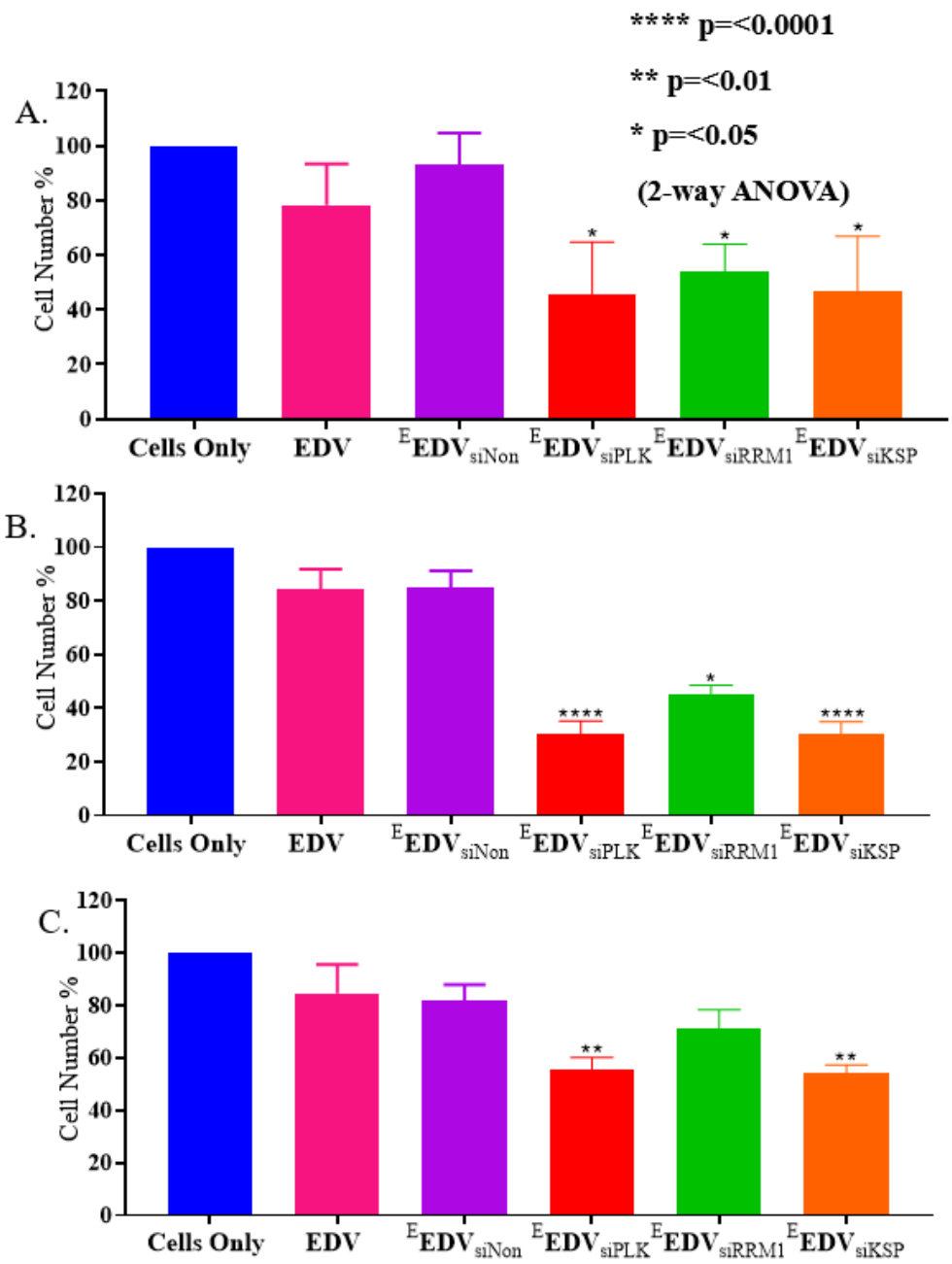

Figure 4.5 Cell growth inhibition in NSCLC hanging drop spheroids after treatment with EDV^{TM}s loaded with PLK1, KSP and RRM1 siRNA. A549 *(A)*, A549-Dox-R *(B)* and H358 *(C)* spheroids were allowed to grow until approximately 300uM when they were treated with 5x10^{8} EDV^{TM}s/spheroid and EDV^{TM}s were targeted to EGFR (E). Treatments were EDV (pink), E-EDV-siNon (purple), E-EDV-siPLK (red), E-EDV-siRRM1(green) and E-EDV-siKSP (orange). Post 72 hours spheroids were collected, and cell number was determined via Trypan Blue staining. Data analysed using GraphPad Prism 8. 2-Way ANOVA with a follow-on Tukey test. n=3 data presented as mean, error bars +/- Std dev.

4.2.5 Targeted- EDV^{TM}s loaded with PLK1 and RRM1 siRNAs decrease gene expression of PLK1 and RRM1

NSCLC hanging drop spheroids *(Figs 4.6 A, B, & C)* were treated with EDV^{TM}s loaded with an siRNA nonsense (siNonsense2), and siRNAs targeting PLK1 and RRM1. The efficiency of the knockdown of these genes was tested using RT-qPCR. There was significant knockdown of PLK1 in both the A549-Dox-R *(Fig. 4.6A)* and H358 *(Fig. 4.6C)* cell lines by the siPLK1 loaded EDV^{TM}s, this also coincided with knockdown from EGFR-EDV-sinonsense2. EGFR-EDV-si-nonsense2 was a negative control not previously used in our experiments. However, this unexpected knockdown result indicated that the nonsense sequence had some homology to siPLK1 sequence. Using the Basic Local Alignment Search Tool (BLAST®) [252], it was discovered that the nonsense sequence that was loaded into our EDV^{TM} has 68% homology to STE20 like kinase (SLK) which is a known regulator of PLK1 and constitutes the mammalian ste-20-like kinase (MST) pathway which is responsible for cell survival [253]. This provides a possible explanation for the unexpected result via indirect gene knockdown of SLK/PLK1. The use of this nonsense sequence was abandoned for further experiments.

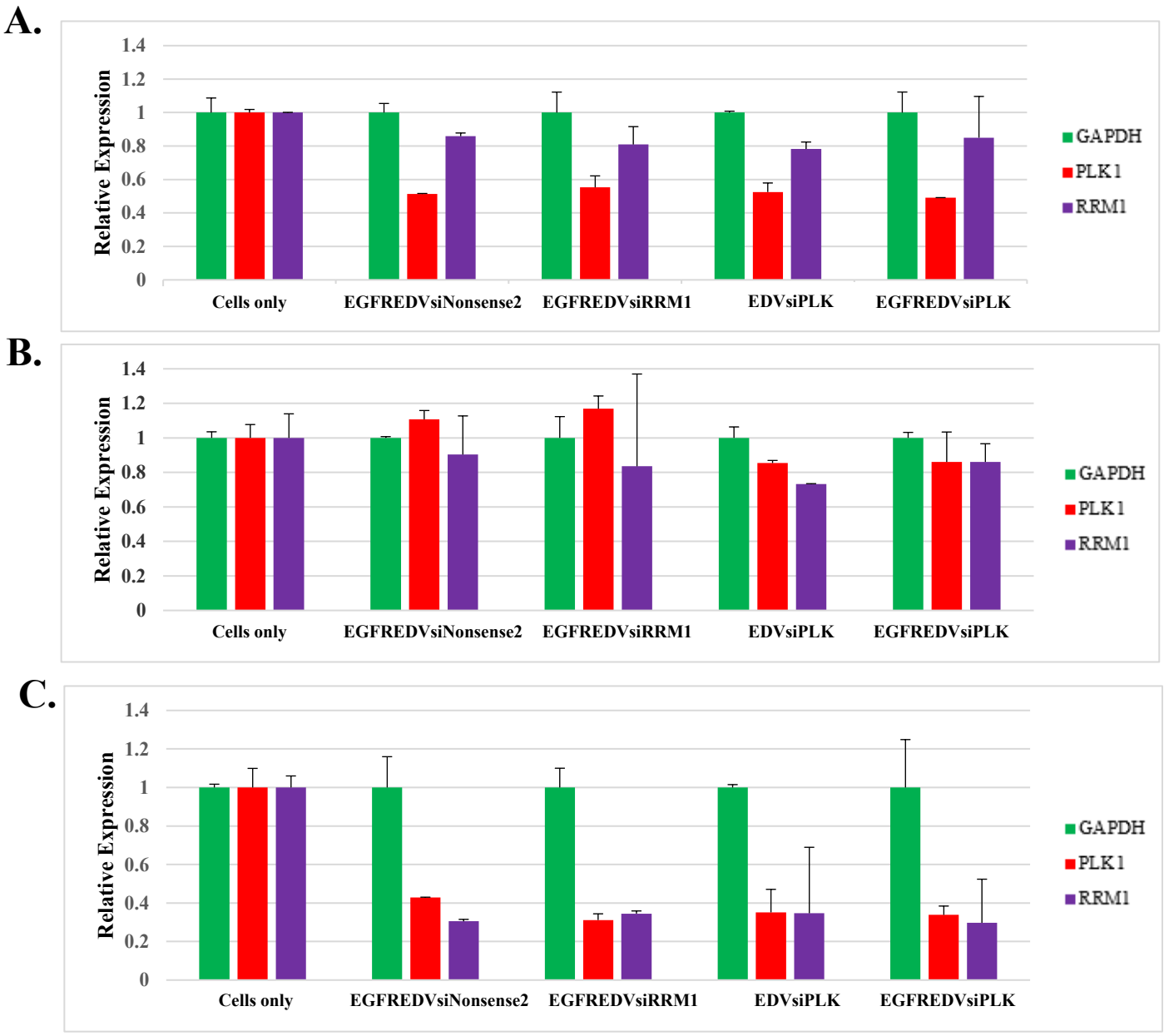

Figure 4.6 RT-qPCR validation of gene knockdown of *PLK1* in NSCLC cell lines. The knockdown of the genes PLK1 (red) and RRM1 (purple) after treatment with EDV^{TM}s loaded with sinonsense2, siPLK1 and siRRM1, was tested in A549-Dox-R *(A),* parental A549 *(B)* and H358 *(C)* cell lines using RT-qPCR. The housekeeping gene (green) used was *GAPDH* and EGFREDVsiNonsense served as a negative control. RT-qPCR carried out using 7500 Software v2.3 and analysed using DataAssist^{TM} v3.01. Error bars +/- Std dev of technical triplicate ($p>0.05$).

4.3 Discussion and Conclusions

The studies in this Chapter set out to determine the efficacy of EDV^{TM}-siRNAs targeting *PLK*1, *RRM*1 and *KSP* using 2 different 3D cell culture models. The initial experiments in this chapter were performed to verify the EGFR status of NSCLC cell lines by flow cytometric analysis. EGFR overexpression is a well-known feature in a variety of cancers with solid tumours [254-259] and specifically NSCLC tumours [246, 247, 260, 261], and therefore, provides a potential target for the EDV^{TM} nanocell technology. The EDV^{TM} is targeted with a bi-specific antibody which allows it to attach to the EGF receptor presenting on tumour cells [168, 203, 205], then the complex has been shown to enter the cancer cell by endocytosis and consequently release its payload of drug or siRNA to ultimately halt tumour cell growth or cause cell death [168, 262]. In this Chapter, we demonstrated significant EGFR expression in the A549 & A549-Dox-R cell lines confirming the use of these cells as suitable targets for EGFR-EDV treatment. Other molecular targets that are currently being explored in NSCLC include the anaplastic lymphoma kinase and ROS1, and there is a shared belief that patients should undergo mutational testing as common practice in the future [263].

Current research involves many types of nanoparticles being loaded with drugs and/or nucleotides to be used to treat many different cancers and diseases [153, 162, 168, 200, 264-266]. Previously there has been development counting nanoparticles in the environment using various techniques including inductively coupled plasma mass spectrometry (ICP-MS), liquid chromatography-mass spectrometry (LC-MS) and laser-induced breakdown spectroscopy, however these methods are unable to discriminate size of particles [267]. However, once nanoparticles are loaded, an important practice is to attempt quantification of the amount of loaded material, which has proven challenging in some cases [268]. Within the field of cancer research, delivery of nanoparticles into live cancer cells has been explored and measured using electron and fluorescent microscopy and drug contents of these nanoparticles were successfully quantitated using High Performance Liquid Chromatography (HPLC), LC-MS and ICP-MS [205, 269]. More recently, the quantification of siRNA duplexes bound to gold nanoparticle surfaces was achieved using a fluorescence-based assay although research involving measurement of siRNA within a nanoparticle is lacking [270].

Visual quantification of nanoparticles *in vitro* has also been investigated by transfecting cells with siRNA that has been labelled with a fluorescent tag and visualising with confocal microscopy [176] . *McCarrol et al.* 2015 visualised the lysosomes carrying siRNA into cells *in vitro* and captured them then releasing their payload. These experiments were expanded *in vivo* in an NSCLC orthotopic model where tumour growth was confirmed using micro-CT analysis or bioluminescent imaging. After treatment with the fluorescently labelled siRNA packaged nanoparticles, the biodistribution of the particles was assessed from frozen sections of the tumour, liver and spleen tissues through confocal microscopy visualisation, with strong fluorescence witnessed in the siRNA/nanoparticle treatment group compared to the siRNA alone group. This finding enforces previous research that free siRNA is eliminated by the body if it is not encapsulated for administration and emphasises the importance of the EDV^{TM} nanocell technology.

While siRNA loaded nanoparticles have been visually quantified, the aim of quantifying the amount of siRNA inside the particle itself has been more challenging. One method of calculating the amount of siRNA within cells has been explored by *Cruz & Houseley* 2014 after siRNA extraction through Hot phenol RNA preparation, GTC-phenol RNA preparation or Small RNA purification, by Quantitative PCR or imaging gels using AIDA (Fuji) or ImageQuant (GE) analysis instruments [271]. Using the quantified amount of siRNA, the researchers calculated the copy number, and the presence of a correlation between high copy number and increased rate of RNAi was investigated. It was found that the greater level of copy number equated to a greater amount of RNA was knocked down. In our study we found that high copy numbers did not necessarily correlate with increased gene knockdown and thus lead to the conclusion that a greater copy number does not necessarily equate to a greater efficacy of siRNA which we hypothesise could be to do with where the target resides in the cell.

In this study, a technique developed by EnGeneIC was utilised to ensure effective loading of an siRNA into the EDV^{TM} by determining the copy number/nanocell using a standard curve of known quantities of nonsense siRNA loaded EDV^{TM}s Specifically the concentration of siRNA for each of the PLK1, RRM1 and KSP siRNA loaded EDV^{TM} samples were measured by staining with an siRNA specific dye, measuring on a fluorometer, and the raw fluorescent values were used against the standard curve to calculate the siRNA concentrations which were in turn used to calculate the copy number. Interestingly we had varying results with EDV^{TM}s

loaded with siPLK, siRRM1 and siKSP ranging from 5000 – 23000 copies siRNA/ EDV^{TM}, much greater payloads than had been found for synthetic nanoparticles [272]. Going forward further work need to be done using the standard curve method used in this study compared to RT-qPCR method of measuring copy number.

The mechanism by which siRNA enters the EDV^{TM} is not fully understood but we hypothesise it is affected by differing charges of the nanoparticle surface, the charge in the channels in the nanocells membrane, as well as the charge of the siRNA itself. We understand that after the 24hrs of incubation of EDV^{TM}/siRNA, loading of siRNA reaches a point of saturation., (EnGeneIC in-house data). Although we are yet to find definitive reasoning behind differing copies of siRNA that is loaded, as previously mentioned we found that the greater copy number didn't equate to superior efficiency in knockdown. In fact, our siRRM1 loaded EDV^{TM}s which had the highest copy number of siRNA per cell showed to be the least effective in cancer cell growth inhibition and ultimately gene knockdown. A possible explanation for this is the importance of the gene or the position in the cell for the siRNA to access it, although further research needs to be done.

As previously mentioned, EnGeneIC investigated the treatment of siRNA targeting MDR1 followed by a chemotherapeutic drug (irinotecan or 5-FU) in the treatment of drug-resistant colon cancer cells. This two-wave treatment caused significant inhibition of tumour growth compared to all control groups [168]. Research has also been conducted to investigate the loading of both an siRNA and a drug simultaneously in a nanoparticle. *Zou et al.* 2012, investigated loading Bcl-2 siRNA into a copolymer and using this alongside Doxorubicin in the treatment of ovarian cancer cells [273]. There was a significant increase in apoptosis after combined treatment compared to siRNA and drug alone controls, which emphasised the synergistic relationship of the two treatments. *Jang et al.* 2016, furthered this research by loading two siRNA targeting MDR1 and BCL2 into nanoparticles and treated MDR KB-V1 cells sequentially with Doxorubicin [274]. Apoptosis was decreased after individual treatment with the siRNAs, when compared to combined treatment. The greatest level of apoptosis was seen when the siRNA combination was combined with doxorubicin treatment. Going forward, this study could be expanded to load two siRNAs into a single EDV^{TM}, for example siPLK1 and siKSP treatments loaded together or in combination with EDV^{TM} carrying drug

For the past 50 years, 2D cell culture has been the standard practice for testing new therapeutics pre-clinically in the field of oncology as the method is simple, cost-effective and non-laborious. However, the limitations of 2D culture, most significantly that they are not a true representation

of a tumour within the body, have resulted in the development of 3D models to observe and treat cancer cells, [275]. Agitation based spheroid formation involves seeding cells on a surface that is constantly moving to prevent any adhesion, resulting in the formation of aggregates that are easily accessable and have the potential to be quite large in dimension [276-278]. Downfalls of this method include significant variation in size and shape of spheroids, the stress of the constant shaking of spheroids and the fact that spheroids are not in indvidual compartments. This technique would not be suitable for many studies including this one, as spheroids could not be individually treated in groups and thus cell growth inhibition, cell cycle and/or cell death could not be monitored or measured with appropriate controls in place.

Another method, liquid overlay, involves cell aggregation on a substrate that is non-adhesive. There is less cell stress since it does not require constant movement and spheroids can be cultured for long periods [277, 279]. Major disadvantages include significant variation of size, shape and quantity of spheroids produced, as well as the laborious task of coating of surfaces in order to enable aggregation. A newer method of spheroid formation that has overcome the re-occuring issue of size and shape variation, is the hanging drop technique, which involves the aggregation of cells at the bottom of a droplet suspended in the air [276, 277, 280]. This method is unique as it offers control of the dimensions of the spheroids as well as limited sheer stress. Limitations are that it is labor intensive, difficult to scale-up and only allows for time restricted cell culture [275].

Most recently there have been specific plates manufactured that allow the creation of 3D spheroids with ease, including the ultra-low binding plates and hanging drop plates. Previous studies have been carried out to investigate the effects of using these two different methods of spheroid formation. *Raghavan et al*. (2016) compared the different spheroid making methodologies including hanging drop and ultra-low binding techniques with ovarian cancer cell lines. The hanging drop methods proved to enhance spheroid compaction and caused greater chemoresistance to cisplatin [281]. These results emphasise the importance of methodology choice and reveals that the hanging drop method produces spheroids that are more likely to represent a tumour mass in the human body. Using the conventional methods, and their resulting spheroids with uncompacted cellular arrangement, may produce results that show treatments to be more effective than they would truly translate *in vivo*.

In this Chapter, we compared the 2 different techniques to culture the spheroids (the ultra-low binding plates and the hanging drop method). We hypothesis that the hanging drop method, with the greater surface area exposed to treatment, would result in greater efficacy of the EDV^{TM}s. A549-Dox-R spheroids in both the hanging drop method as well as the ultra-low

binding plate method were treated with EDV^{TM}s loaded with siRNA for 72hours. Significantly greater growth inhibition of spheroids was observed when using the hanging drop plate in all EDV^{TM} treatment groups compared to the normal low binding plates. This correlates with the previously mentioned research and confirms our hypothesis that the greater surface area exposed allowed greater binding and efficacy of the EDV^{TM}s [281].
Expanding our use of this novel technique, different NSCLC hanging drop spheroids were treated with EDV^{TM}s loaded with siPLK, siKSP and siRRM1 for 72hrs and cell viability was reduced in all cell lines. Cell number was significantly reduced in treatment groups compared to the control groups. We recorded an inhibition of cell growth which coincides with previous *in vitro* studies where we found significant cell cycle arrest after treatment with siRNAs targeting *PLK*1, *KSP* and *RRM*1. As these siRNAs are involved in halting the cell cycle [220] our results showed treated cells were proliferating at a much lower rate. Importantly, we were also able to confirm that EDV^{TM}s are a more effective treatment when using the hanging drop plates compared to the traditional low-binding method of spheroid formation cultured on plates. The hanging drop method allows for all surfaces of the spheroid to be exposed to drugs, targeted EDV^{TM}s which reflects the increase in treatment efficacy using this method.

Finally, an experiment was conducted to test the gene knockdown of NSCLC hanging drop spheroids treated with siRNA loaded EDV^{TM}s and measured by RT-qPCR. There was significant knockdown of PLK1 in both the A549-Dox-R and H358 cell lines by the siPLK1 loaded EDV^{TM}s, albeit our negative control, EGFR-EDV-si-nonsense2 also showed significant knockdown in both PLK1 and RRM1 in the H358 cell line. One reason for this unexpected result is possibly due to the si-nonsense2 control having high homology to the SLK gene, which is a known regulator of PLK1 and influences cell cycle survival. Comparing si-nonsense sequences would be useful before committing a negative control to further experiments. Interestingly, there was also greater knockdown in the A549-Dox-R cell line than its parental A549 cell line. This occurance has also been witnessed in a cisplatin-resistant ovarian cancer cell line ACRP when compared to it's parental A2780 cell line [282].

Overall, in this study we confirmed that siRNAs were efficiently load into EDV^{TM}s with high copy numbers. The best method of spheroid production was deduced and EDV^{TM}s were successfully taken up by hanging drop spheroids with increased efficacy of the siRNAs loaded into the nanocells targeting *PLK*1, *RRM*1 and *KSP* within the cells.

The hanging drop methodology is known to be notoriously difficult, yet has proven to be the most successful in mimicking a tumour environment in the human body, thus it was chosen for this study. Although there was no consistent statistical difference using this methodology in all experiments, we observed a very clear trend of cell growth inhibition after siRNA/treatment which mimicked the monolayer cell culture experiments and this was confirmed in our animal model study. Therefore, supporting the efficacy of these siRNA/EDV^{TM} treatments. Future studies could include apoptosis assays and the use of fluorescently tagged siRNAs to show they are effectively entering the cells contained within the spheroids, to validate the findings of this chapter.

Overall, we demonstrated that cell proliferation of spheroids was successfully inhibited when treated with EDV^{TM}s loaded with siRNA aimed at our target genes.

Chapter 5. Efficacy of EDV^{TM}s loaded with siRNA (*PLK*1, *RRM*1 & *KSP*) to overcome drug resistance in a resistant NSCLC mouse model

5.1 Background

Nanoparticle-based delivery systems has become increasingly popular of the last decade and is now a major part of cancer research [193-199]. Targeted encapsulated drug administration has proven to be more efficacious than systemic administration of drugs since higher concentrations of drugs can be delivered to the tumour (discussed in Chapter 1, sections, 1.6.2 and 1.6.3). Encapsulation of drugs, i.e. in liposomes, micelles, lipid nanoparticles, protein-based particles and polymeric nanoparticles and EDV^{TM}s, protect the drugs from being destroyed by the body's natural defence system [79, 193]. Similarly, when siRNAs are encapsulated within EDV^{TM}s they are protected from being targeted by the body's immune system compared to systemically administered naked siRNA [168]. With the added benefit of being able to target EDV^{TM}s to specific receptors on a tumour, intact siRNA- EDV^{TM}s allow direct delivery inside the tumour cell.

We successfully demonstrated EDV^{TM}-siRNA delivery and potential efficacy using 3D *in vitro* models, as described in Chapter 4. It also known from EnGeneIC research that due to the extravasation of EDV^{TM}s through leaky blood vessels into the tumour micro environment, *in vivo* experiments will necessarily give a 'better" result than in tissue culture. In this Chapter, we examined the effects of the siRNAs loaded EDV^{TM}s in a pre-clinical *in vivo* mouse model. Since drug resistance is the major cause of death in NSCLC patients, we used the drug resistant A549-Dox-R xenograft mouse model established at EnGeneIC.

Aim 3. Test the efficacy of siRNA loaded into EDV^{TM} nanoparticles *in vivo* using an established mouse xenograft model.

To achieve this aim:

First, we tested the efficacy of EDV^{TM}s loaded with siRNAs targeting *PLK*1, *RRM*1 and *KSP* *in vivo* in the A549-Dox-R xenograft mouse model.

Secondly, RT-qPCR analysis was conducted to assess gene knockdown of *PLK*1, *RRM*1 and *KSP* in tumours excised from the A549-Dox-R *in vivo* experiment after undergoing EDV^{TM}-siRNA treatment.

5.2 Results

5.2.1 EDV^{TM}s loaded with PLK1, RRM1 and KSP siRNAs cause tumour growth inhibition in a drug resistant A549-Dox-R xenograft model

EDV^{TM}s loaded with siNonsense, siPLK1, siRRM1 and siKSP were tested *in vivo* using the A549-Dox-R xenograft mouse model *(Figure 5.1)*. After 7 treatment doses tumour volumes of EGFR-EDV-siPLK1 and EGFR-EDV-siKSP treatment groups were measured and found to be significantly smaller than the Saline treatment group. The most important significance was in the reduction in tumour size of EGFR-EDV-siPLK1 and EGFR-EDV-siKSP treated mice compared to the EGFR-EDV-siNonsense treated group *(Figure 5.2)*. Tumours treated with EGFR-EDV-siPLK1, EGFR-EDV-siKSP and EGFR-EDV-siRRM1 were all significantly smaller than the EGFR-EDV-Dox control group.

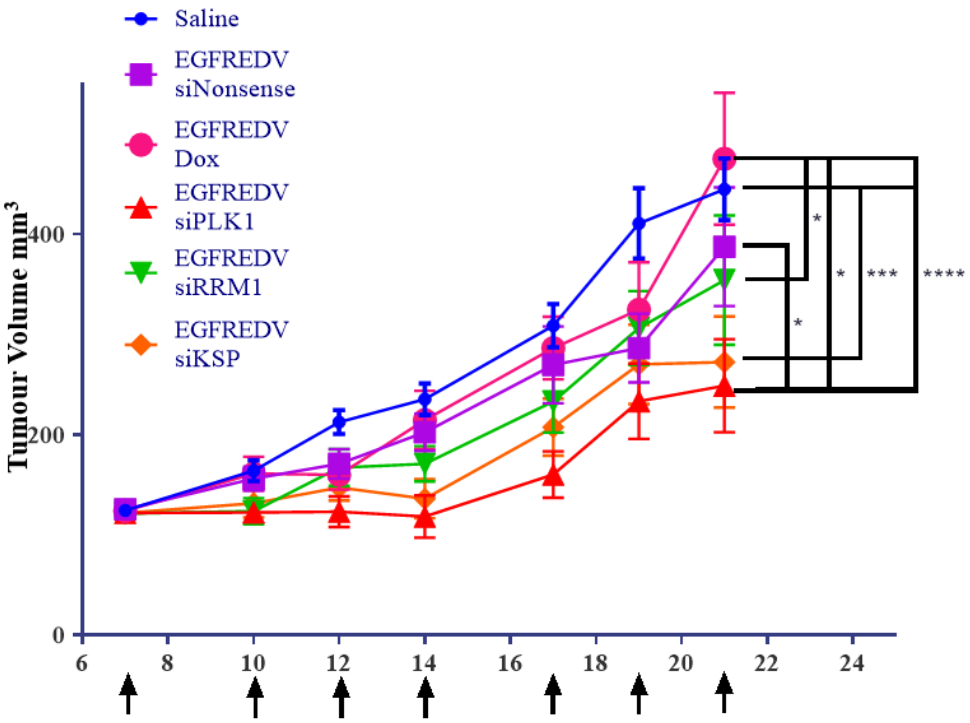

Figure 5.1 EDV^{TM}s loaded with siPLK1 & siKSP demonstrate significant tumour inhibition in A549-Dox-R xenograft. Balb/C nu/nu mice were injected with 5x10^{6} A549-Dox-R cells and tumours grown to 125mm-150mm. 2x10^{9} EDV^{TM}s were administered by intravenous injection, 3 times a week for 2 weeks. Tumours were measured 3 times a week and on completion of the study the tumours were extracted for RT-qPCR analysis of gene knockdown. Error bars +/- Std dev of n=7 mice/treatment. Data entered into GraphPad and a 2 way-ANOVA was performed with a follow-on Tukey test.

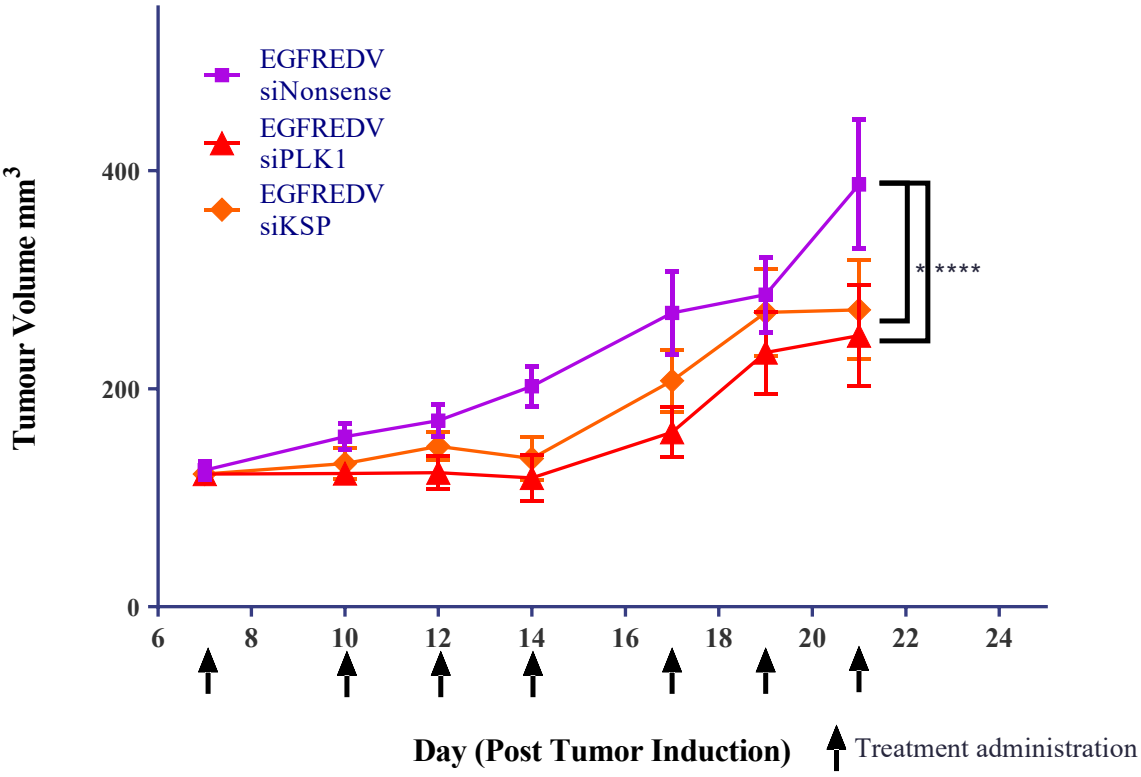

Figure 5.2 EDV^{TM}s loaded with siPLK1 & siKSP demonstrate significant tumour inhibition in A549-Dox-R xenograft compared to siNonsense. Balb/C nu/nu mice were injected with A549-Dox-R cells and EDV^{TM}s administered as described in *Figure 5.1*. Error bars +/- Std dev of n=7 mice/treatment. Data was entered using GraphPad and a 2 way-ANOVA was performed with a follow-on Tukey test.

5.2.2 EDV^{TM}s loaded with PLK1 and KSP siRNAs inhibit gene expression in a drug resistant A549-Dox-R tumour

After successfully inhibiting tumour growth with EDV^{TM}s loaded with siPLK and siKSP *in vivo* we further investigated the efficiency of the siRNAs to knockdown the respective RNAs (PLK and KSP) using RT-qPCR. Knockdown of *PLK*1 was evident in tumours treated with EDV^{TM}s loaded with siPLK1. Surprisingly, siKSP loaded EDV^{TM}s also downregulated *PLK*1. Similar results were observed in tumours treated with EGFR-EDV-siKSP, with decreased expression of *KSP* and *PLK*1 compared to controls (*Figure 5.3 A & B*). Treatment with EGFR-EDV-siRRM1 did not knock-down *RRM1 gene (Figure 5.3 C)* and there was a significant but much smaller inhibition of tumour growth *in vivo* compared to other treatments. However, there was knockdown of *PLK*1 and *KSP* genes (*Figure 5.3 A & B)* after EGFR-EDV-siRRM1 treatment compared to the EGFR-EDV-siNonsense control. Decreased expression of *PLK1* and *KSP* was measured in RNA extracted from tumours treated with EGFR-EDV-Dox which was unexpected *(Figure 5.3 A & B).*

A.

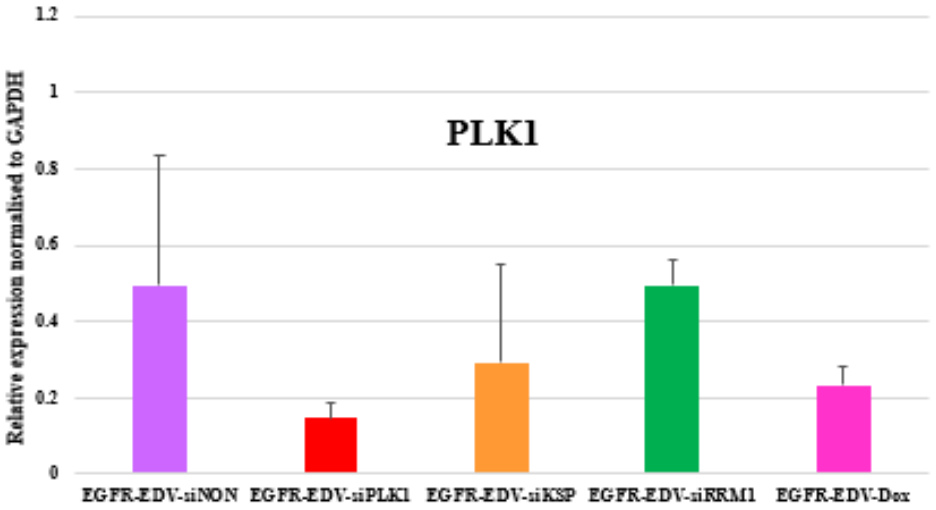
PLK1
Relative expression normalised to GAPDH
1.2
1
0.8
0.6
0.4
0.2
0
EGFR-EDV-siNON
EGFR-EDV-siPLK1
EGFR-EDV-siKSP
EGFR-EDV-siRRM1
EGFR-EDV-Dox

B.

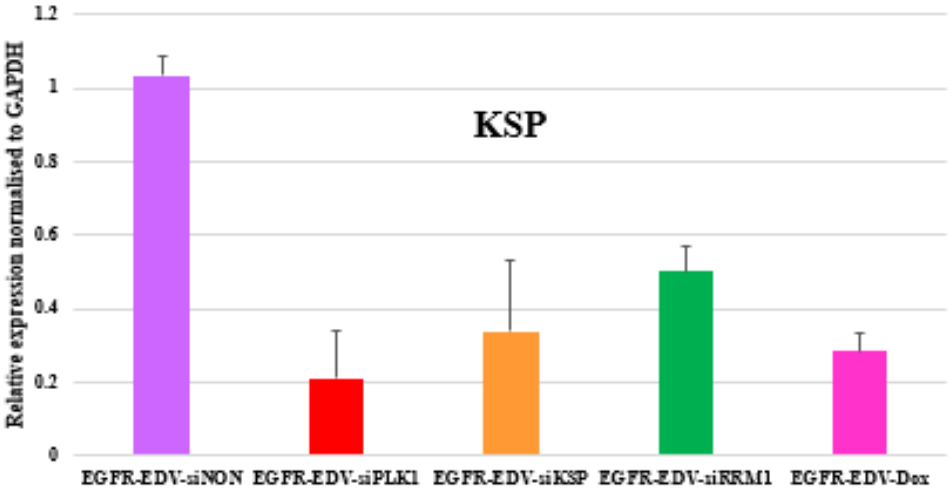
KSP
Relative expression normalised to GAPDH
1.2
1
0.8
0.6
0.4
0.2
0
EGFR-EDV-siNON
EGFR-EDV-siPLK1
EGFR-EDV-siKSP
EGFR-EDV-siRRM1
EGFR-EDV-Dox

C.

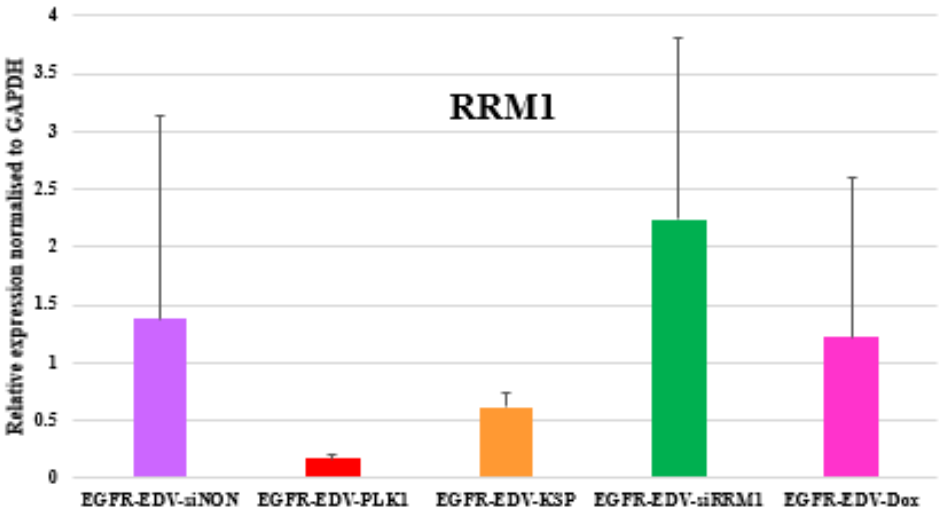
RRM1
Relative expression normalised to GAPDH
4
3.5
3
2.5
2
1.5
1
0.5
0
EGFR-EDV-siNON
EGFR-EDV-PLK1
EGFR-EDV-KSP
EGFR-EDV-siRRM1
EGFR-EDV-Dox

Figure 5.3 Gene knockdown with EDV^{TM}s loaded with siPLK1 & siKSP. The expression of three genes *PLK*1 (A), *KSP* (B), and *RRM*1 (C), was tested in A549-Dox-R tumours treated with EGFR- EDV^{TM}s loaded with siNonsense (purple), siPLK1(red), siKSP (orange), siRRM1 (green) and Doxorubicin (pink) using RT-qPCR. The housekeeping gene used was GAPDH EGFR-EDV siNonsense served as a negative control. RT-qPCR carried out using 7500 Software v2.3 and analysed using DataAssist^{TM} v3.01. Error bars +/- Std dev of technical triplicate, ($p<0.05$).

5.3 Disscusion and Conclusions

Previous *in vivo* studies have used various nanocarriers/particles to transport siRNA to colon, ovarian and lung mouse models with varying results as discussed in *section 1.6.2* [165, 176, 192, 196-198]. Our *in vivo* study demonstrated that EGFR-EDV-siPLK1 and EGFR-EDV-siKSP were effective in inhibiting tumour growth compared to EGFR-EDV-siNon and saline alone respectively in a drug resistant, A549-Dox-R xenograft. After four treatments there was a significant decrease in tumour growth between control groups and siRNA treated groups. However, when there was a 2-day break between treatments, tumours began to regrow in mice targeted with EGFR-EDV-siPLK1 and EGFR-EDV-siKSP. Tumour growth was again inhibited after resumption of treatment with EGFR-EDV-siPLK1 and EGFR-EDV-siKSP when compared to control animals.

In earlier *in vitro* experiments, there was significant cell growth inhibition within spheroids after treatment with EGFR-EDV-siRRM1 as displaed in *Figure 4.3* (A549) and *Figure 4.5* (A549 & A549-Dox-R). However, EGFR-EDV-siRRM1 did not cause cell cycle arrest *in vivo* and limited tumour growth inhibition was observed. Lack of reproducibility from *in vitro* to *in vivo* of siRNA mediated downregulation of target genes has been reported in other studies. s [283, 284] . A study investigating the role of stromal cells in metastasis reported a significant lack of reproducibility between *in vitro* and *in vivo* experiments [283]. This was the consequence of different mechanical properties of stromal cells around a tumour *in vivo* vs *in vitro* resulting in increased levels of intra-tumour stromal remodelling and thus increased metastasis [283]. Furthermore, only 8% of *in vivo* cancer research experiments have been translated into clinical practice. [285]. These findings reveal the need to further improve methodology and mimicking of disease conditions within animal models, particularly in models with intact immune systems.

On the other hand, we have found that EDV^{TM} delivery has translated into the clinic from animal models [201, 203, 204, 207], possibly due to the bacterial origin of the nanocell which may allow them to circumvent the stromal environment of tumours. Thus, we predict that the effective knockdown of *PLK*1 and *KSP,* seen after treatment of EGFR- EDV^{TM}s loaded with corresponding siRNA in our animal model xenograft A549-Dox-R, has the potential to translate into human studies due to the previous success seen in a similar mesothelioma model using EDV^{TM}s loaded with miRNA 16a [207].

In 2018, *Jeong et al.* investigated the role of PLK1 *in vivo* using a mammary adenocarcinoma xenograft resistant to tamoxifen, an antihormone drug for estrogen-positive breast cancer [286]. Similar to the drug resistant NSCLC cell line, A549-Dox-R, used in this study, *PLK*1 was overexpressed in the tamoxifen-resistant MCF-7 cell line (TAMR-MCF-7) [286]. Consequently, cell proliferation was suppressed *in vitro* and tumour growth inhibited *in vivo* after treatment with an ATP-competitive PLK1 inhibitor BI2536. Another interesting result shown by *Jeong et al.* was the significant reduction in expression of the protein Cdc25c, a regulator of G2/M progression and consequently a measure of *PLK*1 activity [286]. This finding coincides with tumour growth regression seen *in vivo* caused by *PLK*1 inhibition. In future studies the quantification of Cdc25c expression will be carried out *in vivo* after treatment of EGFR-EDV-PLK1 to see if they are similarly reduced.

Volasertib, aPLK1 inhibitor drug, has been used in the treatment of anaplastic thyroid carcinoma (ATC), although side effects from treatment include mitotic slippage and endoreduplication leading to cellular resistance (20). In order to overcome this challenge *De Martino et al.* 2018 explored the use of a PI3K inhibitor in combination with volasertib. A synergistic effect between the two was found *in vivo* while treating an immunocompetent allograft T4888M ATC model where tumour growth was successfully inhibited [174]. There was also inhibition of tumour growth in the single treatment groups although interestingly, after two weeks of treatment, the efficacy of volasertib was reduced and tumours started to increase in size.

In this study using the A549-Dox-R xenograft recovery of tumour growth occurred when siRNA treatment was delayed for 48hrs. A possible explanation is that treated cells were in a different phase of cell cycle and thus not affected by the treatment or not enough doses had been administered in the early phase of the treatment. It is possible in our model that the tumour had begun to acquire drug resistance after the initial treatment doses [287].

Decreased gene expression caused by siRNA-encapsulated nanoparticles targeting *PLK*1 and *KSP* has been investigated in colorectal, melanoma and NSCLC *in vivo* models [185, 288, 289]. In this study, RT-qPCR analysis of cDNA from excised A549-Dox-R tumours treated with EGFR-EDV-siPLK1 and EGFR-EDV-siKSP confirmed the expected knockdown of their targets *PLK1* and *KSP* respectively. We also observed decreased expression of *PLK*1 and *KSP* by EGFR-EDV^{TM}s loaded with siKSP and siPLK1 respectively. Both of these genes are mitotic regulators and their corresponding siRNA act as mitotic inhibitors, therefore we hypothesise

that the siRNA targeting one gene (*PLK*1) could off-target the other gene (*KSP*), although further research is needed to support this hypothesis [290].

Interestingly our results also showed a decreased expression of *RRM*1 in groups treated with EGFR-EDV-PLK1 and EGFR-EDV-KSP. *RRM*1 is involved in the G1 DNA replication phase of the cell cycle and therefore the mitotic inhibitors may have some relationship with this gene, though further research needs to be done to explore this theory [229]. Another unexpected result was a reduction of gene expression of *PLK*1 and *KSP* in tumours treated with EGFR-EDV-Dox. These findings were unexpected as they did not translate to our *in vivo* results where tumour growth was not inhibited after treatment with EGFR-EDV-Dox. The A549-Dox-R xenograft experiment is a nude mouse model and therefore EDV^{TM} treatment is expected to stimulate an innate immune response, but without initiating a T-cell response. Further studies in a syngeneic mouse model have shown that the EDV^{TM} can be used to kill cancer cells using a super-cytotoxic drug and this also evokes a cascade of both innate and adaptive immune responses . [262]. Future experiments to test whether functional nucleic acids such as PLK1 can also provoke both innate and adaptive immune responses, will be undertaken in a syngeneic mouse model of lung cancer.

The effect of *KSP* knockdown using siRNA targeting *KSP* delivered in liposomes has also been investigated in ovarian cancer [291]. The liposomes-siRNA complexes were deemed safe and did not elicit adverse immune responses, and caused suppression of tumour growth in the SKOV-3 xenograft. More recently, these siKSP loaded liposomes were used to study drug resistance in ovarian cancer, specifically resistance to KSP inhibitors caused by kinesin functional plasticity [292].
Xenografts derived from patients with platinum-resistant ovarian cancer were treated with the liposome-siRNA complexes in combination with paclitaxel. Tumours analysed with RT-qPCR targeted by liposomes delivered siRNA against KSP showed reduced levels of KSP mRNA compared to negative controls but the efficiency of the knock downs were not as significant as the knockdown achieved by delivery of siRNAs in EDV^{TM}s [292].

Yu et al. 2019 investigated combining siRNA targeting PLK1 and paclitaxel in liposomes *in vivo* using the MCF-7 breast cancer xenograft mouse model [152]. This treatment resulted in increased apoptosis and decreased angiogenesis. Future experiments using the A549-Dox-R xenograft model could focus on testing the effective siRNA EDV^{TM}s in combination with a

drug loaded into EDV^{TM}s simultaneously, or a combination of EDV^{TM}s loaded with siPLK1 and siKSP to provide a synergistic effect and increase overall efficiency and efficacy in inhibiting tumour growth [273, 274]. Future *in vivo* experiments should also explore that the inhibition of tumour growth is specifically a result from knockdown of the target gene as was seen in the *in vitro* experiments of this study.

Overall delivery of siRNAs has been a major issue in oncology. Indeed, as previously mentioned, Alnylam Pharmaceuticals attempted a clinical trial with siPLK1 for solid tumours where the siRNA was delivered by liposomes. Unfortunately, the particles accumulated in the liver and patients experienced deranged liver function tests [151]. Conversely, the EDV^{TM}s have been successfully loaded with functional nucleic acids at therapeutic concentrations and these have been delivered safely and without toxicity into mesothelioma patients [204].
Going forward, our experiments with syngeneic mice bearing NSCLC tumours EDV^{TM}s will be loaded with siPLK1 and siKSP and a plethora of cytokines and infiltration of immune cells into the tumour bed will be measured. Furthermore, as PLK1 has been shown to be a useful target in lung cancer in our animal models, a protocol has also been developed and approved by ethics at 2 major hospitals comparing a super-cytotoxic drug vs siRNA in NSCLC (EnGeneIC in-house data).

This study highlights the exciting possibility that siRNAs against mitotic regulators loaded into EDV^{TM}s will be effective alone or in combination with drug-loaded EDV^{TM}s, and may overcome drug resistance in NSCLC patients who have exhausted treatment options.

Chapter 6. Conclusions and Future Directions

6.1 Conclusions

A common feature of drug resistant lung cancer cells is the overexpression of PLK1, RRM1 & KSP proteins involved in the cell cycle making them potential targets for treatment of drug resistant NSCLCs. One of the major goals of this study was to investigate the potential of siRNAs to downregulate the expression of these genes in order to limit cell growth, and determine their potential in clinical use in drug resistant tumours.

The first aim of this study was to test the knockdown efficiency of siRNA to decrease gene expression of essential cell cycle regulators PLK1, RRM1 & KSP in NSCLC cell lines.
Preliminary results confirmed that *PLK*1 and *KSP* are overexpressed in several NSCLC cell lines and siRNAs targeting for mitotic proteins PLK1 and KSP were shown to be the most effective in causing increased apoptosis, cell cycle arrest and ultimately cell death in NSCLC cell lines *in vitro*.

Our second aim was to test the efficacy of siRNA loaded into EDV^{TM} nanocells *in vitro* using a 3D model to decrease gene expression of *PLK*1, *RRM*1 & *KSP* in NSCLC and cell cycle arrest. We demonstrated significant EGFR expression in the A549 & A549-Dox-R cell lines confirming these cells to be suitable for EGFR-EDV treatment. The siRNA copy number of the loaded EDV^{TM}s was measured and deemed acceptable for therapeutic use according to EnGeneIC quality control guidelines (>3000 copies/EDV^{TM}). Finally, the siRNA-loaded EDV^{TM}s were used to treat NSCLC spheroids using 2 different 3D model cell culture techniques. Significantly greater growth inhibition of spheroids was observed when using the hanging drop plate in all EDV^{TM} treatment groups compared to the normal low binding plates. EDV^{TM}s were successfully taken up by hanging drop spheroids with increased efficacy of the siRNAs loaded into the nanocells targeting *PLK*1, *RRM*1 and *KSP*. Consequently, we demonstrated that cell proliferation of spheroids was successfully inhibited when treated with EDV^{TM}s loaded with siRNA targeting *PLK*1, *RRM*1 and *KSP*.

The final aim of this study was to test the efficacy of siRNA loaded into EDV^{TM} nanocells *in vivo* using an established mouse xenograft model. Firstly, we tested the efficacy of EDV^{TM}s loaded with siRNAs targeting *PLK*1, *RRM*1 and *KSP in vivo* in the A549-Dox-R xenograft mouse model. We demonstrated that EGFR-EDV-siPLK1 and EGFR-EDV-siKSP were effective in inhibiting tumour growth compared to control groups. RT-qPCR analysis was

conducted to measure the efficiency of gene knockdown of *PLK*1, *RRM*1 and *KSP* in tumours excised from the A549-Dox-R *in vivo* experiment after undergoing EDV^{TM}-siRNA treatment. Tumours treated with EGFR-EDV-siPLK1 and EGFR-EDV-siKSP had significant knockdown of their targets *PLK1* and *KSP* respectively.

In summary, in this study, three different techniques were used in preclinical experiments to determine the efficacy of specific targeted EGFR-EDV^{TM}-siRNAs to kill NSCLCs. Firstly, I performed *in vitro* gene/protein knockdown of the naked siRNAs, siPLK1, siRRM1 and siKSP in NSCLC cells to determine cell death. Although siPLK1 and siKSP proved to be the most efficacious in the 2D culture system, we decided to continue using all three siRNAs in EGFR-EDV^{TM} 3D culture experiments as 3D cell cultures are more physiologically relevant and predictive of the human tumour outcome.

Comparison of the 3D hanging drop method with the conventional 3D matrigel plates demonstrated that the hanging drop method resulted in more effective uptake of the EGFR-EDV^{TM}-siRNA nanoparticles given the greater surface area exposure, as demonstrated by fluorescent microscopy and flow cytometry. Even though the cell death in the 3D spheroid model was not highly significance, there was a clear trend of cell/spheroid growth inhibition in all experiments and therefore the decision was made to further test the siRNA/EDV^{TM} treatment *in vivo* using drug resistant A549-Dox-R xenografts. Tumour growth inhibition after treatment with EGFR-EDV^{TM}s loaded with siPLK1 and siKSP was successful. While each of the chosen methods has it's difficulties, the progressive approach, from 2D to 3D *in vitro* culture to the *in vivo* mouse xenograft model demonstrated the advantages and negatives of each method. Importantly, though uptake of EGFR-EDV^{TM}-siRNAs didn't necessarily dictate immediacy of cell death in 3D spheroids, overall spheroid size (growth) was observed. Importantly, EGFR-EDV^{TM}-siRNAs treatment in xenograft models were successful in causing tumour growth inhibition.

Conclusion, in this study we have shown *in vitro* and *in vivo* that EDV^{TM}s can deliver siRNAs to hanging drop 3D spheroids and into a mouse xenograft model to inhibit cell and tumour growth. This study highlights the exciting possibility that siRNAs against mitotic regulators and loaded into EDV^{TM}s could be effective alone or in combination with drug-loaded EDV^{TM}s, and may overcome drug resistance in NSCLC patients.

6.2 Future Directions

Going forward the A549-Dox-R xenograft model could be utilised further with a focus on testing the effective siRNA EDV^{TM}s in combination with a drug (Doxorubicin or 682 [262]), loaded into EDV^{TM}s separately, or with a combination of EDV^{TM}s loaded with siPLK1 and siKSP. This would highlight whether the combination would result in a synergistic effect and increase overall efficiency. We would also like to investigate whether an increase in the number of doses/week would allow for a greater concentration of payload into the tumour bed early in the treatment regime.

Future experiments to test whether EDV^{TM}s carrying functional nucleic acids such as siPLK1 can also provoke both innate and adaptive immune responses, will be undertaken in a syngeneic mouse model of lung cancer. Syngeneic mice bearing NSCLC tumours will be treated with EDV^{TM}s loaded with siPLK1 and siKSP, and several cytokines and infiltration of immune cells into the tumour bed will be measured. Furthermore, as *PLK*1 has been shown to be a useful target in lung cancer in our animal models, a protocol has also been developed and approved by ethics at 2 major hospitals comparing a super-cytotoxic drug, 682 vs siRNA-PLK1 in NSCLC (EnGeneIC in-house data).

Chapter 7. References

1. endmemo.com. *EndMemo DNA/RNA copy number calculator* 2019 September 10 201]; Available from: http://endmemo.com/bio/dnacopynum.php.
2. Siegel, R.L., et al., *Colorectal cancer statistics, 2017.* CA: a cancer journal for clinicians, 2017. **67**(3): p. 177-193.
3. Shaw, A.T., et al., *Crizotinib versus chemotherapy in advanced ALK-positive lung cancer.* New England Journal of Medicine, 2013. **368**(25): p. 2385-2394.
4. Farkona, S., E.P. Diamandis, and I.M. Blasutig, *Cancer immunotherapy: the beginning of the end of cancer?* BMC medicine, 2016. **14**(1): p. 73.
5. Tatiparti, K., et al., *siRNA delivery strategies: a comprehensive review of recent developments.* Nanomaterials, 2017. **7**(4): p. 77.
6. Dang, C.V., et al., *Drugging the 'undruggable' cancer targets.* Nat Rev Cancer, 2017. **17**(8): p. 502-508.
7. Aagaard, L. and J.J. Rossi, *RNAi therapeutics: principles, prospects and challenges.* Advanced drug delivery reviews, 2007. **59**(2-3): p. 75-86.
8. Bartlett, D.W. and M.E. Davis, *Impact of tumor-specific targeting and dosing schedule on tumor growth inhibition after intravenous administration of siRNA-containing nanoparticles.* Biotechnology and bioengineering, 2008. **99**(4): p. 975-985.
9. McNamara II, J.O., et al., *Cell type–specific delivery of siRNAs with aptamer-siRNA chimeras.* Nature biotechnology, 2006. **24**(8): p. 1005.
10. Sørensen, D.R., M. Leirdal, and M. Sioud, *Gene silencing by systemic delivery of synthetic siRNAs in adult mice.* Journal of molecular biology, 2003. **327**(4): p. 761-766.
11. Kawakami, S. and M. Hashida, *Targeted delivery systems of small interfering RNA by systemic administration.* Drug metabolism and pharmacokinetics, 2007. **22**(3): p. 142-151.
12. Naing, A., et al., *EphA2 gene targeting using neutral liposomal small interfering RNA (EPHARNA) delivery: A phase I clinical trial*. 2017, American Society of Clinical Oncology.
13. Morrison, C., *Alnylam prepares to land first RNAi drug approval.* Nat Rev Drug Discov, 2018. **17**(3): p. 156-157.
14. van Zandwijk, N., et al., *Safety and activity of microRNA-loaded minicells in patients with recurrent malignant pleural mesothelioma: a first-in-man, phase 1, open-label, dose-escalation study.* The Lancet Oncology, 2017. **18**(10): p. 1386-1396.

15. Hirsch, F.R., et al., *Lung cancer: current therapies and new targeted treatments.* The Lancet, 2017. **389**(10066): p. 299-311.
16. Australia, A.G.C. *Lung Cancer Statistics* 2018 21 March 2018; Available from: < https://lung-cancer.canceraustralia.gov.au/statistics>.
17. *Australian Institute of Health and Welfare in Cancer -*

Cancer in Australia Australian Institute of Health and Welfare in Cancer

2017; Available from: https://www.aihw.gov.au/getmedia/3da1f3c2-30f0-4475-8aed-1f19f8e16d48/20066-cancer-2017.pdf.aspx?inline=true.
18. Organisation, W.H. *Cancer*. 2018; Available from: <http://www.who.int/en/news-room/fact-sheets/detail/cancer>.
19. Society, A.C. *What is Non-small cell lung cancer?* 2018 2018 [cited 2018; Available from: < https://www.cancer.org/cancer/non-small-cell-lung-cancer/about/what-is-non-small-cell-lung-cancer.html>.
20. Party, C.C.A.L.C.G.W., *Clinical practice guidelines for the treatment of lung cancer*. 2018.
21. Baggstrom, M.Q., et al., *Third-generation chemotherapy agents in the treatment of advanced non-small cell lung cancer: a meta-analysis.* Journal of Thoracic Oncology, 2007. **2**(9): p. 845-853.
22. Lazzari, C., et al., *Historical evolution of second-line therapy in non-small cell lung cancer.* Frontiers in medicine, 2017. **4**: p. 4.
23. Neel, D.S. and T.G. Bivona, *Resistance is futile: overcoming resistance to targeted therapies in lung adenocarcinoma.* NPJ precision oncology, 2017. **1**(1): p. 3.
24. Xue, et al., *Evolution from genetics to phenotype: reinterpretation of NSCLC plasticity, heterogeneity, and drug resistance.* Protein & cell, 2017. **8**(3): p. 178-190.
25. Mansoori, B., et al., *The Different Mechanisms of Cancer Drug Resistance: A Brief Review.* Advanced pharmaceutical bulletin, 2017. **7**(3): p. 339.
26. Meacham, C.E. and S.J. Morrison, *Tumour heterogeneity and cancer cell plasticity.* Nature, 2013. **501**(7467): p. 328.
27. Basak, U., et al., *Deciphering the Cancer Puzzle: Cancer Stem Cells Being the Pivotal Piece.* J Stem cell Res Transplant, 2017. **49**: p. 1025.
28. Thiery, J.P., et al., *Epithelial-mesenchymal transitions in development and disease.* cell, 2009. **139**(5): p. 871-890.

29. Sui, H., et al., *Epithelial-mesenchymal transition and drug resistance: role, molecular mechanisms, and therapeutic strategies.* Oncology research and treatment, 2014. **37**(10): p. 584-589.
30. Sun, Y., et al., *Metabolic and transcriptional profiling reveals pyruvate dehydrogenase kinase 4 as a mediator of epithelial-mesenchymal transition and drug resistance in tumor cells.* Cancer & metabolism, 2014. **2**(1): p. 20.
31. Shien, K., et al., *Acquired resistance to EGFR inhibitors is associated with a manifestation of stem cell–like properties in cancer cells.* Cancer research, 2013. **73**(10): p. 3051-3061.
32. Bhatia, S., et al., *The challenges posed by cancer heterogeneity.* Nature biotechnology, 2012. **30**(7): p. 604.
33. Shea, M., D.B. Costa, and D. Rangachari, *Management of advanced non-small cell lung cancers with known mutations or rearrangements: latest evidence and treatment approaches.* Therapeutic advances in respiratory disease, 2016. **10**(2): p. 113-129.
34. Olaussen, K. and S. Postel-Vinay, *Predictors of chemotherapy efficacy in non-small-cell lung cancer: a challenging landscape.* Annals of Oncology, 2016. **27**(11): p. 2004-2016.
35. Jeong, S.H., et al., *Expression of Bcl-2 predicts outcome in locally advanced non-small cell lung cancer patients treated with cisplatin-based concurrent chemoradiotherapy.* Lung Cancer, 2010. **68**(2): p. 288-294.
36. Kim, E.S., et al., *Copper transporter CTR1 expression and tissue platinum concentration in non-small cell lung cancer.* Lung cancer, 2014. **85**(1): p. 88-93.
37. (ASCO, A.S.o.C.O. *Lung Cancer - Non-Small Cell: Types of Treatment*. 2019 01/2019 [cited 2019 27 October]; Available from: https://www.cancer.net/cancer-types/lung-cancer-non-small-cell/types-treatment
38. Melguizo, C., et al., *Modulation of MDR1 and MRP3 gene expression in lung cancer cells after paclitaxel and carboplatin exposure.* International journal of molecular sciences, 2012. **13**(12): p. 16624-16635.
39. Rossi, A. and M. Di Maio, *Platinum-based chemotherapy in advanced non-small-cell lung cancer: optimal number of treatment cycles.* Expert review of anticancer therapy, 2016. **16**(6): p. 653-660.
40. Fidias, P.M., et al., *Phase III study of immediate compared with delayed docetaxel after front-line therapy with gemcitabine plus carboplatin in advanced non–small-cell lung cancer.* Journal of Clinical Oncology, 2008. **27**(4): p. 591-598.

41. Socinski, M.A., et al., *Treatment of stage IV non-small cell lung cancer: Diagnosis and management of lung cancer: American College of Chest Physicians evidence-based clinical practice guidelines.* Chest, 2013. **143**(5): p. e341S-e368S.
42. Chang, Q., et al., *First-line pemetrexed/carboplatin or cisplatin/bevacizumab compared with paclitaxel/carboplatin/bevacizumab in patients with advanced non-squamous non-small cell lung cancer with wild-type driver genes: A real-world study in China.* 2019. **10**(5): p. 1043-1050.
43. Gobbini, E., et al., *Real-world outcomes according to treatment strategies in ALK-rearranged non-small-cell lung cancer (NSCLC) patients: an Italian retrospective study.* 2019: p. 1-8.
44. Lindeman, N.I., et al., *Molecular testing guideline for selection of lung cancer patients for EGFR and ALK tyrosine kinase inhibitors: guideline from the College of American Pathologists, International Association for the Study of Lung Cancer, and Association for Molecular Pathology.* J Thorac Oncol, 2013. **8**(7): p. 823-59.
45. Lindeman, N.I., et al., *Updated Molecular Testing Guideline for the Selection of Lung Cancer Patients for Treatment With Targeted Tyrosine Kinase Inhibitors: Guideline From the College of American Pathologists, the International Association for the Study of Lung Cancer, and the Association for Molecular Pathology.* Arch Pathol Lab Med, 2018. **142**(3): p. 321-346.
46. Agency, E.M., *Summary of Product Characteristics - Tarceva (erlotinib), Iressa (gefitinib).* 2014.
47. Riely, G.J., et al., *Prospective assessment of discontinuation and reinitiation of erlotinib or gefitinib in patients with acquired resistance to erlotinib or gefitinib followed by the addition of everolimus.* Clinical cancer research, 2007. **13**(17): p. 5150-5155.
48. Ghafoor, Q., et al., *Epidermal Growth Factor Receptor (EGFR) Kinase Inhibitors and Non-Small Cell Lung Cancer (NSCLC)–Advances in Molecular Diagnostic Techniques to Facilitate Targeted Therapy.* Pathology & Oncology Research, 2017: p. 1-9.
49. Zhou, C., et al., *Erlotinib versus chemotherapy as first-line treatment for patients with advanced EGFR mutation-positive non-small-cell lung cancer (OPTIMAL, CTONG-0802): a multicentre, open-label, randomised, phase 3 study.* The lancet oncology, 2011. **12**(8): p. 735-742.

50. Tetsu, O., et al., *Drug resistance to EGFR inhibitors in lung cancer.* Chemotherapy, 2016. **61**(5): p. 223-235.
51. Yu, H., et al., *Analysis of Mechanisms of Acquired Resistance to EGFR TKI therapy in 155 patients with EGFR-mutant Lung Cancers.* Clinical cancer research, 2013: p. clincanres. 2246.2012.
52. Zhang, B., et al., *Complex epidermal growth factor receptor mutations and their responses to tyrosine kinase inhibitors in previously untreated advanced lung adenocarcinomas.* Cancer, 2018. **124**(11): p. 2399-2406.
53. Ou, S.-H.I. and R.A. Soo, *Dacomitinib in lung cancer: a "lost generation" EGFR tyrosine-kinase inhibitor from a bygone era?* Drug design, development and therapy, 2015. **9**: p. 5641.
54. Mok, T., et al., *Dacomitinib versus gefitinib for the first-line treatment of advanced EGFR mutation positive non-small cell lung cancer (ARCHER 1050): A randomized, open-label phase III trial*. 2017, American Society of Clinical Oncology.
55. Administration, U.S.F.D. *FDA approves dacomitinib for metastatic non-small cell lung cancer*. 2018 26 November 2018; Available from: https://www.fda.gov/drugs/drug-approvals-and-databases/fda-approves-dacomitinib-metastatic-non-small-cell-lung-cancer.
56. Jänne, P.A., et al., *AZD9291 in EGFR inhibitor–resistant non–small-cell lung cancer.* New England Journal of Medicine, 2015. **372**(18): p. 1689-1699.
57. Yang, J.C.-H., et al., *Osimertinib in pretreated T790M-positive advanced non–small-cell lung cancer: AURA study phase II extension component.* Journal of Clinical Oncology, 2017. **35**(12): p. 1288-1296.
58. Mok, T.S., et al., *Osimertinib or platinum–pemetrexed in EGFR T790M–positive lung cancer.* New England Journal of Medicine, 2017. **376**(7): p. 629-640.
59. Helena, A.Y., et al., *A phase I, dose escalation study of oral ASP8273 in patients with non–small cell lung cancers with epidermal growth factor receptor mutations.* 2017. **23**(24): p. 7467-7473.
60. Oxnard, G.R., et al., *Preliminary results of TATTON, a multi-arm phase Ib trial of AZD9291 combined with MEDI4736, AZD6094 or selumetinib in EGFR-mutant lung cancer*. 2015, American Society of Clinical Oncology.
61. Yang, J.C.-H., et al., *Osimertinib Plus Durvalumab versus Osimertinib Monotherapy in EGFR T790M–Positive NSCLC following Previous EGFR TKI Therapy: CAURAL Brief Report.* 2019. **14**(5): p. 933-939.

62. AstraZeneca. *Osimertinib Plus Savolitinib in EGFRm+/MET+ NSCLC Following Prior Osimertinib (SAVANNAH)*. 2019 October 8 2019; Available from: https://clinicaltrials.gov/ct2/show/NCT03778229
63. Ramalingam, S.S., et al., *Overall survival with osimertinib in untreated, EGFR-mutated advanced NSCLC.* 2020. **382**(1): p. 41-50.
64. Akamatsu, H., et al., *Phase I/II Study of Osimertinib With Bevacizumab in EGFR-mutated, T790M-positive Patients With Progressed EGFR-TKIs: West Japan Oncology Group 8715L (WJOG8715L).* 2019.
65. Higuchi, T., et al., *Osimertinib regressed an EGFR-mutant lung-adenocarcinoma bone-metastasis mouse model and increased long-term survival.* 2020. **13**(10): p. 100826.
66. Mazza, V. and F. Cappuzzo, *Treating EGFR mutation resistance in non-small cell lung cancer–role of osimertinib.* The application of clinical genetics, 2017. **10**: p. 49.
67. Xing, P., et al., *Clinical outcomes of various resistance mechanisms of osimertinib in Chinese advanced non-small cell lung cancer patients*. 2019, American Society of Clinical Oncology.
68. Naing, A., et al., *Pegilodecakin combined with pembrolizumab or nivolumab for patients with advanced solid tumours (IVY): a multicentre, multicohort, open-label, phase 1b trial.* 2019. **20**(11): p. 1544-1555.
69. Hecht, J.R., et al., *Immunologic and tumor responses of pegilodecakin with 5-FU/LV and oxaliplatin (FOLFOX) in pancreatic ductal adenocarcinoma (PDAC).* 2020: p. 1-11.
70. Wang, S., S. Cang, and D. Liu, *Third-generation inhibitors targeting EGFR T790M mutation in advanced non-small cell lung cancer.* Journal of hematology & oncology, 2016. **9**(1): p. 34.
71. Zhang, W., et al., *Olmutinib (BI1482694/HM61713), a novel epidermal growth factor receptor tyrosine kinase inhibitor, reverses ABCG2-mediated multidrug resistance in cancer cells.* 2018. **9**: p. 1097.
72. Tan, D.S., et al., *Safety and efficacy of nazartinib (EGF816) in adults with EGFR-mutant non-small-cell lung carcinoma: a multicentre, open-label, phase 1 study.* 2020.
73. Sukrithan, V., et al., *Emerging drugs for EGFR-mutated non-small cell lung cancer.* 2019. **24**(1): p. 5-16.
74. Soda, M., et al., *Identification of the transforming EML4–ALK fusion gene in non-small-cell lung cancer.* Nature, 2007. **448**(7153): p. 561.

75. Solomon, B.J., et al., *First-line crizotinib versus chemotherapy in ALK-positive lung cancer.* New England Journal of Medicine, 2014. **371**(23): p. 2167-2177.
76. Engelman, J.A. and P.A. Jänne, *Mechanisms of acquired resistance to epidermal growth factor receptor tyrosine kinase inhibitors in non–small cell lung cancer.* Clinical Cancer Research, 2008. **14**(10): p. 2895-2899.
77. Santarpia, M., et al., *Spotlight on ceritinib in the treatment of ALK+ NSCLC: design, development and place in therapy.* Drug design, development and therapy, 2017. **11**: p. 2047.
78. Alexander, P.B. and X.-F. Wang, *Resistance to receptor tyrosine kinase inhibition in cancer: molecular mechanisms and therapeutic strategies.* Frontiers of medicine, 2015. **9**(2): p. 134-138.
79. Soria, J.-C., et al., *First-line ceritinib versus platinum-based chemotherapy in advanced ALK-rearranged non-small-cell lung cancer (ASCEND-4): a randomised, open-label, phase 3 study.* The Lancet, 2017. **389**(10072): p. 917-929.
80. Camidge, D.R., et al., *Brigatinib versus crizotinib in ALK-positive non–small-cell lung cancer.* 2018. **379**(21): p. 2027-2039.
81. Wakelee, H., K. Kelly, and M.J. Edelman, *50 Years of progress in the systemic therapy of non-small cell lung cancer.* Am Soc Clin Oncol Educ Book, 2014: p. 177-89.
82. Young, A., D. Lou, and F. McCormick, *Oncogenic and wild-type Ras play divergent roles in the regulation of mitogen-activated protein kinase signaling.* Cancer discovery, 2013. **3**(1): p. 112-123.
83. Kim, H., et al., *Ubiquitin C-terminal hydrolase-L1 is a key regulator of tumor cell invasion and metastasis.* Oncogene, 2009. **28**(1): p. 117.
84. Zhang, J., et al., *Targeting KRAS-mutant non-small cell lung cancer: challenges and opportunities.* Acta biochimica et biophysica Sinica, 2015. **48**(1): p. 11-16.
85. Yip, P.Y., *Phosphatidylinositol 3-kinase-AKT-mammalian target of rapamycin (PI3K-Akt-mTOR) signaling pathway in non-small cell lung cancer.* Translational lung cancer research, 2015. **4**(2): p. 165.
86. Kakegawa, S., et al., *Clinicopathological features of lung adenocarcinoma with KRAS mutations.* Cancer, 2011. **117**(18): p. 4257-4266.
87. Kempf, E., et al., *KRAS oncogene in lung cancer: focus on molecularly driven clinical trials.* European Respiratory Review, 2016. **25**(139): p. 71-76.

88. Zarredar, H., et al., *Potential Molecular Targets in the Treatment of Lung Cancer Using siRNA Technology.* Cancer investigation, 2018: p. 1-22.
89. Del Re, M., et al., *Implications of KRAS mutations in acquired resistance to treatment in NSCLC.* Oncotarget, 2018. **9**(5): p. 6630.
90. Román, M., et al., *KRAS oncogene in non-small cell lung cancer: clinical perspectives on the treatment of an old target.* Molecular cancer, 2018. **17**(1): p. 33.
91. Riely, G.J., et al., *A phase II trial of Salirasib in patients with lung adenocarcinomas with KRAS mutations.* Journal of Thoracic Oncology, 2011. **6**(8): p. 1435-1437.
92. Chabon, J.J., et al., *Circulating tumour DNA profiling reveals heterogeneity of EGFR inhibitor resistance mechanisms in lung cancer patients.* Nature communications, 2016. **7**: p. 11815.
93. Gatalica, Z., et al., *BRAF mutations are potentially targetable alterations in a wide variety of solid cancers.* Kidney, 2015. **6**: p. 341.
94. Passiglia, F., et al., *KRAS inhibition in non–small cell lung cancer: Past failures, new findings and upcoming challenges.* 2020. **137**: p. 57-68.
95. Yuan, X., et al., *Recent Advances of SHP2 Inhibitors in Cancer Therapy: Current Development and Clinical Application.* 2020.
96. Chan, B.A. and B.G. Hughes, *Targeted therapy for non-small cell lung cancer: current standards and the promise of the future.* Translational lung cancer research, 2015. **4**(1): p. 36.
97. Alidzanovic, L., et al., *The VEGF rise in blood of bevacizumab patients is not based on tumor escape but a host-blockade of VEGF clearance.* Oncotarget, 2016. **7**(35): p. 57197.
98. Sandler, A., et al., *Paclitaxel–carboplatin alone or with bevacizumab for non–small-cell lung cancer.* New England Journal of Medicine, 2006. **355**(24): p. 2542-2550.
99. Clarke, J.M. and H.I. Hurwitz, *Understanding and targeting resistance to anti-angiogenic therapies.* Journal of gastrointestinal oncology, 2013. **4**(3): p. 253.
100. Masuda, C., et al., *Bevacizumab counteracts VEGF-dependent resistance to erlotinib in an EGFR-mutated NSCLC xenograft model.* International journal of oncology, 2017. **51**(2): p. 425-434.
101. Tolaney, S.M., et al., *Role of vascular density and normalization in response to neoadjuvant bevacizumab and chemotherapy in breast cancer patients.* Proceedings of the National Academy of Sciences, 2015. **112**(46): p. 14325-14330.

102. Saito, H., et al., *Erlotinib plus bevacizumab versus erlotinib alone in patients with EGFR-positive advanced non-squamous non-small-cell lung cancer (NEJ026): interim analysis of an open-label, randomised, multicentre, phase 3 trial.* 2019. **20**(5): p. 625-635.
103. Daoud, A. and Q.S. Chu, *Targeting Novel but Less Common Driver Mutations and Chromosomal Translocations in Advanced Non-Small Cell Lung Cancer.* Frontiers in oncology, 2017. **7**: p. 222.
104. Hainsworth, J.D., et al., *Targeted therapy for non-small cell lung cancer (NSCLC) with HER2, BRAF, or hedgehog alterations: Interim data from MyPathway*. 2017, American Society of Clinical Oncology.
105. Bronte, G., et al., *Targeting RET-rearranged non-small-cell lung cancer: future prospects.* 2019. **10**: p. 27.
106. Falchook, G.S., et al., *Effect of the RET inhibitor vandetanib in a patient with RET fusion-positive metastatic non-small-cell lung cancer.* 2016. **34**(15): p. e141-e144.
107. Drilon, A., et al., *Efficacy of Selpercatinib in RET Fusion–Positive Non–Small-Cell Lung Cancer.* 2020. **383**(9): p. 813-824.
108. Editor, O. *Lung cancer trial of RET inhibitor selpercatinib achieves durable responses in majority of patients with RET gene fusions*. 2020 [cited 2020 September 2]; Available from: https://oncologynews.com.au/lung-cancer-trial-of-ret-inhibitor-selpercatinib-achieves-durable-responses-in-majority-of-patients-with-ret-gene-fusions/.
109. Miller, J.F. and M. Sadelain, *The journey from discoveries in fundamental immunology to cancer immunotherapy.* Cancer Cell, 2015. **27**(4): p. 439-49.
110. Helmy, K.Y., et al., *Cancer immunotherapy: accomplishments to date and future promise.* Ther Deliv, 2013. **4**(10): p. 1307-20.
111. Forde, P.M., J.R. Brahmer, and R.J. Kelly, *New Strategies in Lung Cancer: Epigenetic Therapy for Non–Small Cell Lung Cancer.* Clinical Cancer Research, 2014. **20**(9): p. 2244-2248.
112. Farinde, A. *Drug–Receptor Interactions*. 2016 October, 2016 10 May 2018
]; Available from: < https://www.msdmanuals.com/en-au/professional/clinical-pharmacology/pharmacodynamics/drug%E2%80%93receptor-interactions.
113. Davies, M., *New modalities of cancer treatment for NSCLC: focus on immunotherapy.* Cancer management and research, 2014. **6**: p. 63.

114. Carter, B.W., et al., *Immunotherapy in Non–Small Cell Lung Cancer Treatment.* Journal of thoracic imaging, 2017. **32**(5): p. 300-312.
115. Khalil, D.N., et al., *The future of cancer treatment: immunomodulation, CARs and combination immunotherapy.* Nature reviews Clinical oncology, 2016. **13**(5): p. 273.
116. Gridelli, C., et al., *Second-line treatment of advanced non-small cell lung cancer non-oncogene addicted: new treatment algorithm in the era of novel immunotherapy.* Curr Clin Pharmacol, 2018.
117. Moya-Horno, I., et al., *Combination of immunotherapy with targeted therapies in advanced non-small cell lung cancer (NSCLC).* Ther Adv Med Oncol, 2018. **10**: p. 1758834017745012.
118. Tsiara, A., et al., *Implementation of immunotherapy in the treatment of advanced non-small cell lung cancer (NSCLC).* Ann Transl Med, 2018. **6**(8): p. 144.
119. Filippi, A.R., et al., *Locally-advanced non-small cell lung cancer: shall immunotherapy be a new chance?* J Thorac Dis, 2018. **10**(Suppl 13): p. S1461-S1467.
120. Ernani, V. and A.K. Ganti, *Immunotherapy in treatment naive advanced non-small cell lung cancer.* J Thorac Dis, 2018. **10**(Suppl 3): p. S412-S421.
121. Taunk, N.K., et al., *Immunotherapy and radiation therapy for operable early stage and locally advanced non-small cell lung cancer.* Transl Lung Cancer Res, 2017. **6**(2): p. 178-185.
122. Wrangle, J.M., et al., *ALT-803, an IL-15 superagonist, in combination with nivolumab in patients with metastatic non-small cell lung cancer: a non-randomised, open-label, phase 1b trial.* The Lancet Oncology, 2018. **19**(5): p. 694-704.
123. Parker, B.S., J. Rautela, and P.J. Hertzog, *Antitumour actions of interferons: implications for cancer therapy.* Nature Reviews Cancer, 2016. **16**(3): p. 131.
124. Tarhini, A.A., H. Gogas, and J.M. Kirkwood, *IFN-α in the treatment of melanoma.* The Journal of Immunology, 2012. **189**(8): p. 3789-3793.
125. Jiang, T., C. Zhou, and S. Ren, *Role of IL-2 in cancer immunotherapy.* Oncoimmunology, 2016. **5**(6): p. e1163462.
126. Sharma, R., S.M. Fu, and S.-T. Ju, *IL-2: a two-faced master regulator of autoimmunity.* Journal of autoimmunity, 2011. **36**(2): p. 91-97.
127. Kamensek, U., et al., *Clinically Usable Interleukin 12 Plasmid without an Antibiotic Resistance Gene: Functionality and Toxicity Study in Murine Melanoma Model.* Cancers, 2018. **10**(3): p. 60.

128. Daud, A.I., et al., *Phase I trial of interleukin-12 plasmid electroporation in patients with metastatic melanoma.* Journal of clinical oncology, 2008. **26**(36): p. 5896.
129. Athie, A., et al., *Analysis of copy number alterations reveals the lncRNA ALAL-1 as a regulator of lung cancer immune evasion.* 2020. **219**(9).
130. editor, O. *Researchers identify RNA molecule that helps lung cancer cells evade immune system*. 2020 28 August 2020; Available from: https://oncologynews.com.au/category/tumour-stream/lung-cancer/.
131. Ohaegbulam, K.C., et al., *Human cancer immunotherapy with antibodies to the PD-1 and PD-L1 pathway.* Trends Mol Med, 2015. **21**(1): p. 24-33.
132. Brahmer, J., et al., *Nivolumab versus docetaxel in advanced squamous-cell non–small-cell lung cancer.* New England Journal of Medicine, 2015. **373**(2): p. 123-135.
133. Connolly, E., I. Nordman, and G.J.J.o.T.O. Mallesara, *Advanced NSCLC Treatment and Outcomes After Nivolumab.* 2018. **13**(10).
134. Lynch, T.J., et al., *Ipilimumab in combination with paclitaxel and carboplatin as first-line treatment in stage IIIB/IV non–small-cell lung cancer: results from a randomized, double-blind, multicenter phase II study.* Journal of clinical oncology, 2012. **30**(17): p. 2046-2054.
135. Hodi, F.S., et al., *Improved survival with ipilimumab in patients with metastatic melanoma.* New England Journal of Medicine, 2010. **363**(8): p. 711-723.
136. Tomasini, P., et al., *Ipilimumab: its potential in non-small cell lung cancer.* Therapeutic advances in medical oncology, 2012. **4**(2): p. 43-50.
137. Hellmann, M.D., et al., *Nivolumab plus ipilimumab in advanced non–small-cell lung cancer.* 2019. **381**(21): p. 2020-2031.
138. Cyriac, G. and L. Gandhi. *Emerging biomarkers for immune checkpoint inhibition in lung cancer*. in *Seminars in cancer biology*. 2018. Elsevier.
139. Herbst, R.S., et al., *A study of MPDL3280A, an engineered PD-L1 antibody in patients with locally advanced or metastatic tumors*. 2013, American Society of Clinical Oncology.
140. Rittmeyer, A., et al., *Atezolizumab versus docetaxel in patients with previously treated non-small-cell lung cancer (OAK): a phase 3, open-label, multicentre randomised controlled trial.* The Lancet, 2017. **389**(10066): p. 255-265.
141. ONA Editor, O.N. *IASLC WCLC 2020: Addition of sintilimab to pemetrexed and platinum improved progression-free survival in NSCLC*. 2020 [cited 2020 September 2]; Available from: https://oncologynews.com.au/iaslc-wclc-2020-addition-of-

sintilimab-to-pemetrexed-and-platinum-improved-progression-free-survival-in-nsclc/#:~:text=survival%20in%20NSCLC-,IASLC%20WCLC%202020%3A%20Addition%20of%20sintilimab%20to%20pemetrexed%20and%20platinum,progression%2Dfree%20survival%20in%20NSCLC&text=The%20median%20progression%20free%20survival,5.0%20months).

142. Yang, Y., et al., *Efficacy and safety of sintilimab plus pemetrexed and platinum as first-line treatment for locally advanced or metastatic nonsquamous non-small cell lung cancer: a randomized, double-blind, phase 3 study (ORIENT-11).* 2020.
143. Kim, Y.-D., et al., *Pattern of cancer/testis antigen expression in lung cancer patients.* International journal of molecular medicine, 2012. **29**(4): p. 656-662.
144. Vansteenkiste, J.F., et al., *Efficacy of the MAGE-A3 cancer immunotherapeutic as adjuvant therapy in patients with resected MAGE-A3-positive non-small-cell lung cancer (MAGRIT): a randomised, double-blind, placebo-controlled, phase 3 trial.* The Lancet Oncology, 2016. **17**(6): p. 822-835.
145. Institute, H.L.M.C.C.a.R., *Phase II Study to Assess the Safety and Immunogenicity of recMAGE-A3+AS15 ASCI With or Without Poly IC:LC ClinicalTrials.gov Identifier: NCT01437605* 2018.
146. Neninger, E., et al., *Combining an EGF-based cancer vaccine with chemotherapy in advanced nonsmall cell lung cancer.* Journal of immunotherapy, 2009. **32**(1): p. 92-99.
147. Popa, X., et al., *Anti-EGF antibodies as surrogate biomarkers of clinical efficacy in stage IIIB/IV non-small-cell lung cancer patients treated with an optimized CIMAvax-EGF vaccination schedule.* 2020. **9**(1): p. 1762465.
148. Li, H., et al., *Antitumor activity of EGFR-specific CAR T cells against non-small-cell lung cancer cells in vitro and in mice.* Cell death & disease, 2018. **9**(2): p. 177.
149. Heymach, J. *NY-ESO-1^{c259}T for Advanced NSCLC - ClinicalTrials.gov Identifier: NCT02588612*. 2020; Available from: <https://clinicaltrials.gov/ct2/show/NCT02588612>
150. Fire, A., et al., *Potent and specific genetic interference by double-stranded RNA in Caenorhabditis elegans.* nature, 1998. **391**(6669): p. 806.
151. Hu, B., et al., *Therapeutic siRNA: state of the art.* 2020. **5**(1): p. 1-25.
152. Yu, S., et al., *Co-delivery of paclitaxel and PLK1-targeted siRNA using aptamer-functionalized cationic liposome for synergistic anti-breast cancer effects in vivo.* 2019. **15**(6): p. 1135-1148.

153. Li, F., et al., *Co-delivery of VEGF siRNA and etoposide for enhanced anti-angiogenesis and anti-proliferation effect via multi-functional nanoparticles for orthotopic non-small cell lung cancer treatment.* 2019. **9**(20): p. 5886.
154. Rao, D.D., et al., *siRNA vs. shRNA: similarities and differences.* 2009. **61**(9): p. 746-759.
155. Stein, R.A. *RNA Silencing Finds Its Therapeutic Voice*. 2020 [cited 2020 April 2]; Available from: https://www.genengnews.com/insights/rna-silencing-finds-its-therapeutic-voice/.
156. Rothschild, S.I., *Targeted therapies in non-small cell lung cancer—beyond EGFR and ALK.* Cancers, 2015. **7**(2): p. 930-949.
157. Siebring-van Olst, E., et al., *A genome-wide siRNA screen for regulators of tumor suppressor p53 activity in human non-small cell lung cancer cells identifies components of the RNA splicing machinery as targets for anticancer treatment.* Molecular oncology, 2017. **11**(5): p. 534-551.
158. Liu, K., et al., *The siRNA cocktail targeting VEGF and HER2 inhibition on the proliferation and induced apoptosis of gastric cancer cell.* Molecular and cellular biochemistry, 2014. **386**(1-2): p. 117-124.
159. Kunze, D., et al., *Simultaneous siRNA-mediated knockdown of antiapoptotic BCL2, Bcl-xL, XIAP and survivin in bladder cancer cells.* International journal of oncology, 2012. **41**(4): p. 1271-1277.
160. Gupta, K., et al., *Neutrophil gelatinase–associated lipocalin is expressed in osteoarthritis and forms a complex with matrix metalloproteinase 9.* Arthritis & Rheumatism: Official Journal of the American College of Rheumatology, 2007. **56**(10): p. 3326-3335.
161. Yang, Y., et al., *Nanoparticle delivery of pooled siRNA for effective treatment of non-small cell lung caner.* Molecular pharmaceutics, 2012. **9**(8): p. 2280-2289.
162. Perepelyuk, M., et al., *siRNA-Encapsulated Hybrid Nanoparticles Target Mutant K-ras and Inhibit Metastatic Tumor Burden in a Mouse Model of Lung Cancer.* Molecular Therapy-Nucleic Acids, 2017. **6**: p. 259-268.
163. Golan, T., et al., *RNAi therapy targeting KRAS in combination with chemotherapy for locally advanced pancreatic cancer patients.* Oncotarget, 2015. **6**(27): p. 24560.
164. Ltd, S. *The LODER Platform*. 2017 13 August 2018]; Available from: http://silenseed.com/?page_id=2424.

165. Xue, W., et al., *Small RNA combination therapy for lung cancer.* Proceedings of the National Academy of Sciences, 2014. **111**(34): p. E3553-E3561.
166. Mehta, A., et al., *Targeting KRAS mutant lung cancer cells with siRNA-loaded bovine serum albumin nanoparticles.* 2019. **36**(9): p. 133.
167. Mao, C.-Q., et al., *Synthetic lethal therapy for KRAS mutant non-small-cell lung carcinoma with nanoparticle-mediated CDK4 siRNA delivery.* Molecular Therapy, 2014. **22**(5): p. 964-973.
168. MacDiarmid, J.A., et al., *Sequential treatment of drug-resistant tumors with targeted minicells containing siRNA or a cytotoxic drug.* Nature biotechnology, 2009. **27**(7): p. 643.
169. Liu, Z., Q. Sun, and X. Wang, *PLK1, A potential target for cancer therapy.* Translational oncology, 2017. **10**(1): p. 22-32.
170. Gumireddy, K., et al., *ON01910, a non-ATP-competitive small molecule inhibitor of Plk1, is a potent anticancer agent.* Cancer cell, 2005. **7**(3): p. 275-286.
171. Rudolph, D., et al., *BI 6727, a Polo-like kinase inhibitor with improved pharmacokinetic profile and broad antitumor activity.* Clinical cancer research, 2009. **15**(9): p. 3094-3102.
172. O'neil, B., et al., *A phase II/III randomized study to compare the efficacy and safety of rigosertib plus gemcitabine versus gemcitabine alone in patients with previously untreated metastatic pancreatic cancer.* Annals of Oncology, 2015. **26**(9): p. 1923-1929.
173. Ellis, P.M., et al., *A Randomized, Open-Label Phase II Trial of Volasertib as Monotherapy and in Combination With Standard-Dose Pemetrexed Compared With Pemetrexed Monotherapy in Second-Line Treatment for Non–Small-Cell Lung Cancer.* Clinical lung cancer, 2015. **16**(6): p. 457-465.
174. De Martino, D., et al., *PI3K blockage synergizes with PLK1 inhibition preventing endoreduplication and enhancing apoptosis in anaplastic thyroid cancer.* 2018. **439**: p. 56-65.
175. Affatato, R., et al., *Identification of PLK1 as a New Therapeutic Target in Mucinous Ovarian Carcinoma.* 2020. **12**(3): p. 672.
176. McCarroll, J.A., et al., *Therapeutic targeting of polo-like kinase 1 using RNA-interfering nanoparticles (iNOPs) for the treatment of non-small cell lung cancer.* Oncotarget, 2015. **6**(14): p. 12020.

177. Wang, Z.-X., et al., *Overexpression of polo-like kinase 1 and its clinical significance in human non-small cell lung cancer.* The international journal of biochemistry & cell biology, 2012. **44**(1): p. 200-210.
178. Greco, K.A., et al., *PLK-1 silencing in bladder cancer by siRNA delivered with exosomes.* Urology, 2016. **91**: p. 241. e1-241. e7.
179. Rivlin, N., et al., *Mutations in the p53 tumor suppressor gene: important milestones at the various steps of tumorigenesis.* Genes & cancer, 2011. **2**(4): p. 466-474.
180. Yang, L. and M. Karin, *Roles of tumor suppressors in regulating tumor-associated inflammation.* Cell death and differentiation, 2014. **21**(11): p. 1677.
181. Sur, S., et al., *Abstract# LB-31: A new panel of isogenic human cancer cells suggests a therapeutic approach for cancers with inactivated p53*. 2009, AACR.
182. Kawata, E., et al., *Intravenous administration of PLK-1 siRNA with atelocollagen as an in vivo drug delivery system (DDS) successfully prevents the growth of murine liver metastasis of non small cell lung cancer*. 2007, AACR.
183. Kawata, E., et al., *Administration of PLK-1 small interfering RNA with atelocollagen prevents the growth of liver metastases of lung cancer.* Molecular cancer therapeutics, 2008. **7**(9): p. 2904-2912.
184. Demeure, M.J., et al., *A phase I/II study of TKM-080301, a PLK1-targeted RNAi in patients with adrenocortical cancer (ACC)*. 2016, American Society of Clinical Oncology.
185. Hu, X.-X., Y.-H. Wang, and J.-Y. Zhang, *Downregulation of VEGF and KSP Gene Expression Inhibits Proliferation of A549 Cells.*
186. Burnett, J.C. and J.J. Rossi, *RNA-based therapeutics: current progress and future prospects.* Chemistry & biology, 2012. **19**(1): p. 60-71.
187. Jordheim, L.P., et al., *The ribonucleotide reductase large subunit (RRM1) as a predictive factor in patients with cancer.* The lancet oncology, 2011. **12**(7): p. 693-702.
188. Davidson, J.D., et al., *An increase in the expression of ribonucleotide reductase large subunit 1 is associated with gemcitabine resistance in non-small cell lung cancer cell lines.* Cancer research, 2004. **64**(11): p. 3761-3766.
189. Bepler, G., et al., *RRM1 modulated in vitro and in vivo efficacy of gemcitabine and platinum in non-small-cell lung cancer.* Journal of Clinical Oncology, 2006. **24**(29): p. 4731-4737.

190. Souglakos, J., et al., *Ribonucleotide reductase subunits M1 and M2 mRNA expression levels and clinical outcome of lung adenocarcinoma patients treated with docetaxel/gemcitabine.* British journal of cancer, 2008. **98**(10): p. 1710.
191. Lam, J.K., et al., *siRNA Versus miRNA as Therapeutics for Gene Silencing.* Mol Ther Nucleic Acids, 2015. **4**: p. e252.
192. Polyak, D., et al., *Systemic delivery of siRNA by aminated poly (α) glutamate for the treatment of solid tumors.* Journal of Controlled Release, 2017. **257**: p. 132-143.
193. Ragelle, H., et al., *Nanoparticle-based drug delivery systems: a commercial and regulatory outlook as the field matures.* Expert opinion on drug delivery, 2017. **14**(7): p. 851-864.
194. Nakamura, Y., et al., *Nanodrug delivery: is the enhanced permeability and retention effect sufficient for curing cancer?* Bioconjugate chemistry, 2016. **27**(10): p. 2225-2238.
195. Petros, R.A. and J.M. DeSimone, *Strategies in the design of nanoparticles for therapeutic applications.* Nature reviews Drug discovery, 2010. **9**(8): p. 615.
196. Dong, H., H.S. Parekh, and Z.P. Xu, *Enhanced cellular delivery and biocompatibility of a small layered double hydroxide–liposome composite system.* Pharmaceutics, 2014. **6**(4): p. 584-598.
197. Krivitsky, A., et al., *Structure–Function Correlation of Aminated Poly (α) glutamate as siRNA Nanocarriers.* Biomacromolecules, 2016. **17**(9): p. 2787-2800.
198. Su, J., et al., *Silencing microRNA by interfering nanoparticles in mice.* Nucleic acids research, 2011. **39**(6): p. e38-e38.
199. Elbatanony, R.S., et al., *Afatinib-loaded inhalable PLGA nanoparticles for localized therapy of non-small cell lung cancer (NSCLC)—Development and in-vitro efficacy.* 2020: p. 1-17.
200. MacDiarmid, J.A., et al., *Bacterially-derived nanocells for tumor-targeted delivery of chemotherapeutics and cell cycle inhibitors.* Cell cycle, 2007. **6**(17): p. 2099-2105.
201. Whittle, J.R., et al., *First in human nanotechnology doxorubicin delivery system to target epidermal growth factor receptors in recurrent glioblastoma.* Journal of Clinical Neuroscience, 2015. **22**(12): p. 1889-1894.
202. Taylor, K., et al. *Nanocell targeting using engineered bispecific antibodies*. in *MAbs*. 2015. Taylor & Francis.

203. Solomon, B.J., et al., *A first-time-in-human phase I clinical trial of bispecific antibody-targeted, paclitaxel-packaged bacterial minicells.* PloS one, 2015. **10**(12): p. e0144559.
204. Reid, G., et al., *Clinical development of TargomiRs, a miRNA mimic-based treatment for patients with recurrent thoracic cancer.* Epigenomics, 2016. **8**(8): p. 1079-1085.
205. MacDiarmid, J.A., et al., *Bacterially derived 400 nm particles for encapsulation and cancer cell targeting of chemotherapeutics.* Cancer cell, 2007. **11**(5): p. 431-445.
206. MacDiarmid, J.A. and H. Brahmbhatt, *Minicells: versatile vectors for targeted drug or si/shRNA cancer therapy.* Current opinion in biotechnology, 2011. **22**(6): p. 909-916.
207. Kao, S.C., et al., *A significant metabolic and radiological response after a novel targeted microRNA-based treatment approach in malignant pleural mesothelioma.* American journal of respiratory and critical care medicine, 2015. **191**(12): p. 1467-1469.
208. Reid, G., et al., *Restoring expression of miR-16: a novel approach to therapy for malignant pleural mesothelioma.* Annals of oncology, 2013. **24**(12): p. 3128-3135.
209. Potticary, J., *New delivery option for anticancer drugs demonstrated in a clinical trial*. 2013, FUTURE MEDICINE LTD UNITEC HOUSE, 3RD FLOOR, 2 ALBERT PLACE, FINCHLEY CENTRAL, LONDON, N3 1QB, ENGLAND.
210. Glover, A.R., et al., *MicroRNA-7 as a tumor suppressor and novel therapeutic for adrenocortical carcinoma.* Oncotarget, 2015. **6**(34): p. 36675.
211. Gomex, M., *New Ammo In The War On Brain Cancer*, in *CBS New York News.* 2018.
212. Livak, K.J. and T.D.J.m. Schmittgen, *Analysis of relative gene expression data using real-time quantitative PCR and the 2− ΔΔCT method.* 2001. **25**(4): p. 402-408.
213. Shi, W., et al., *Significance of Plk1 regulation by miR-100 in human nasopharyngeal cancer.* 2010. **126**(9): p. 2036-2048.
214. Shimizu, J., et al., *mRNA expression of RRM1, ERCC1 and ERCC2 is not associated with chemosensitivity to cisplatin, carboplatin and gemcitabine in human lung cancer cell lines.* 2008. **13**(4): p. 510-517.
215. Wolter, P., et al., *Central spindle proteins and mitotic kinesins are direct transcriptional targets of MuvB, B-MYB and FOXM1 in breast cancer cell lines and are potential targets for therapy.* 2017. **8**(7): p. 11160.
216. Valente, V., et al., *Selection of suitable housekeeping genes for expression analysis in glioblastoma using quantitative RT-PCR.* 2009. **10**(1): p. 17.

217. Tschaharganeh, D., et al., *Non-specific effects of siRNAs on tumor cells with implications on therapeutic applicability using RNA interference.* Pathology & Oncology Research, 2007. **13**(2): p. 84-90.
218. Mann, G.J., et al., *Ribonucleotide reductase M1 subunit in cellular proliferation, quiescence, and differentiation.* Cancer Res, 1988. **48**(18): p. 5151-6.
219. Rahman, M.A., et al., *Systemic Delivery of siRNA-Nanoparticles Targeting RRM2 Suppresses Head and Neck Tumor Growth.* Journal of Controlled Release, 2012. **159**(3): p. 384-392.
220. Lee, S.-Y., C. Jang, and K.-A. Lee, *Polo-like kinases (plks), a key regulator of cell cycle and new potential target for cancer therapy.* Development & reproduction, 2014. **18**(1): p. 65.
221. Zheng, Z., et al., *DNA synthesis and repair genes RRM1 and ERCC1 in lung cancer.* 2007. **356**(8): p. 800-808.
222. Grolmusz, V.K., et al., *Cell cycle dependent RRM2 may serve as proliferation marker and pharmaceutical target in adrenocortical cancer.* 2016. **6**(9): p. 2041.
223. Tao, W., et al., *Induction of apoptosis by an inhibitor of the mitotic kinesin KSP requires both activation of the spindle assembly checkpoint and mitotic slippage.* Cancer cell, 2005. **8**(1): p. 49-59.
224. Wolf, G., et al., *Prognostic significance of polo-like kinase (PLK) expression in non-small cell lung cancer.* Oncogene, 1997. **14**(5): p. 543.
225. Ceppi, P., et al., *ERCC1 and RRM1 gene expressions but not EGFR are predictive of shorter survival in advanced non-small-cell lung cancer treated with cisplatin and gemcitabine.* Annals of Oncology, 2006. **17**(12): p. 1818-1825.
226. Sarli, V. and A.J.C.C.R. Giannis, *Targeting the kinesin spindle protein: basic principles and clinical implications.* 2008. **14**(23): p. 7583-7587.
227. Database, G.T.H.G. *PLK1 Gene (Protein Coding)*

Polo Like Kinase 1. 2020 [cited 20 2 February]; Available from: https://www.genecards.org/cgi-bin/carddisp.pl?gene=PLK1.

228. Database, G.T.H.G. *KIF11 Gene (Protein Coding)*

Kinesin Family Member 11. 2020 [cited 2020 2 February]; Available from: https://www.genecards.org/cgi-bin/carddisp.pl?gene=KIF11.

229. Database, G.T.H.G. *RRM1 Gene (Protein Coding)*

Ribonucleotide Reductase Catalytic Subunit M1

2020 [cited 2020 2 February]; Available from: https://www.genecards.org/cgi-bin/carddisp.pl?gene=RRM1&keywords=rrm1.

230. Database, G.T.H.G. *RRM2 Gene (Protein Coding)*

Ribonucleotide Reductase Regulatory Subunit M2. 2020 [cited 2020 2 February]; Available from: https://www.genecards.org/cgi-bin/carddisp.pl?gene=RRM2&keywords=rrm2.

231. Wlodkowic, D., J. Skommer, and Z. Darzynkiewicz, *Flow cytometry-based apoptosis detection*, in *Apoptosis*. 2009, Springer. p. 19-32.

232. Spänkuch-Schmitt, B., et al., *Effect of RNA silencing of polo-like kinase-1 (PLK1) on apoptosis and spindle formation in human cancer cells.* Journal of the National Cancer Institute, 2002. **94**(24): p. 1863-1877.

233. Malich, G., B. Markovic, and C.J.T. Winder, *The sensitivity and specificity of the MTS tetrazolium assay for detecting the in vitro cytotoxicity of 20 chemicals using human cell lines.* 1997. **124**(3): p. 179-192.

234. O'Toole, S.A., et al., *The MTS assay as an indicator of chemosensitivity/resistance in malignant gynaecological tumours.* 2003. **27**(1): p. 47-54.

235. Gray, P.J., et al., *Identification of human polo-like kinase 1 as a potential therapeutic target in pancreatic cancer.* 2004. **3**(5): p. 641-646.

236. Tao, Y.-F., et al., *Inhibiting PLK1 induces autophagy of acute myeloid leukemia cells via mammalian target of rapamycin pathway dephosphorylation.* 2017. **37**(3): p. 1419-1429.

237. Doan, C.C., et al., *Downregulation of Kinesin Spindle Protein Inhibits Proliferation, Induces Apoptosis and Increases Chemosensitivity in Hepatocellular Carcinoma Cells.* 2015. **19**(1): p. 1.

238. Ying, B., R.B.J.B. Campbell, and b.r. communications, *Delivery of kinesin spindle protein targeting siRNA in solid lipid nanoparticles to cellular models of tumor vasculature.* 2014. **446**(2): p. 441-447.

239. Marra, E., et al., *Kinesin spindle protein SiRNA slows tumor progression.* Journal of cellular physiology, 2013. **228**(1): p. 58-64.

240. Sagawa, M., et al., *Ribonucleotide reductase catalytic subunit M1 (RRM1) as a novel therapeutic target in multiple myeloma.* 2017. **23**(17): p. 5225-5237.

241. Vogel, C. and E.M.J.N.r.g. Marcotte, *Insights into the regulation of protein abundance from proteomic and transcriptomic analyses.* 2012. **13**(4): p. 227-232.

242. Miyamoto, S.i., et al., *Discrepancies between the gene expression, protein expression, and enzymatic activity of thymidylate synthase and dihydropyrimidine dehydrogenase in human gastrointestinal cancers and adjacent normal mucosa.* 2001. **18**(4): p. 705-713.

243. Rocha-Martins, M., B. Njaine, and M.S.J.P.o. Silveira, *Avoiding pitfalls of internal controls: validation of reference genes for analysis by qRT-PCR and Western blot throughout rat retinal development.* 2012. **7**(8).

244. Daga, N., et al., *Growth-restricting effects of siRNA transfections: a largely deterministic combination of off-target binding and hybridization-independent competition.* 2018. **46**(18): p. 9309-9320.

245. Draz, M.S., et al., *Nanoparticle-mediated systemic delivery of siRNA for treatment of cancers and viral infections.* 2014. **4**(9): p. 872.

246. Yang, C.-H., et al., *EGFR over-expression in non-small cell lung cancers harboring EGFR mutations is associated with marked down-regulation of CD82.* Biochimica et Biophysica Acta (BBA)-Molecular Basis of Disease, 2015. **1852**(7): p. 1540-1549.

247. Hirsch, F., M. Varella-Garcia, and F.J.O. Cappuzzo, *Predictive value of EGFR and HER2 overexpression in advanced non-small-cell lung cancer.* 2009. **28**(1): p. S32-S37.

248. Jang, M., et al., *Design of a platform technology for systemic delivery of siRNA to tumours using rolling circle transcription.* 2015. **6**(1): p. 1-12.

249. Van Loo, P., et al., *Allele-specific copy number analysis of tumors.* 2010. **107**(39): p. 16910-16915.

250. Miele, E., et al., *Nanoparticle-based delivery of small interfering RNA: challenges for cancer therapy.* 2012. **7**: p. 3637.

251. Xu, X., M.C. Farach-Carson, and X.J.B.a. Jia, *Three-dimensional in vitro tumor models for cancer research and drug evaluation.* 2014. **32**(7): p. 1256-1268.

252. Johnson, M., et al., *NCBI BLAST: a better web interface.* Nucleic Acids Research, 2008. **36**(suppl_2): p. W5-W9.

253. Park, B.H. and Y.H.J.B.R. Lee, *Phosphorylation of SAV1 by mammalian ste20-like kinase promotes cell death.* 2011. **44**: p. 584-589.

254. Kalyankrishna, S. and J.R.J.J.o.C.O. Grandis, *Epidermal growth factor receptor biology in head and neck cancer.* 2006. **24**(17): p. 2666-2672.

255. Destro, A., et al., *EGFR overexpression in malignant pleural mesothelioma: an immunohistochemical and molecular study with clinico-pathological correlations.* 2006. **51**(2): p. 207-215.
256. Park, H.S., et al., *High EGFR gene copy number predicts poor outcome in triple-negative breast cancer.* 2014. **27**(9): p. 1212-1222.
257. Spano, J.-P., et al., *Impact of EGFR expression on colorectal cancer patient prognosis and survival.* 2005. **16**(1): p. 102-108.
258. Peraldo-Neia, C., et al., *Epidermal Growth Factor Receptor (EGFR) mutation analysis, gene expression profiling and EGFR protein expression in primary prostate cancer.* 2011. **11**(1): p. 31.
259. Sheng, Q. and J.J.B.j.o.c. Liu, *The therapeutic potential of targeting the EGFR family in epithelial ovarian cancer.* 2011. **104**(8): p. 1241-1245.
260. Antonicelli, A., et al., *EGFR-targeted therapy for non-small cell lung cancer: focus on EGFR oncogenic mutation.* 2013. **10**(3): p. 320.
261. Pirker, R., et al., *EGFR expression as a predictor of survival for first-line chemotherapy plus cetuximab in patients with advanced non-small-cell lung cancer: analysis of data from the phase 3 FLEX study.* 2012. **13**(1): p. 33-42.
262. Sagnella, S.M., et al., *Cyto-Immuno-Therapy for Cancer: A Pathway Elicited by Tumor-Targeted, Cytotoxic Drug-Packaged Bacterially Derived Nanocells.* 2020. **37**(3): p. 354-370. e7.
263. Griffin, R. and R.A.J.O.J. Ramirez, *Molecular Targets in Non–Small Cell Lung Cancer.* 2017. **17**(4): p. 388-392.
264. Risnayanti, C., et al., *PLGA nanoparticles co-delivering MDR1 and BCL2 siRNA for overcoming resistance of paclitaxel and cisplatin in recurrent or advanced ovarian cancer.* 2018. **8**(1): p. 7498.
265. Byeon, H.J., et al., *Doxorubicin-loaded nanoparticles consisted of cationic-and mannose-modified-albumins for dual-targeting in brain tumors.* Journal of Controlled Release, 2016. **225**: p. 301-313.
266. Xu, P.-Y., et al., *Overcoming multidrug resistance through inhalable siRNA nanoparticles-decorated porous microparticles based on supercritical fluid technology.* 2018. **13**: p. 4685.
267. López-Serrano, A., et al., *Nanoparticles: a global vision. Characterization, separation, and quantification methods. Potential environmental and health impact.* 2014. **6**(1): p. 38-56.

268. Shang, J. and X.J.C.S.R. Gao, *Nanoparticle counting: towards accurate determination of the molar concentration.* 2014. **43**(21): p. 7267-7278.
269. Arsov, Z., et al., *Fluorescence microspectroscopy as a tool to study mechanism of nanoparticles delivery into living cancer cells.* 2011. **2**(8): p. 2083-2095.
270. Melamed, J.R., et al., *Quantification of siRNA duplexes bound to gold nanoparticle surfaces*, in *Biomedical Nanotechnology*. 2017, Springer. p. 1-15.
271. Cruz, C. and J.J.E. Houseley, *Endogenous RNA interference is driven by copy number.* 2014. **3**: p. e01581.
272. Zhong, C., et al., *Determination of plasmid copy number reveals the total plasmid DNA amount is greater than the chromosomal DNA amount in Bacillus thuringiensis YBT-1520.* 2011. **6**(1): p. e16025.
273. Zou, S., et al., *Enhanced apoptosis of ovarian cancer cells via nanocarrier-mediated codelivery of siRNA and doxorubicin.* 2012. **7**: p. 3823.
274. Jang, M., H.D. Han, and H.J.J.S.r. Ahn, *A RNA nanotechnology platform for a simultaneous two-in-one siRNA delivery and its application in synergistic RNAi therapy.* 2016. **6**: p. 32363.
275. Costa, E.C., et al., *Spheroids formation on non-adhesive surfaces by liquid overlay technique: Considerations and practical approaches.* 2018. **13**(1): p. 1700417.
276. Zanoni, M., et al., *3D tumor spheroid models for in vitro therapeutic screening: a systematic approach to enhance the biological relevance of data obtained.* 2016. **6**(1): p. 1-11.
277. Breslin, S. and L.J.D.d.t. O'Driscoll, *Three-dimensional cell culture: the missing link in drug discovery.* 2013. **18**(5-6): p. 240-249.
278. Edmondson, R., et al., *Three-dimensional cell culture systems and their applications in drug discovery and cell-based biosensors.* 2014. **12**(4): p. 207-218.
279. Costa, E.C., et al., *Optimization of liquid overlay technique to formulate heterogenic 3D co-cultures models.* 2014. **111**(8): p. 1672-1685.
280. Timmins, N., S. Dietmair, and L.J.A. Nielsen, *Hanging-drop multicellular spheroids as a model of tumour angiogenesis.* 2004. **7**(2): p. 97-103.
281. Raghavan, S., et al., *Comparative analysis of tumor spheroid generation techniques for differential in vitro drug toxicity.* 2016. **7**(13): p. 16948.
282. Li, J., et al., *Gene expression response to cisplatin treatment in drug-sensitive and drug-resistant ovarian cancer cells.* 2007. **26**(20): p. 2860-2872.

283. Friedl, P.J.E., *Reproducibility in Cancer Biology: Rethinking research into metastasis.* 2019. **8**: p. e53511.
284. Steger-Hartmann, T. and M.J.C.O.i.T. Raschke, *Translating in vitro to in vivo and animal to human.* 2020. **23**: p. 6-10.
285. Mak, I.W., N. Evaniew, and M.J.A.j.o.t.r. Ghert, *Lost in translation: animal models and clinical trials in cancer treatment.* 2014. **6**(2): p. 114.
286. Jeong, S.B., et al., *Essential role of polo-like kinase 1 (Plk1) oncogene in tumor growth and metastasis of tamoxifen-resistant breast cancer.* 2018. **17**(4): p. 825-837.
287. Housman, G., et al., *Drug resistance in cancer: an overview.* Cancers, 2014. **6**(3): p. 1769-1792.
288. Malhotra, M., et al., *Systemic siRNA delivery via peptide-tagged polymeric nanoparticles, targeting PLK1 gene in a mouse xenograft model of colorectal cancer.* 2013. **2013**.
289. Gutteridge, R.E.A., et al., *Targeted knockdown of polo-like kinase 1 alters metabolic regulation in melanoma.* 2017. **394**: p. 13-21.
290. Dharmapuri, S., et al., *Intratumor RNA interference of cell cycle genes slows down tumor progression.* 2011. **18**(7): p. 727-733.
291. Lee, J., H.J.J.B. Ahn, and b.r. communications, *PEGylated DC-Chol/DOPE cationic liposomes containing KSP siRNA as a systemic siRNA delivery Carrier for ovarian cancer therapy.* 2018. **503**(3): p. 1716-1722.
292. Lee, J., et al., *KSP siRNA/paclitaxel-loaded PEGylated cationic liposomes for overcoming resistance to KSP inhibitors: Synergistic antitumor effects in drug-resistant ovarian cancer.* 2020. **321**: p. 184-197.